JOURNAL OF THE

Electrochemical Society

LIBRARY
UNIVERSITY OF UTAH
FEB 7 1951
SALT LAKE CITY

Vol. 98, No. 2 February, 1951

Published Monthly by

THE ELECTROCHEMICAL SOCIETY

Enthone announces eight new METAL FINISHING PRODUCTS

WATERSHEDDING LIQUIDS

New watershedding liquids for rapid, complete stain-free drying of metals, such as copper, brass, silver and gold.

METAL STRIPPER—A

An alkaline stripper for dissolving nickel, silver, copper, brass, zinc, cadmium and gold from steel. No electric current is necessary.

CLEANER—160

A new alkali cleaner for anodic and cathodic cleaning of copper and brass, at high current density. A companion product to many other alkali cleaners for zinc, steel and aluminum.

STRIPPER—S49

A non-flammable solvent type stripper for lacquers and enamels.

WRITE FOR LITERATURE ON PRODUCTS DESCRIBED. ALSO CHECK LIST OF OVER 60 PRODUCTS FOR METAL FINISHING.

Enthone inc

442 ELM STREET
NEW HAVEN, CONN.

Journal of the

Electrochemical Society

FEBRUARY, 1951 VOLUME 98 • NUMBER 2

CONTENTS

Measurement of and Effect of Temperature on Electrical Resistance of Glass Electrodes. *Edgar L. Eckfeldt and George A. Perley* 37

A Micro Solution-Potential Measuring Technique. *L. W. Smith and V. J. Pingel* 48

Dichromate Reduction Rate at a Steel Surface in Air-Free, Acetic Acid Solution. *Norman Hackerman and Ray M. Hurd* 51

Potential-pH Diagram of Lead and its Applications to the Study of Lead Corrosion and to the Lead Storage Battery. *Paul Delahay, Marcel Pourbaix, and Pierre Van Rysselberghe* 57

Potential-pH Diagram of Silver. Construction of the Diagram—Its Applications to the Study of the Properties of the Metal, its Compounds, and its Corrosion. *Paul Delahay, Marcel Pourbaix, and Pierre Van Rysselberghe* 65

Electronic Instrumentation for Overvoltage Measurements. *Dimitrios Staicopoulos, Ernest Yeager, and Frank Hovorka* 68

Luminescence of K_4MnCl_6 and KCl (Pb + Mn). *Robert J. Ginther* 74

Current Affairs

Washington Spring Meeting 25C

Summer Corrosion Course at M.I.T. 26C

News Notes 26C

Section News 27C

Personals 27C

New Members 28C

Announcements from Publishers 28C

Book Reviews 29C

Notes from Industry 30C

Employment Situations 30C

H. H. Uhlig, *Editor*

Norman Hackerman, *Technical Editor* F. L. LaQue, *Business Manager* R. M. Burns, *Consultant*

Eleanor Reid, *Managing Editor* H. B. Linford, *Associate Editor* U. B. Thomas, *Associate Editor* R. G. Ellis, *Advertising Manager*

Divisional Editors

J. M. Bialosky, *Corrosion* Abner Brenner, *Electrodeposition* N. C. Cahoon, *Battery* H. C. Froelich, *Electronics*

W. C. Gardiner, *Industrial Electrolytic* A. E. Pavlish, *Electrothermic* R. R. Ralston, *Electric Insulation* W. D. Robertson, *Theoretical* Sherlock Swann, Jr., *Electro-Organic*

Published monthly by The Electrochemical Society, Inc., Mt. Royal and Guilford Aves., Baltimore 2, Md., combining the Journal and Transactions of The Electrochemical Society. Editorial Office: 235 W. 102nd St., New York 25, N. Y. Statements and opinions given in articles and papers in the Journal of The Electrochemical Society are those of the contributors, and The Electrochemical Society assumes no responsibility for them. Subscription: $8.50 to members, $12.00 to nonmembers. Single copies $1.00 to members, $1.25 to nonmembers. Copyright 1951 by The Electrochemical Society. Entered as second-class matter November 15, 1947, at the Post Office at Baltimore, Md., under the act of August 24, 1912.

How to Determine Impurities in Electroplating Solutions

Of all methods for determining minute impurities in plating baths, the most practical is the *colorimetric.* The principle utilized is simple: color intensity, due to presence of a colored constituent, is directly proportional to the concentration of that constituent.

USE OF THE COLORIMETRIC METHOD

This method requires the measuring of light transmitted by solutions.

Intensity of the transmitted light is measured by photoelectric means to attain a high degree of accuracy. No two solutions of different character will have transmittancy curves of exactly the same shape, hence, a solution under test is usually compared to a reference solution free of impurities. Calibration curves plotted from a series of runs facilitate determinations. Summaries of techniques used to determine four different impurities follow:

LEAD IN NICKEL PLATING BATHS

Lead is separated from interfering ions by extraction with a carbon tetrachloride solution of dithizone in the presence of potassium cyanide. After removal of the excess dithizone with alkaline potassium cyanide, the transmittancy of the solution is measured and the quantity of lead present determined from a calibration curve.

IRON IN NICKEL PLATING BATHS

Iron is separated from the other metallic ions by precipitation with cupferron. The iron cupferride is extracted with amyl acetate and then returned to the aqueous solution by shaking the amyl acetate extract with nitric acid. The iron is then reduced with hydroxylamine hydrochloride. O-phenanthroline is added, and the pH is adjusted with sodium acetate. Finally, the light transmission of the ferrous o-phenanthroline complex is measured.

MANGANESE IN NICKEL PLATING BATHS

The manganese is oxidized to permanganate by sodium periodate in an acid mixture of phosphoric and perchloric acids. The transmission of the solution is then measured.

COPPER IN NICKEL PLATING BATHS

Copper is isolated from the other constituents in the plating bath by precipitation with 2-mercaptobenzothiazole and extraction of the precipitate with amyl acetate. The color is then developed by addition of dibutyl amine and carbon disulfide. After the solution has been diluted with ethyl alcohol, its transmittancy is measured.

A.E.S. RESEARCH PROGRAM

The American Electroplaters' Society is conducting a comprehensive research program and has developed useful information on current plating problems. International Nickel, in addition to its other support of this program, feels that it will be a further service to make copies of these A.E.S. Research Reports available.

For an authoritative, detailed, 48-page study of this subject, we offer you a free copy of the A.E.S. Research Report, Serial No. 3, entitled *"Determination of Impurities in Electroplating Solutions."* Write us for your copy, now.

• • •

Because of unusually heavy industrial and defense demand, rationing of nickel has been in force since July 1st. On January 1, 1951, National Production Authority Order M-14, respecting the consumption of primary nickel, went into effect.

We shall continue to issue information on new developments and user experience with nickel-containing materials as we believe that dissemination of such data can help to promote the intelligent utilization of critical materials, so essential in these times.

EMBLEM OF INCO SERVICE TRADE MARK

THE INTERNATIONAL NICKEL COMPANY, INC. 67 WALL STREET NEW YORK 5, N. Y.

Editorial

The Electric Eel

MICHAEL FARADAY'S curiosity was far-reaching, and his intuitive sense of scientific order amazing, even in light of knowledge today. One of his interesting series of experiments concerned the gymnotus or electric eel found in small fresh-water rivers which flow into the Atlantic Ocean at Venezuela and the Guianas. They may measure $2\frac{1}{2}$ to 4 feet in length, and have the unique method of catching other fish by stunning them with a high voltage discharge through the water. Faraday was interested in the origin of electricity, whatever its source, which stimulated his curiosity about the electric eel. "The existence of animals," he said, "able to give the same concussion to the living system as the electrical machine, the voltaic battery, and the thunderstorm,—it became of growing importance to identify the living power which they possess, with that which man can call into action from inert matter, and by him called electricity."

Faraday obtained a specimen of gymnotus from a Mr. Porter who had brought it to England from South America in August of 1838. He found that electric shocks from the eel were powerful when the "hands were placed in a favorable position, i.e., one on the body near the head and the other near the tail." The nearer the hands were together, the less powerful was the shock. Using copper leads instead, Faraday noticed that a galvanometer was much affected—much more, for example, than from a cell made by placing zinc and platinum electrodes above and below the tongue. The deflection was always in the same direction; in other words, the gymnotus was a source of intermittent direct current with positive pole near the head and negative pole near the tail. By sending the eel's impulse through 22 feet of silk-covered wire in the form of a solenoid, he found that a steel needle placed within the solenoid became magnetic. A similar impulse, furthermore, was used successfully to electrolyze a potassium iodide solution soaked in paper. Faraday looked for a heating effect by the piscatorial electricity, but of this he was not sure. However, the impulse could be made to produce an electric spark when one of the copper conductors was rubbed over a steel file connected to the other conductor. There seemed to be no doubt but that the gymnotus was a source of bona fide electricity.

Faraday, perennially with an eye to the quantitative, estimated before the

(*Continued on next page*)

days of the voltmeter that the shock he received from his obliging eel was like that of a "good voltaic battery of perhaps 100 or more pairs of plates of which the circuit is completed for a moment only." From this we might infer that the eel could deal at least 150 volts. In addition, the eel could supply repeated—two or three—shocks within a short interval of time, but, if excited too often, it became fatigued and the shocks diminished. Peculiar it was that despite the strong electric impulse sufficient to stun a small fish, the eel itself was apparently so adapted as to be unaffected by the same or even greater impulse that simultaneously traveled through its body. Also apparent, Faraday said, was that the eel knew when his victim had the proper conductivity permitting shock. For example, the hands in contact with or near the eel received repeated shocks, but a glass rod or the galvanometer circuit received one or two impulses and was thereafter ignored.

Faraday suggested that the gymnotus produced electricity by a mechanism probably related to the conversion of nervous energy into electricity. For did not an electric shock produce a nervous stimulus? The reverse might also be true. Faraday thought of proving this by sending a current through the body of a fatigued gymnotus in the opposite direction and thereby restoring the electrical capacities of the eel. He also suggested investigating whether the current generated by one side of the gymnotus put into action the electricity-producing organs on the other side. Would the response be the same if the nerves to the organs were first cut? These are some of the experiments Faraday suggested and wanted to do. However, other matters were more pressing, and so the mystery of the electric eel remains, waiting for still other experimenters of more-than-usual curiosity to unravel the answers.

Add the gymnotus to a long list of challenges awaiting young men about to enter the field of electrochemistry.

Measurement of and Effect of Temperature on Electrical Resistance of Glass Electrodes[1]

EDGAR L. ECKFELDT AND GEORGE A. PERLEY

Leeds & Northrup Company, Philadelphia, Pennsylvania

ABSTRACT

The apparent irregularities observed in measuring the electrical resistance of glass electrodes, as reported in the literature, are explained by the dielectric properties of glass. The use of d.c. is recommended, and the need for caution in the use of a.c. is indicated. An experimental technique is described which hastens the measurement with d.c. when dielectric absorption is bothersome. An experimental study is reported dealing with the effect of temperature on the resistance of glass electrodes, including ones of Corning 015 glass and others made from three newer pH-responsive glasses. The experimental results do not agree with previously employed equations. The Rasch and Hinrichsen relationship, $\log R = B/T + A$, in which the logarithm of the resistance varies linearly with the reciprocal of the absolute temperature, is preferred. A nomograph is given for the glasses studied. The temperature-resistance behavior of Corning 015 glass is mathematically the same for membranes immersed in solution and for the dry glass at elevated temperatures.

INTRODUCTION

The electrical resistance of the pH-responsive glass membrane is an important property of a glass electrode, since for any particular type of measuring equipment there is an upper limit of resistance beyond which errors of measurement become significant.

Glass electrodes have peculiar properties that present problems in resistance measurements. The literature on this subject consequently reflects some perplexity and lack of agreement on methods and results, and the practical and theoretical usefulness of the existing information on resistance has been limited. Various d-c methods of measuring the resistance have been reported and appear to give concordant results (4, 5, 6, 8, 11, 16). Reported a-c resistances are much lower than the corresponding values with d.c., and the a-c values vary with frequency (2, 12, 15). The differences between d-c and a-c values have been attributed to errors of "polarization" presumed to be present in the d-c measurements (12, 15). The first part of this paper discusses the significances of d-c and a-c resistances, shows why the two methods give different values, and justifies and recommends the use of d.c. for glass electrodes.

The question of the temperature-resistance relationship is also considered. Reported relationships of immersed glass electrodes, including those of Corning 015 glass, are all of the general form

$$\log R = A + Bt \qquad \text{(I)}$$

in which R is the resistance, A and B are constants, and t is the temperature (2, 3, 22). The resistance of glass not immersed in solutions has been expressed very often by a different general equation, originally given by Rasch and Hinrichsen (20), namely

$$\log R = A + B/T. \qquad \text{(II)}$$

T is the absolute temperature, and the other symbols are the same as in equation (I). Corning 015 glass at elevated temperatures and not in contact with solution follows this second equation (25). The question arises as to whether Corning 015 glass changes its temperature-resistance relationship when in contact with aqueous solutions. The latter portion of this paper describes an experimental study in which the second equation is found valid for all glass electrodes studied, including Corning 015 glass.

SIGNIFICANCES OF D-C AND A-C RESISTANCES[2]

It is accepted practice to define resistance as that "property of an electric circuit or of any body that may be used as part of an electric circuit which determines for a given current the rate at which electric energy is converted into heat or radiant energy, and which has a value such that the product of the resistance and the square of the current gives the rate of conversion of energy" (1). This definition does not seem feasible to use with glass electrodes, since the amount of heat generated with the necessarily low currents is vanishingly small. This definition is useful, nevertheless, in explaining the influence of a loss-producing phenomenon on the electrical resistance of a material.

[1] Manuscript received January 27, 1949. This paper prepared for delivery before the Philadelphia Meeting, May 4 to 7, 1949.

[2] The following indicate general references for the material of this section: (14), (18), (26).

Ohm's law gives a convenient way of measuring resistance, but it may not be applied to all circuits. It may be used, however, when a constant voltage results in an unvarying current in the substance being measured. The voltage, E, used in the calculation must not include electromotive forces outside the substance, such as might arise at its boundary or at auxiliary electrodes. Such extraneous electromotive forces, E_c, commonly oppose the applied voltage, and Ohm's law must be modified when they are present to

$$E - E_c = RI. \qquad \text{(III)}$$

The evidence indicates that with glass electrodes extraneous counterelectromotive forces are of inconsequential magnitude and may be ignored in using Ohm's law.

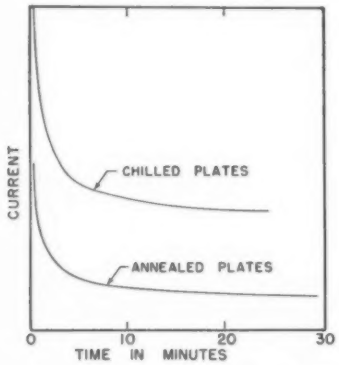

FIG. 1. Dielectric absorption in an opal borosilicate glass, from the work of Guyer.

Complications, nevertheless, will arise in measuring the resistance of glass electrodes. Glass is primarily a dielectric and exhibits only slight electrical conductivity. The measurement of resistance thus will be markedly influenced by dielectric properties. It appears that the literature on glass electrodes does not adequately relate the influence of dielectric phenomena to the problem of measuring resistance.

Dielectric Properties of Glass

Dielectric absorption in glass and glass electrodes tends to become more pronounced as the temperature is lowered and the resistance of the glass increases. The mechanisms responsible are not completely understood, but it is helpful, not only in measuring the resistance but also in considering other aspects of the glass electrode, to have a knowledge of these phenomena.

Fig. 1, taken from the work of Guyer (10), shows what happens when a voltage is applied to different plates of a borosilicate glass. The curves show that initially the current falls sharply and then slowly levels off at a finite value. The current that flows comprises not only that required to charge the geometric capacity, which component very rapidly falls to zero, but also at least two other components. These two latter components are manifestations of the imperfect nature of the dielectric, and, as they are primarily responsible for converting electrical energy into heat, are of especial interest in a discussion of resistance.

One of these heating components, the conduction current, is not a function of time and in many cases satisfactorily obeys Ohm's law. The migration of alkali metal ions within the glass network appears to be responsible for the conduction current. The measurement of d-c resistance of glass electrodes depends upon measuring only this conduction-current component.

The other heating component, the so-called absorption current, decreases with time and slowly decays to zero. It is anomalous in nature and unique and specific for each dielectric. Apparently this current is a manifestation of a slow rearrangement or distortion of the internal structure of the glass caused by the electric field, dissipation of electric energy into heat accompanying the process. Taylor (24) has shown a remarkable analogy between the absorption current and delayed elastic effects.

The passage of an absorption current results in an accumulation of charge in the glass. A brief short circuit of the glass does not suffice to discharge the glass completely, and subsequently a difference of potential will arise across the glass. This is termed residual charge. Only by protracted short-circuiting of the glass (or by letting it stand for a long period) can all of the residual charge be removed.

The measuring technique described later demonstrates the principle of superposition, another aspect of dielectric absorption. A striking example of this principle occurs when a glass which exhibits dielectric absorption is charged for a long period, and then is charged briefly with the polarity of the charging voltage reversed. If this glass is now discharged, the direction of flow of the discharge current will be found at first to be consistent with the polarity of the voltage of the latter short charging period, but eventually the direction of flow of the discharge current will reverse itself and become consistent with the former longer charging period.

Dielectric Loss and Measurements with A.C.

Dielectric loss refers to the loss of electric energy as heat due to a changing electric field, this heat arising not only from the conduction-current component but also from the absorption-current component. In glass at room temperature, the magnitude of the latter component depends very much on

frequency and may greatly exceed the conduction-current component. Thus the value of resistance depends very much upon the frequency used to measure it, and the value with d.c. may differ radically from values found with a.c., the a-c values differing among themselves.

This explains why reported values of resistance of glass electrodes with d.c. may be as much as thirty or more times greater than corresponding values with a.c. The duration of even a quick d-c measurement in a given instance may be long compared with the speed of the absorptive change, so dielectric absorption passes unnoticed. However, measurements with a.c. under corresponding conditions may result in an absorption current having a very significant component in phase with the applied field. Such an in-phase component of current results in a loss of energy within the glass, thereby adding an a-c conductivity component to that conductivity of the glass which would be observed by a d-c measurement alone. This increased conductivity corresponds to the lower resistance observed in an a-c resistance measurement. The a-c measurement involves an additional phenomenon (or phenomena) and, therefore, has a more complicated significance than the d-c measurement.

D-C Resistance

The pH-indicating potential of the glass electrode is a d-c potential, and pH measuring techniques employed with this d-c potential will be affected not by a-c resistances but only by the d-c resistance of the electrode, as Dole (7) has pointed out. The question arises as to how reliable is a d-c measurement in giving the desired property. Complications from dielectric phenomena can be overcome by proper measurement of the conduction-current component as described later. Possible complications arising from an extraneous counterelectromotive force must be considered, as these would vitiate the simple use of Ohm's law. The following facts seem to support the viewpoint that the d-c measurement does not introduce an extraneous counterelectromotive force [corresponding to E_c of equation (III)], and that the simple use of Ohm's law is valid:

1. D-C resistances are independent of the applied voltage (15). If a counterelectromotive force were present, it might reasonably be expected not to be proportional to the voltage.

2. In the absence of chemical attack, d-c resistances are constant with solutions of different pH and different composition (22), factors which might be expected to vary the counterelectromotive force if one did exist.

3. Exceedingly small currents flow in the commonly used methods of measuring d-c resistance of glass electrodes, and correspondingly minute amounts of substances are involved in the electrolysis. Thus, if one volt is used in measuring 100 megohms, only 10^{-8} ampere flows, which corresponds to less than one-hundredth of a microgram of sodium (or lithium) in one hour.

4. D.C. has been used for many years at ordinary temperatures in measuring the resistance of specimens of glass which are not in the form of glass electrodes nor immersed in aqueous solutions. Morey (17) cites the need for techniques to prevent polarization, not at ordinary temperatures but only above 100°C.

5. The d-c resistance of glass at ordinary temperatures (not in glass electrodes nor immersed in aqueous solutions) shows remarkable continuity with a-c values at high temperatures, both groups following the law of Rasch and Hinrichsen (13, 21). This speaks against an interfering element being present and suggests that a single phenomenon is being observed.

The results of the present experimental study support the viewpoint that no significant counterelectromotive force is present in the d-c measurement of glass electrodes. The agreement of the temperature-resistance values with a simple mathematical equation over a considerable temperature range argues against the presence of complicating effects, and indicates that a single phenomenon is being observed.

The value of resistance as calculated using Ohm's law from a properly made d-c measurement is accepted as a true ohmic resistance of the glass.

Measuring the d-c Resistance

In many cases, especially above room temperature, dielectric absorption does not interfere with a simple d-c measurement. In such instances a straightforward measuring procedure may be employed (4, 5, 6, 8, 11, 16).

At lower temperatures, however, dielectric absorption becomes troublesome. Even at room temperature certain lithia types of pH-responsive glass show dielectric absorption, and the resistance of these becomes very difficult to measure as the temperature is lowered. An attempt to measure the conduction current is complicated by the changing value of the current which may persist for hours. In the example of Fig. 1, even after 30 minutes the current is still changing somewhat, and it would not be strictly valid to take the current at that time. A premature reading will give a value of resistance which is too low, since apparent resistance will be low initially and will rise progressively finally approaching a constant value. By waiting long enough, the conduction-current component can be obtained, since the other current components eventually will decrease to zero while the conduction-current component remains constant.

The experimental part of the present study, in those instances where dielectric absorption was bothersome, employed a novel procedure to reduce the tediousness of the measurements. The viewpoint was taken that separate processes contribute to the absorption current, and that each adjusts itself to the electric field at its own rate. Thus the slowness of the observed current in reaching constancy is caused essentially by the slowest of these processes. It was found experimentally that equilibrium with a particular applied field could be reached more quickly by applying initially a constant voltage for a short time and then lowering the voltage somewhat, causing it to come into agreement with that particular induced condition in the glass which corresponded to the slowest process.

Fig. 2 illustrates what happens in the presence of dielectric absorption when the voltage is suddenly lowered somewhat, after an initial period of subjecting a glass electrode to a constant voltage. The curves of this figure represent *apparent* values of

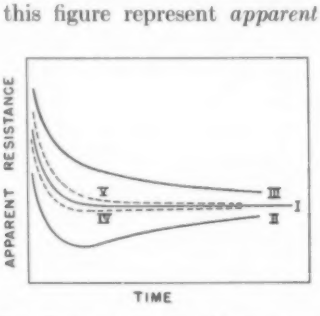

FIG. 2. The effect of lowering the impressed voltage in the presence of dielectric absorption.

resistances by Ohm's law, as would be obtained from the changing currents and the particular voltages employed. Curve I results when the voltage is lowered the correct amount; there is an initial rapid fall corresponding to the readjustment of the more rapid process (or processes) to the new voltage, and then the apparent resistance becomes constant. The constant conduction current is realized, and the corresponding value of resistance as calculated from Ohm's law is the accepted d-c resistance of the glass.

Usually the first trial is not successful in producing Curve I. Curve II shows insufficient lowering of the voltage. After the initial rapid fall, caused as before, the trend reverses and the apparent resistance increases, but at a slower rate than in the absence of a readjustment of the voltage. Curve III shows too great a lowering; there is the initial rapid fall, followed by a continuing slow downward trend.

In practice it is not necessary to produce Curve I, which in itself would be a tedious procedure. After the initial period any value of current taken from Curve II will yield a value of resistance which is somewhat lower than the accepted value, while a value selected from a similar point on Curve III will yield a value of resistance somewhat higher than the accepted value. The direction of the trend after the initial period indicates whether the voltage change was too little or too much. Thus the accepted value can be obtained with any desired precision by successively modifying the voltage so as to straddle Curve I more and more closely, as for example by Curves IV and V. Usually, four or five trials will suffice to give an acceptable value.

EXPERIMENTAL

The change of d-c resistance of glass electrodes with temperature was studied experimentally by measuring twelve electrodes of glasses of four different compositions, at selected temperatures in the range from about 8° to 75°C. The measuring assembly was designed to afford close control over the important variables and to provide versatility and ease of operation. The components were, for the most part, standard instruments.

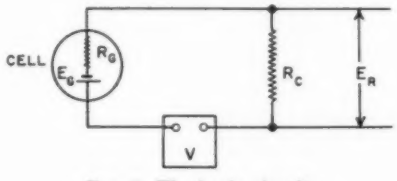

FIG. 3. The basic circuit

Method of Measurement

The method employed in measuring the resistance is basically similar to that employed by Guyer (9) in his study of the electrical behavior of glass at room temperature, and to that employed by Corzo (5) in his study of glass electrodes. The problems which confronted Guyer are analogous to those which arise in measuring the resistance of glass electrodes. The present method differs from these, however, in that it measures the electromotive force of the glass electrode cell, whatever it may be, and includes it in the equation for the calculation of resistance.

The basic circuit is shown in Fig. 3. The potential of the glass cell is represented by E_g and its resistance by R_g. An adjustable, known source of voltage in the circuit is represented by V, and a calibrated resistor of known value by R_c. The potential of the glass electrode cell, E_g, is first measured as in the customary way for measuring pH. This must be done before the glass acquires a charge if dielectric absorption is pronounced. Then the value E_R is measured with R_c and V introduced as in Fig. 3. Resistances in the circuit other than R_g and R_c

are negligible, and the resistance of the glass is given by the relationship

$$R_G = R_C\left(\frac{V + E_G - E_R}{E_R}\right). \qquad \text{(IV)}$$

An examination of this relationship reveals that the most favorable conditions for measuring the resistance exist when the calibrated resistor approximately equals the resistance of the glass (when $V + E_G$ is approximately twice E_R). When the calibrated resistor is greatly different, the accuracy of measurement is less. Since the resistance of glass changes markedly with temperature, it is desirable to have a number of calibrated resistors to cover the range to be measured.

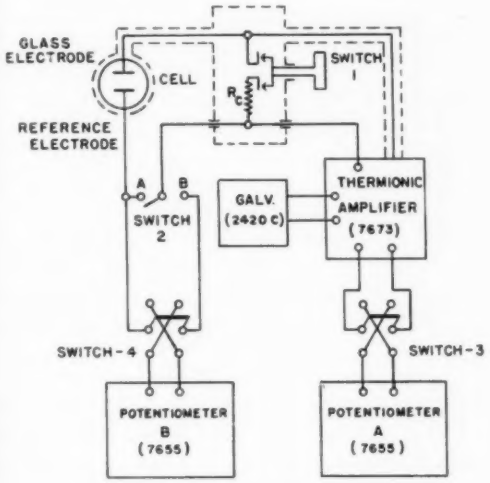

FIG. 4. The measuring circuit

Apparatus

Electrical Circuit.—The actual circuit is given in Fig. 4. The standard components are indicated by the L&N numbers appearing thereon. The potentiometers are the portable type with a range of 0 to 1.11 volts. The amplifier, described by Cherry (4), is designed for a very high impedance of input.

Potentiometer A is used to counterbalance the input voltage to the amplifier and thus serves to measure that voltage. Potentiometer B supplies the adjustable, known voltage V, an acceptable procedure since the circuit which is supplied has insignificant conductance. The polarities of the potentiometers are readily reversed by their respective reversing switches, 3 and 4.

The high-resistance portion of the circuit is indicated with shielding in Fig. 4, and requires, as is commonly known, excellent insulation and protection from electrostatic fields. The conductors and connectors are the types used in pH equipment. Switch 1 has insulating parts of Plexiglas and is mounted along with the interchangeable calibrated resistor inside a metal can as indicated. The remainder of the circuit is assembled with ordinary insulation and wiring precautions.

The potential of the glass cell, E_G, may be measured with switch 1 in the open position and switch 2 in the A position. The value of E_R may then be obtained with switch 1 closed and with switch 2 in the B position. These values along with the known values of V and R_C yield with equation (IV) the value of resistance of the glass.

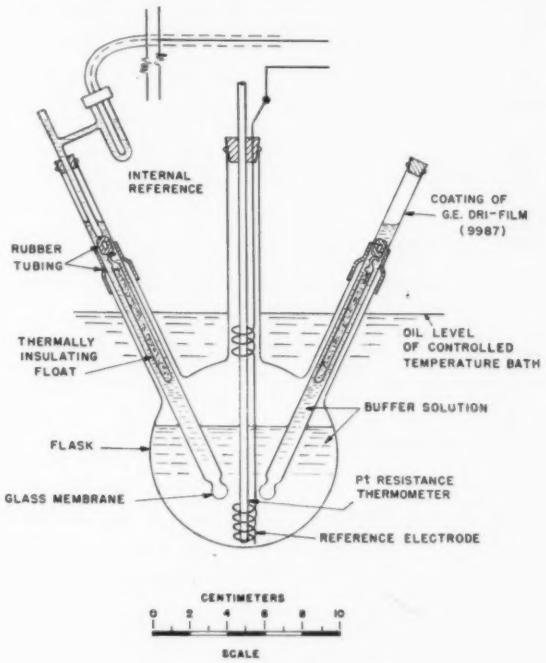

FIG. 5. The cell assembly

Calibrated Resistors.—Four calibrated resistors were used to cover the range of measured resistances. Three were received from the Victoreen Instrument Company and had values as follows: 11.5, 91.2, and 1010 megohms. The fourth, on hand from previous work, had a resistance of 376 megohms.

These were calibrated by first measuring the resistance of the lowest one in a conventional way using a Wheatstone bridge and sensitive galvanometer. This was used to calibrate the next higher one using the circuit of Fig. 4, and so on. Particular care was exercised to obtain good relative values, rather than exact absolute values.

The effect of temperature on these standards during the measurements was inconsequential, since

their temperature coefficients were not excessive and the room temperature varied only slightly during the course of the work.

Cell Assembly.—The twelve electrodes under test were assembled in two specially blown flasks, as shown in Fig. 5. Each flask, with nominal volume of 500 ml, had six side-arms for electrodes. These assemblies were immersed as indicated in a controlled-temperature bath, capable of maintaining regulation of the order of ±0.001°C. The metal lining of the tank was connected electrically to the shielding of the circuit and thus shielded the electrode assembly. A platinum resistance thermometer with Mueller bridge (L&N No. 8163-A and 8069, respectively) gave the temperature of the solution in which the glass electrodes were immersed. The National Bureau of Standards furnished the constants of the thermometer.

The same buffer solution was used inside and outside the electrodes. It was approximately 7 pH and was composed of diabasic sodium phosphate (0.03 molal), monobasic potassium phosphate (0.03 molal), and sodium chloride (0.02 molal).

TABLE I. *Compositions of the pH-responsive glasses* (mole per cent)

Designation of glass	Li_2O	Na_2O	Cs_2O	CaO	BaO	La_2O_3	SiO_2
Corning 015	—	21.4	—	6.4	—	—	72.2
L & N 402	25	—	—	—	8.4	—	66.6
L & N 379	25	—	2	2	5	3	63
L & N 399	28	—	2	—	5	2	63

The reference electrode was a length of silver wire, formed as shown. The lower portion was coated with silver chloride by anodic electrolysis in a solution of hydrochloric acid.

A calomel electrode with salt bridge as shown was the internal reference. In making a sequence of measurements this was moved from electrode to electrode as required. The two reference electrodes were different and, in general, were not at the same temperature. Thus the cell had a net potential, constant over any measuring period and included in calculating resistance as has been described.

A glass float, containing glass wool, fitted closely inside the stem of each glass electrode. A short section of rubber tubing inside the stem held the float in place. This float reduced longitudinal transfer of heat. The exposed portion of the stem of each electrode was protected against electrical leakage by G.E. Dri-Film No. 9987, applied as a 5 per cent solution in carbon tetrachloride.

pH-Responsive Bulbs

The pH-responsive membranes were in the form of bulbs of the Haber type and were similar in size and ruggedness to those of modern commercial electrodes. Each bulb contained about one decigram of glass and measured a little less than one centimeter in diameter. The thickness of the membranes averaged about 0.1 mm. The bulbs were blown on stems of lead-glass which has high electrical resistance.

The resistance of the glass in electrodes depends upon thermal history and other factors, and accordingly no attempt was made to ascertain the precise specific resistance. With the above dimensions, however, and the assumption that about two-thirds of the sphere is involved, a factor of 200 cm is derivable for converting the measured to the specific resistance. This, of course, may be used only as a guide in estimating the order of magnitude of the specific resistance.

The compositions (in mole per cent) of the pH-responsive glasses are given in Table I. The figures for Corning 015 glass were taken from published information. The figures for the L&N glasses were obtained from chemical analyses of representative batches. The 015 glass was purchased from the Corning Glass Works; the others were prepared in this laboratory. L&N glass 399 is intended for use at ordinary temperatures, while the other two are for use at higher temperatures. One of the present authors has prepared information on pH-responsive glasses, including the above newer glasses (19).

Procedure

The experimental part of this study was done intermittently over a period of five months. The bulk of the work consisted of two series of runs at selected temperatures, one before and the other after protracted heating of the electrodes at 75°C. The electrodes were also subjected to preparatory and incidental testing.

The electrodes were blown at the beginning of the work and were not put in contact with solution until about two and one-half months had passed. They were then mounted and assembled as previously described. Four or five days of soaking elapsed before the first values of resistance were taken. In the latter period of testing, the bulbs always stayed in contact with the buffer solution, and during the idle time between runs, remained at room temperature.

To insure thermal equilibrium before taking readings, several hours were allowed to elapse with the bath controlled at the desired temperature. Temperatures taken inside the flasks during the periods of measuring differed by no more than one- or two-hundredths of a degree from those taken in the oil, and by even less than this from the reported values.

The question arose concerning whether the above waiting time was adequate at the lower temperatures. A test was made in which one flask of elec-

trodes was held for about ten hours at 10° above, and another flask for about ten hours at 10° below, the particular temperature of the bath (14.35°C). Both flasks were then placed in the bath at the same time and were brought into thermal equilibrium with the bath as rapidly as possible. Measurements of resistance were made during the subsequent twenty-four hours. No evidence was obtained to indicate that time was required for the resistance to adjust itself to the new temperature, although the test was conducted in such a way that rapid changes which might have been completed within the first hour or so would not have been noticed.

The readings were taken as previously described. The value of the impressed voltage (V) was usually about one volt. Preliminary tests with one-tenth volt gave the same results as those with one volt, showing that these glasses obey Ohm's law. This is in agreement with the observations of others (15).

During the measurements, the polarity of the impressed voltage was reversed from time to time to avoid any possible cumulative effect of passing current through the electrodes always in the same direction. The direction of current flow through the bulb made no difference in the value of resistance. Moreover, so long as dielectric absorption was negligible, the reading was obtained without noticeable delay upon reversing the voltage. With marked dielectric absorption, however, the reading was delayed, as would be expected.

A previous section explains how the taking of readings was facilitated in the presence of dielectric absorption, and this procedure was employed when needed.

The first series of runs includes the following successive temperatures: 25.01°, 14.35°, 8.45°, 36.02°, 48.63° 61.46°C. It was originally planned to conclude the work with a final set of readings at about 75°C, but in the course of this run (actually at 74.52°C) the resistances of two or three of the electrodes were uncertain, indicating changing values. Accordingly, the electrodes were left at this temperature overnight for a total period of about 18 hours with the hope that the values would become stable. The next day readings were continued, and this time there was no evidence of change.

Because of this, a second series of runs, including all but the lowest of the previous temperatures, was performed in the following sequence: 74.52°, 48.63°, 61.46°, 25.01°, 14.35°, 36.02°C. It was not difficult to re-establish these particular temperatures by virtue of the method of control built into the controlled-temperature bath.

TABLE II. *Resistances of the electrodes* (values in megohms)

Temp °C	Series*	Corning 015 Glass			L & N 402 Glass			L & N 379 Glass			L & N 399 Glass		
		Electrode No.			Electrode No.			Electrode No.			Electrode No.		
		1	2	3	4	5	6	7	8	9	10	11	12
8.45	I	1790	890	990	3700	2240	2440	3800	4000	2840	460	550	520
14.35	I	940	460	520	1890	1160	1180	1920	2040	1430	241	287	267
	II	1000	480	560	3300	1560	1610	1940	2250	1630	267	360	610
25.01	I	330	158	181	530	360	360	610	660	460	82	99	86
	II	340	159	190	930	440	470	620	670	480	85	99	156
36.02	I	119	56	66	161	98	120	200	219	152	25.8	28.6	28.9
	II	122	57	68	253	131	143	196	224	162	27.0	33.	46.
48.63	I	42	19.7	23.5	48	29.9	38	64	71	49	8.8	9.5	9.8
	II	42	19.2	23.3	64	36	42	66	72	51	10.4	11.1	12.5
61.46	I	15.4	7.2	8.6	15.1	9.7	12.6	21.4	23.9	16.6	3.2	3.4	3.5
	II	15.3	7.0	8.5	18.9	10.6	12.7	20.6	23.1	16.7	3.3	3.5	4.0
74.52	II	5.9	2.72	3.3	5.9	3.7	4.6	7.5	8.4	5.9	1.21	1.26	1.36

* Series I was performed before protracted heating at 74.52°C; Series II, afterward.

Results

The resistances, calculated using equation (IV), are presented in Table II. The majority of these values represent single measurements. In a fair number of instances, however, multiple measurements were available, and averages are presented.

The results appear also in the graphs of Fig. 6, 7, 8, and 9. The resistance on a logarithmic scale is plotted against the reciprocal of the absolute temperature. Series I appears in Fig. 6 and 7, while

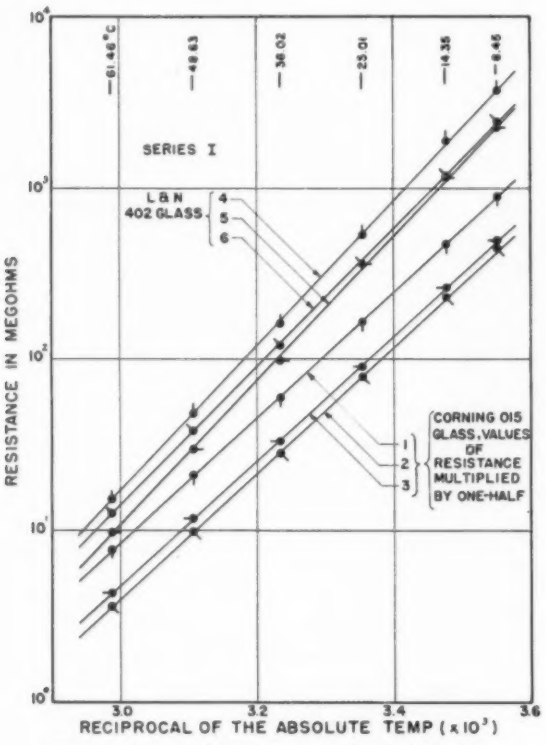

FIG. 6. Data of Series I, electrodes 1 through 6

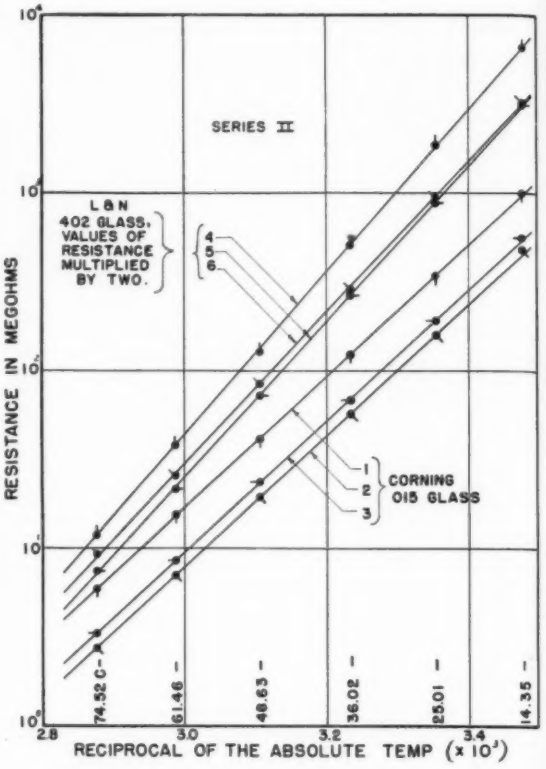

FIG. 8. Data of Series II, electrodes 1 through 6

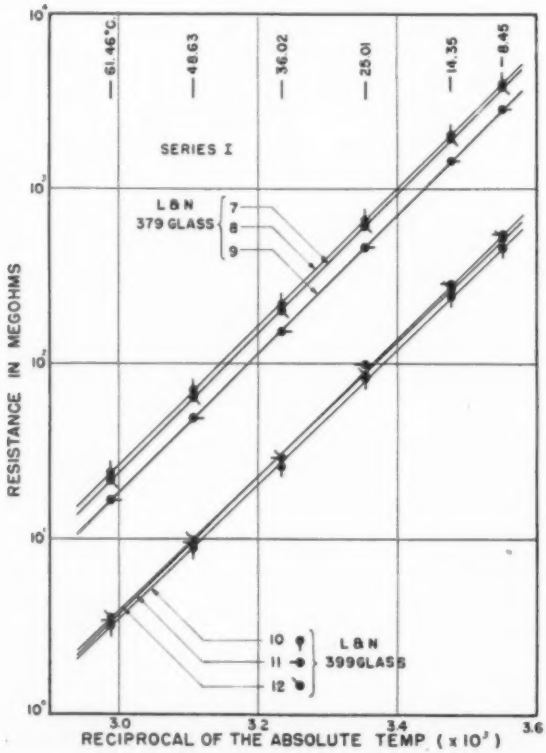

FIG. 7. Data of Series I, electrodes 7 through 12

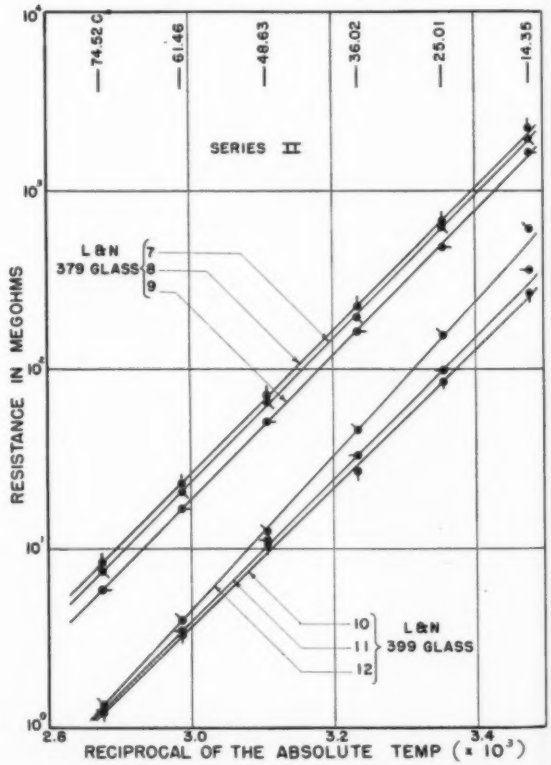

FIG. 9. Data of Series II, electrodes 7 through 12

Series II appears in Fig. 8 and 9. In Fig. 6 the values of resistance for Corning 015 glass are multiplied by one-half to prevent crowding of the two sets of curves, and for the same reason in Fig. 8, the values for L&N 402 glass are multiplied by two. The temperature in degrees centigrade is given for each set of points to aid in interpreting the temperature scale.

Multiple measurements allowed a study of reproducibility. Usually values agreed well, deviations from the average being less than one or two per cent. Occasionally, however, a value deviated as much as ten per cent, for no apparent reason.

In general, the values for a given electrode lie close to the straight line which has been drawn through them. Hence the graphs show that these

TABLE III. *Slope constants of the glasses*

Glass	Electrode No.	Values of B ($\times 10^{-3}$)		Values of Q ($\times 10^{-3}$)	
		Series I*	Series II*	Series I*	Series II*
Corning 015	1	3.7	3.7	16.9	16.9
	2	3.7	3.7	16.9	16.9
	3	3.6	3.7	16.5	16.9
L & N 402	4	4.3	4.6	19.6	21.0
	5	4.2	4.4	19.2	20.1
	6	4.1	4.3	18.7	19.6
L & N 379	7	4.0	4.0	18.3	18.3
	8	4.0	4.0	18.3	18.3
	9	4.0	4.0	18.3	18.3
L & N 399	10	3.8	3.9	17.4	17.8
	11	3.9	4.0	17.8	18.3
	12	3.8	4.3	17.4	19.6

* Series I was performed before protracted heating at 74.52°C; Series II, afterward.

glass electrodes follow the Rasch and Hinrichsen law

$$\log_{10} R_G = A + B/T \qquad \text{(V)}$$

in which R_G is the observed resistance (in megohms), T the absolute temperature, and A and B are constants.

The value of A depends on the particular dimensions of the membrane as well as on the intrinsic character of the glass, and thus this constant does not have basic significance. The value of B, however, representing the slope of the curve, is independent of the membrane dimensions, and is related to the nature of the glass. The larger the value of B, the more rapidly will the resistance change with temperature. Calculated values of B are given in Table III, which also shows, for the sake of comparison, the slope constant expressed as Q's in the same way as the results of Lengyel and Blum (13). Values of B were converted to values of Q by the relationship

$$Q = 2.3\,RB = 4.57\,B \qquad \text{(VI)}$$

in which R is the gas constant in calories per degree per mole.

Fig. 10 is a nomograph constructed to express equation (V). If the resistance of an electrode is known at a particular temperature, this nomograph affords a rapid means of estimating the resistance at any other temperature, or of estimating the temperature at which the resistance will be a specified value. The nomograph is used by placing a straightedge between known values of resistance and temperature,

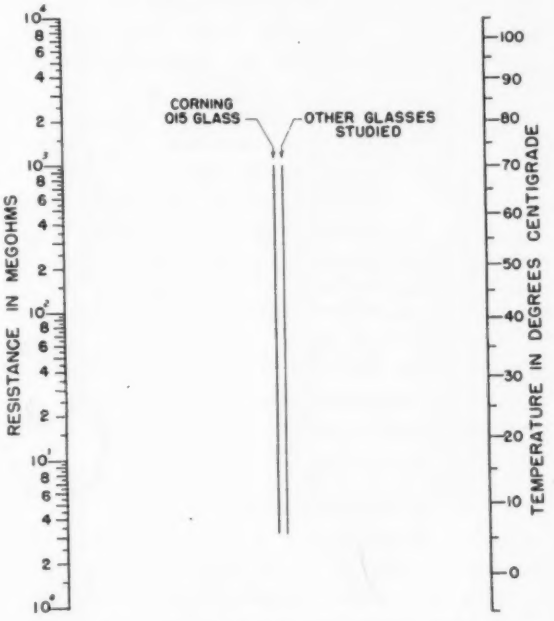

FIG. 10. Nomograph of the temperature-resistance relationship of the glass electrode.

and noting the point of intersection with one of the central vertical lines, depending on the type of glass. This point, when aligned with either a second temperature or resistance, yields the corresponding value of the other variable.

The position of the central pivoting point establishes the values of the constants, A and B; vertical displacement varies A, while horizontal displacement varies B. The value of B for Corning 015 glass was taken as 3700. Values of B in Table III for L&N glasses 399 and 402 are less constant. In Series I, however, the values for L&N glasses 379, 399, and 402 average very close to 4000, which value was used in the nomograph in placing the vertical line for these glasses.

Discussion

During the course of the investigation the feeling gradually developed that highly reproducible values of resistance could not be obtained for glass electrodes despite repeated attempts to refine technique.

Comparison of Series I and II

The differences between Series I and II, observable in Table II, indicate that electrodes tend to increase their resistance when immersed in hot solutions. The 25°C resistances of electrodes 4 and 12 almost doubled in going from Series I to II. Although large changes in the 25°C resistance occurred in only two or three instances, all others showed at least some increase. The effect of heating also tended to increase the slope constant as Table III shows. It is interesting to note that in the two cases of large resistance change the slope constants also underwent the largest changes.

These changes are understandable when it is realized that the glass in the electrodes is in a chilled condition. As a result, the specific resistance is much lower than it would be with annealed glass. Other studies in our laboratory bear out Beckman's (3) observations in this respect, and indicate that by annealing, the resistance of electrodes may be increased by a factor of as much as four or five. The curves of Fig. 1 also show this same effect for plates of borosilicate glass. It is not surprising, therefore, to have found a change caused by the hot solution, the apparent effect of which was to change the glasses partially toward a more annealed condition.

Temperature-Resistance Relationship

The results clearly show that resistance and temperature are related in accordance with equations (II) and (V), the Rasch and Hinrichsen law (20). This is contrary to the results of previous investigations.

The question arises as to how well the constants of this study for Corning 015 glass agree with the published work of Taylor and Kraissl (25) on the resistance of this same glass. Their relationship is that of equation (II) and (V), the constants of which we calculated from their graph to give

$$\log_{10} \rho = -1.62 + \frac{3800}{T} \qquad \text{(VII)}$$

where ρ is the specific resistance and T the absolute temperature. Equation (VII) represents measurements made from about 100° to 400°C, the glass being not in contact with aqueous solutions. This slope constant is 3800, very close to the average value of 3700 found in the present work for Corning 015 glass.

Equation (VII) gives, by extrapolation, a specific resistance for 015 glass of about 1.3×10^{11} ohm-cm at 25°C. A rough approximation of the specific resistance of the 015 electrodes can be made as follows. Their average measured resistance is about 2×10^8 ohms at 25°C. If this is multiplied by 200 cm (the approximate factor previously mentioned) the result is 4×10^{10} ohm-cm for the specific resistance. But since the electrodes are in a chilled condition, this figure may not be compared directly with the extrapolated value at 25°C. If allowance is made for the chilled condition by multiplying, say, by a factor of four or five (the approximate correction for the chilled condition previously mentioned) there is remarkably good agreement.

Kahler and DeEds (11) obtained a specific resistance of 3.6×10^{10} ohm-cm at 22.3°C for electrodes of 015 composition. It is assumed that this is for the chilled condition, and this figure agrees fairly well with the corresponding value of the present study, 4×10^{10} ohm-cm at 25°C.

The slope constants as Q's in Table III fall nicely within the range of values found by Lengyel and Blum (13) for their glasses. Their values range from 16,200 to 23,000, while the present ones range from 16,500 to 21,000.

The nomograph of Fig. 10 can be used to obtain precise values for Corning 015 and L&N 379 glasses. With the other two glasses, however, some uncertainty will exist because of the inherent changeability of the slope. Nevertheless a fair approximation should result if the right-hand line is used for these glasses.

It is interesting to check the nomograph against published values for 015 glass electrodes. The results of Kahler and DeEds (11) for one electrode, 1200 megohms at 5°C and 12 megohms at 55°C, agree exceptionally well. The measurements of Corzo (5) also agree. His data show, incidentally, that the resistance and implicit slope values tend to increase slightly with heating (or standing), as in the present study.

If the logarithm of the resistance is plotted against the temperature using the present data, following the previously accepted practice of equation (I), the points lie on lines having definite curvature. This is suggested in two of the sources (2, 22) which note that their slope constants tend to decrease slightly with increasing temperature. Thus it is believed that this way of expressing the temperature-resistance relationship may be only approximately valid for pH glasses, being useful only over a restricted temperature range.

Stevels (23) discusses the effect of temperature on the electrical conductivity of glass. He attempts to explain why some glasses follow a simple logarithmic

relationship with temperature, while others follow the Rasch and Hinrichsen law. In his picture, "abnormal glasses" are characterized by a relatively open structure of the silicon-oxygen network, and the conducting ions are able to jump rather unhindered, thus causing the glass to follow the Rasch and Hinrichsen law. The desirability of low resistance in a pH glass automatically operates to favor a glass of such character. From this it would appear that glasses suitable for pH work are of the "abnormal" type, and would thus follow the Rasch and Hinrichsen law.

Conclusions

Possible complications in measuring the electrical resistance of glass electrodes include extraneous counterelectromotive forces and dielectric phenomena. The weight of evidence indicates that extraneous counterelectromotive forces are inconsequential and may be ignored. Dielectric phenomena may lead to complications such as the changing nature of the measuring current caused by dielectric absorption (with d.c.), and the dependence of resistance on the frequency (with a.c.).

The use of d.c. is recommended for evaluating the resistance of the glass electrode. By measuring only the conduction-current component of the glass, the d-c resistance can be obtained using Ohm's law. This appears to be the true ohmic resistance of the glass.

When dielectric absorption is bothersome it is desirable, in measuring the conduction-current component, to employ an adjustable voltage across the glass membrane, thereby avoiding the long waiting time required with a fixed voltage. After a short initial period the voltage is lowered and adjusted to make it agree with the induced condition in the glass corresponding to the slowest absorptive process.

The equations previously used for expressing the temperature-resistance relationship of glass electrodes do not fit the present data. The Rasch and Hinrichsen law is preferred in which the logarithm of the resistance follows a linear relationship with the reciprocal of the absolute temperature. It is convenient to use this relationship in the form of a nomograph as shown in Fig. 10.

The temperature-resistance relationship obtained for Corning 015 glass electrodes immersed in aqueous solutions is identical to that given in the literature for the dry glass from 100° to 400°C, both sets of data following the Rasch and Hinrichsen law. Moreover, the respective constants are in agreement. From this it may be inferred that the fundamental process of conduction is not dissimilar in the two cases.

Acknowledgments

The authors wish to express appreciation to their colleagues, especially to Dr. W. G. Amey, Mr. R. H. Cherry, and Dr. P. H. Dike, for their many helpful suggestions and acts of assistance during the course of this study.

Any discussion of this paper will appear in a Discussion Section, to be published in the December 1951 issue of the Journal.

References

1. "American Standard Definitions of Electrical Terms," p. 32, American Institute of Electrical Engineers, New York (1941).
2. A. H. W. Aten, Louise Boerlage, and J. E. Garsen, *Chem. Weekblad*, **37**, 158 (1940).
3. A. O. Beckman, as quoted by Malcolm Dole, "The Glass Electrode," John Wiley & Sons, Inc., p. 152, New York (1941).
4. R. H. Cherry, *Trans. Electrochem. Soc.*, **72**, 33 (1937).
5. R. H. Corzo, "The Change of the Asymmetry Potential and Resistance of the Glass Electrode with the Temperature," Thesis, Northwestern University (June 1940).
6. Malcolm Dole, "The Glass Electrode," John Wiley & Sons, Inc., p. 66, New York, (1941).
7. *Ibid.*, p. 71.
8. L. W. Elder, Jr., *J. Am. Chem. Soc.*, **51**, 3266 (1929).
9. E. M. Guyer, *J. Am. Ceram. Soc.*, **16**, 607 (1933).
10. E. M. Guyer, as quoted by George W. Morey, "The Properties of Glass," Reinhold Publishing Corp., p. 475, New York (1938).
11. H. Kahler, and Floyd DeEds, *J. Am. Chem. Soc.*, **53**, 2998 (1931).
12. Ludwig Kratz, *Z. Elektrochem.*, **49**, 474 (1943).
13. B. Lengyel and E. Blum, *Trans. Faraday Soc.*, **30**, 461 (1934).
14. J. T. Littleton and G. W. Morey, "The Electrical Properties of Glass," John Wiley & Sons, Inc., New York (1933).
15. Duncan A. MacInnes and Donald Belcher, *J. Am. Chem. Soc.*, **53**, 3315 (1931).
16. D. A. MacInnes and Malcolm Dole, *J. Am. Chem. Soc.*, **52**, 29 (1930).
17. George W. Morey, "The Properties of Glass,' Reinhold Publishing Co., p. 446 and p. 448, New York (1938).
18. George W. Morey, "The Properties of Glass," Reinhold Publishing Co., New York (1938).
19. George A. Perley, *Anal. Chem.*, **21**, 394 (1949).
20. Ewald Rasch and F. Willy Hinrichsen, *Z. Elektrochem.*, **14**, 41 (1908).
21. Denis M. Robinson, *Physics*, **2**, 52 (1932).
22. Hj. Saechtling, H. Richter, and H. C. Rosenthal, *Z. Elektrochem.*, **45**, 79 (1939).
23. J. M. Stevels, "Progress in the Theory of the Physical Properties of Glass," Elsevier Publishing Co., Chap. III, New York (1948).
24. Nelson W. Taylor, *J. Applied Phys.*, **12**, 753 (1941).
25. W. C. Taylor and F. Kraissl, as quoted by Malcolm Dole, "The Glass Electrode," John Wiley & Sons, Inc., p. 152, New York (1941).
26. J. B. Whitehead, "Lectures on Dielectric Theory and Insulation," McGraw-Hill Book Co., Inc., New York (1927).

A Micro Solution-Potential Measuring Technique[1]

L. W. Smith

Cornell Aeronautical Laboratory, Inc., Buffalo, New York

AND

V. J. Pingel

Fansteel Metallurgical Corporation, North Chicago, Illinois

ABSTRACT

A technique for measuring the solution potential of a metal or alloy on a micro scale has been developed. It consists of electrically insulating the polished and etched surface of the metal specimen with a transparent plastic film, puncturing the film over any desired microconstituent with the aid of a specially adapted hardness tester, and then determining the solution potential at the point of puncture. In this manner it is possible to examine an alloy of normal grain size at high magnifications (up to 566 ×) and obtain the solution potential of any desired part of the microstructure.

Introduction

Solution potential measurements have long been a means of predicting the corrosion susceptibility of groups of metals or alloys when exposed to various corrosion mediums. It is possible in this way to determine the feasibility of using two different metals or alloys in close contact under conditions where electrolytic action may take place. However, when an alloy is to be used alone the corrosion susceptibility cannot be conclusively predicted by solution potential measurements of the alloy as a single unit. It then becomes necessary to determine the solution potential of the various microconstituents and grain areas of the alloy. In the course of a project on the stabilization of 24S-type aluminum alloys against intergranular corrosion by element additions, it was deemed necessary to develop a suitable method of studying the internal solution potential characteristics of the various alloy systems. The methods described by Mears and Brown (1) using fine tubulus or moistened fiber and the waxing techniques were not desirable due to the need of growing large sized grains.

The specific potential measuring problem involved is illustrated in the first two figures. Fig. 1 shows a copper-aluminum alloy structure (4.5 Cu, balance Al) that has resulted by air cooling from a solution temperature of 910°F. The white grain boundaries have been copper depleted and thus have a more electronegative solution potential than the adjacent areas. In the presence of an electrolyte this white portion of the grain boundary is anodic to the grain boundary precipitate (black) and the solid solution grain interior. Fig. 2 shows the effect of an electrolyte on such a grain structure when present in a wrought specimen. The attack is intergranular and proceeds along the depleted grain boundary areas. The reports of Rawdon (2), Dix (3), and Mutchler (4), as well as many others, discuss this type of corrosion on the copper-aluminum alloys.

Procedure

The metal specimen is first mounted in Lucite or Bakelite and then polished and etched in the conventional manner. A thin transparent film of plastic coating is then applied with an eye dropper and allowed to dry. Fig. 3 shows a coated specimen ready for examination. It should be noted that the entire specimen is not coated. An uncoated area is left open to facilitate electrical contact.

The specimen is then immersed in the electrolyte and tested for electrical insulation. After electrical insulation has been verified, the specimen is ready for microscopic observation and the selection of the desired area for solution potential measurement. Fig. 4 shows the Tukon Hardness Tester adapted with a special indenter for puncturing the insulating film over the grain area being investigated. Very light indenter loads are used. These range from 45 grams to 100 grams. The tip of the indenter is ground to the shape of a truncated cone. Fig. 5 shows the shape of the indention when made directly on a metal specimen without the plastic film.

After the small puncture has been made through the plastic film, it is again ready to be submerged in the electrolyte with the small punctured area below the surface of the liquid. The solution potential of the small area at the point of puncture is then determined with the potentiometer. Fig. 6 and 7 are photomicrographs of an indention taken through the plastic coating before and after the solution

[1] Manuscript received August 2, 1950. This paper prepared for delivery before the Chicago Meeting, October 12 to 15, 1949.

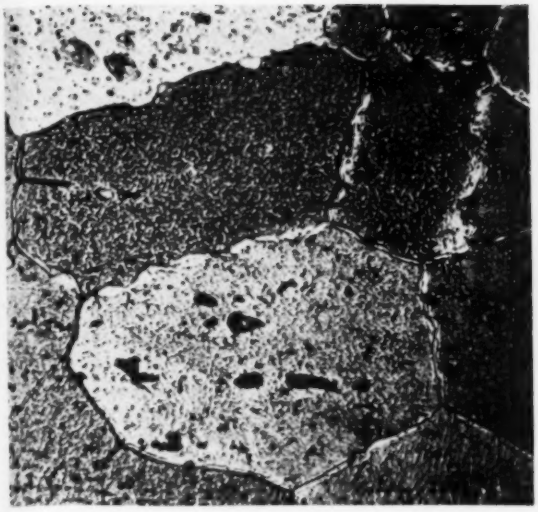

FIG. 1. Grain structure of cast aluminum alloy (4.5 Cu, balance Al). Air cooled from 910° F. Heavy Keller's etch. The white grain boundaries have been depleted of copper. Original magnification was 750; the print has been reduced to half size.

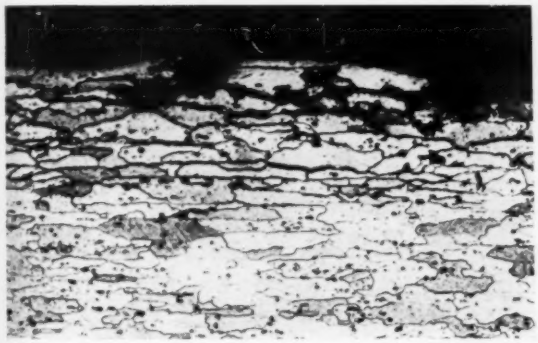

FIG. 2. Grain structure of wrought aluminum alloy (4.5 Cu, balance Al). Air cooled from 910° F. Six-hour exposure to standard intergranular salt and peroxide corrosion solution. Light Keller's etch. The attack is along the depleted grain boundaries. Original magnification was 100; the print has been reduced to half size.

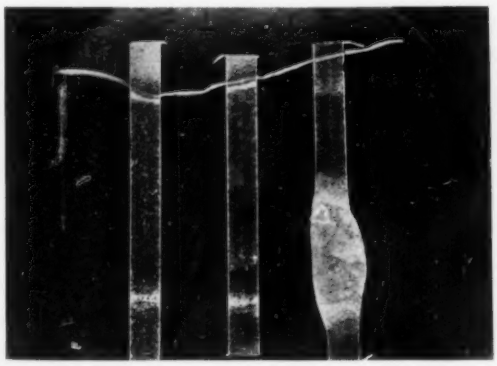

FIG. 3. Plastic coated metallurgical mount. All surfaces are electrically insulated except the small area at top which allows contact with the electrode holder. 3×.

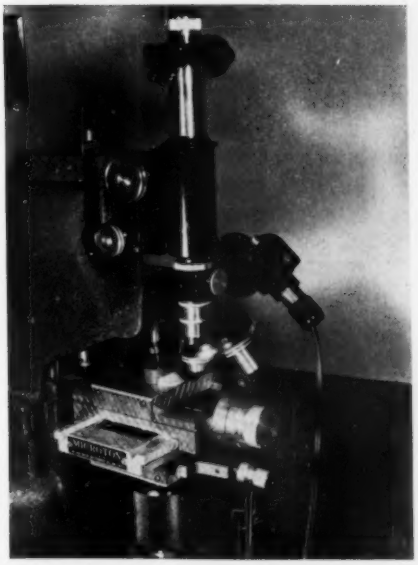

FIG. 4. Specimen under special indenter mounted in standard Tukon Hardness Tester making small puncture through the electrically insulating plastic film.

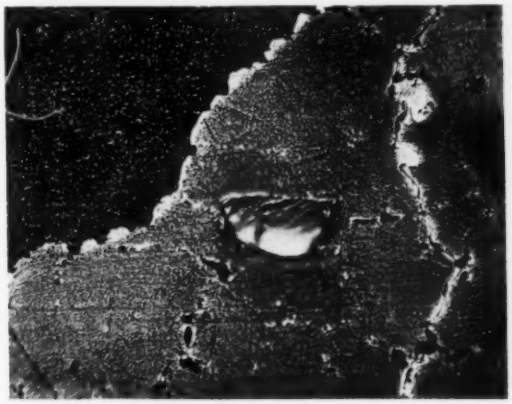

FIG. 5. Photomicrograph of 4.5% Cu-95.5% Al alloy air-cooled from 1018° F showing depleted zones and shape of indenture when made on uncoated specimen. Indenture is approximately 0.0013 in. across the long diameter. Keller's etch. 500×.

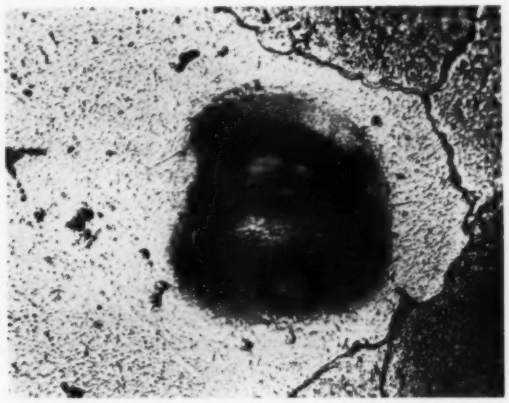

FIG. 6. Photomicrograph taken through the plastic coating showing indenture in center of grain before specimen was immersed in electrolyte for solution potential measurement. Keller's etch. 500×.

potential was measured. It may be seen that the area over which the potential was taken has been confined to the center of the grain.

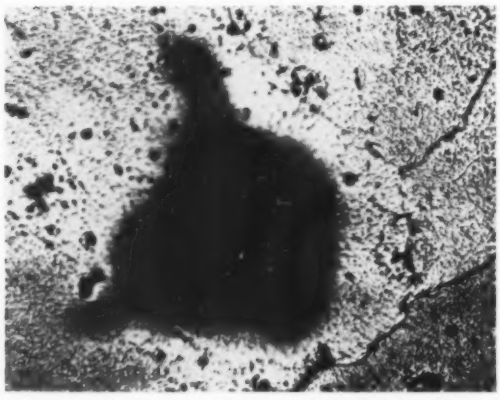

FIG. 7. Photomicrograph of same area as Fig. 6 after specimen was immersed in the electrolyte and tested for solution potential. Note that electrolyte has not undercut the plastic film as shown by the location of the corrosion products. Keller's etch. 500×.

DISCUSSION

The transparent plastic coating now being used is ethyl cellulose dissolved in various solvents which control the drying time to approximately five minutes. Lucite mounts have been found best suited for the technique. Bakelite mounts are not satisfactory because of the inability to get the plastic coating to bond well with the Bakelite. Several different solvents and combinations of solvents have been tried with the desired effects being the least amount of stress cracking of the Lucite mount, the least amount of wrinkling of the coating, and short time room temperature drying. Ether, alcohol, ethyl acetate, butyl acetate, and amyl acetate have been somewhat satisfactory. A plastic coating solution containing by weight 9 per cent ethyl cellulose, 18 per cent petroleum naptha, 55 per cent toluol, and 18 per cent ethyl alcohol has been found most satisfactory.

Several types and shapes of indenters have been investigated including the standard Tukon and Vickers indenters. A sharpened phonograph needle with the tip having the shape of a truncated cone has proved the most satisfactory.

The electrolyte used in these solution potential studies consists of a 1*N* solution of NaCl containing 0.3 per cent of H_2O_2. Approximately 5 drops of a solution of 5 per cent aerosol are added per 100 cm³ of the electrolyte as a wetting agent. It has been found that the addition of aerosol does not appreciably, if at all, affect the solution potential measurements except to facilitate the entrance of the electrolyte into the small indention. It has also been found that etching the specimen, to make the selection of the desired indention location possible, has no effect on the resultant solution potential because of the fresh cut made by the indenter. The possibility of the indenter causing cold working of the metal has not been thoroughly investigated. Indications are that it does not affect the solution potential values.

RESULTS

Investigations carried out in developing this micro solution-potential measuring technique have shown the values obtained to be accurate and reliable. The solution potential value obtained when the entire specimen of a precipitation hardening alloy such as the Cu-Al alloys is used will be that of the most anodic constituent or grain area. Using this fact it is possible to predict the relative corrosion properties of a group of similar Cu-Al alloys by comparing solution potential values taken in the center of the grains with those taken across the grain boundary so that at least a portion of indenter is in a depleted zone. Values obtained in this manner for cast specimens homogenized at 1018°F and air cooled in order to obtain depleted grain boundaries and susceptibility to intergranular corrosion are as follows:

2S Aluminum Control Specimen	
Entire specimen	−0.83 volt
Through indention in plastic coating	−0.83 volt
Heat 13, 4.5% Cu, 95.5% Al	
Entire specimen	−0.75 volt
Depleted grain boundary area	−0.74 volt
Center of grain	−0.68 volt
Heat 30, 4.5% Cu, 94.5% Al, 1.0% In	
Entire specimen	−0.97 volt
Depleted grain boundary area	−0.97 volt
Center of grain	−0.79 volt
Heat 36, 4.5% Cu, 94.5% Al, 1.0% Cr	
Entire specimen	−0.72 volt
Depleted grain boundary area	−0.71 volt
Center of grain	−0.66 volt

Other experiments were run on weld specimens and standard aluminum alloys with satisfactory results. With further improvements in the transparent coating and with an improved cutting and smaller indenter, it should be possible to use this method for determining micro solution-potential values not only for aluminum alloys but also for stainless steels and for other metallurgical problems.

Any discussion of this paper will appear in a Discussion Section, to be published in the December 1951 issue of the JOURNAL.

REFERENCES

1. R. B. MEARS AND R. H. BROWN, *Ind. Eng. Chem.*, **33**, 1001 (1941).
2. H. S. RAWDON, *Nat. Advisory Comm. Aeronaut. Tech. Note* 282, 283, 284, 285 (April 1928); 304 (February 1929); 304 (May 1929).
3. E. H. DIX, JR., *Nat. Advisory Comm. Aeronaut. Tech. Note* 259 (August 1927).
4. W. MUTCHLER, *J. Research Nat. Bur. Standards* **25**, 75 (December 1940).

Dichromate Reduction Rate at a Steel Surface in Air-free, Acetic Acid Solution[1]

NORMAN HACKERMAN AND RAY M. HURD

Department of Chemistry, University of Texas, Austin, Texas

ABSTRACT

A system was devised in which aqueous solutions of $K_2Cr_2O_7$ and of acetic acid could be brought in contact with steel coupons in the absence of air. The rate of reduction of the dichromate was determined as a function of time by titration and spectrophotometrically. Changes in pH were also followed. Rates were measured with various initial concentrations of dichromate and of acetic acid and for several areas of steel surface. The effects of temperature, presence of NaCl, presence of oxygen, and order of addition of the solutions were studied. There was measurable loss of dichromate in all cases except those in which air was deliberately added. In general, the rate curves became level before all of the dichromate was reduced, with the maximum loss about 60 per cent. It was concluded that dichromate at 400 ppm was a fairly effective inhibitor to the corrosion of steel down to pH 3.0 in the absence of oxygen even with 1000 ppm NaCl present. A mechanism for the reaction and of the corrosion inhibition is proposed.

INTRODUCTION

Despite the extensive use of chromates and dichromates to inhibit corrosion, the nature of the protection afforded by these chemicals has not yet been established to the satisfaction of all investigators. It is most widely accepted that the metal surface becomes separated from the corrosive medium by formation of a tightly adhering film of hydrated metallic oxides. However, there appears to be an additional effect, most apparent on initial contact between metal and chromate. For example, in 0.01*N* $K_2Cr_2O_7$ the electrode potential of iron becomes more electropositive by 0.24 volt in an hour and then remains constant at this value (1). Other such instances have been reported and form the basis for a postulate to the effect that chromate passivates by making the surface more noble. It has been pointed out (2), however, that corrosion might occur in spite of such an indication of passivity and, as a matter of fact, the validity of the potential-time method as a means of indicating passivity has been questioned.

Even though the metal may not be rendered passive by the chromate, in most cases the surface is soon covered with a film which consists mainly of ferric oxide and small amounts of chromic oxide, according to Hoar and Evans (3). Evans (4) attributes the inhibitive power of chromates to the production of just such a film in physical contact with the surface. This is said to occur by interaction of chromate with the ferrous ions formed at a discontinuity in the original air-oxide film, the new film then sealing off the discontinuity. Such a mechanism, drawn directly from the chemistry of the system, is generally substantiated by Darrin in his papers on corrosion control with chromate (5).

Most of the work with chromates has been in either neutral or slightly alkaline solutions. In fact, if the inhibitive action is due to the formation of a mixed Fe_2O_3—Cr_2O_3 protective coating, then, as is indicated by Evans (4), chromates would be ineffective in acid solutions, since the film would dissolve. However, the addition of chromates to a number of originally highly corrosive gas condensate wells has been found to afford good protection from corrosion (6), even though the pH of the aqueous fluid was estimated to be 3.5–4.5 and the system was anaerobic. The loss in weight of steel coupons exposed to these gas well streams has already been investigated (7), but consumption of chromate could not be measured accurately in the field. Also there is not much published material concerning the rate of chromate loss due to steel in air-free acidic systems. Since the concentration of oxygen might be the rate-determining factor and mask the kinetics of the chromate-steel reaction, it was considered desirable to carry out the experimental work under anaerobic conditions.

EXPERIMENTAL

An apparatus was constructed which would insure the complete absence of oxygen from the system and at the same time provide for the introduction and withdrawal of the solutions, for flow of nitrogen, and for stirring. A diagram of this apparatus is shown in Fig. 1. Some of the precautions which were taken to exclude oxygen from the system are as follows: glass seals were made throughout the nitrogen and

[1] Manuscript received July 28, 1950. This paper prepared for delivery before the Buffalo Meeting, October 11 to 13, 1950.

solution lines; a mercury seal stirrer was used; the reaction chamber was sealed to a Bakelite top with a rubber gasket; and the entire chamber was immersed in a water bath.

Tank nitrogen was freed of residual oxygen by passing it through two solutions of acidified vanadyl sulfate, after a process described by Meites and Meites (8). All lines leading to and from the reaction chamber were thoroughly flushed with a stream of this purified nitrogen before each run. The potassium chromate and acetic acid solutions were prepared from distilled water which had been boiled and stored under an atmosphere of nitrogen. After the solutions had been made up, they were again saturated with nitrogen and stored in the water bath to bring them to the reaction temperature. Finally,

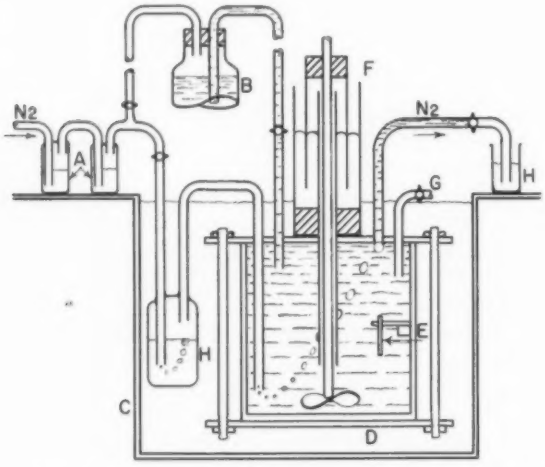

FIG. 1. Diagram of the apparatus. A, vanadyl sulfate solutions; B, reaction solution; C, thermostat; D, reaction vessel; E, steel coupons; F, stirrer; G, sample port; H, bubblers containing water.

when the solutions were introduced, they were made to fill the reaction vessel completely, thereby removing any traces of air which may have remained after the nitrogen flushing. During the course of the runs nitrogen was slowly but continuously bubbled through the solutions.

C. P. chemicals were used throughout. The steel surface was supplied in the form of SAE 1020 steel coupons, the surface areas of which were approximately 25 cm^2 per side, or 50 cm^2 per coupon. Preparation of the metal surface consisted of polishing first with 1/0 emery paper, then with 3/0 sandpaper, rinsing with acetone, and drying with tissue. The edges of the coupons were coated with a thin layer of paraffin to avoid possible excessive effects at areas of metal stress.

Procedure

The general experimental procedure is given below, where the letters refer to Fig. 1. The reacting solution was first made up to the desired concentrations of acetic acid and potassium dichromate and stored in the thermostat (C). The coupons were polished and then sealed into the reaction vessel (D), and more water was added to the bath until the top of the jar was covered. Nitrogen was allowed to flow through the system for about ten minutes, during which time the bottle containing the solution was removed from the thermostat and sealed in at (B). By diverting the flow of nitrogen into the bottle (B), the solution was forced over into the reacti vessel. Note that the solution filled the jar complet before it began to flow from the exit nitrogen lin After the solution was transferred, the flow of nitrogen was returned to the reaction vessel. Samples of the solution were removed by simply closing off the exit nitrogen stream and opening the sample port (G), thus forcing some of the solution out of the jar.

Approximately 5-ml samples were withdrawn and analyzed for both hydrogen ion and dichromate concentrations. Hydrogen ion was measured with a Beckman model "M" pH meter, which gave an estimated accuracy of ±0.03 pH unit in the range used. Dichromate concentration was at first determined by a standard titrimetric procedure in which a measured excess of standard ferrous ion was added to the sample, and the excess ferrous ion titrated with standard dichromate. Because of the small sample size, however, this method gave only fair accuracy. In some of the later work the analyses were made with a Beckman model "DU" spectrophotometer, with greatly increased accuracy and reproducibility. The acetic acid in the samples did not absorb at the wavelength used for the analyses (430 mμ), but ferric ion did. This interference was eliminated by adding to each sample a tiny crystal of ammonium bifluoride, which removed the ferric ion by formation of the colorless complex, FeF_6^{---}.

RESULTS

The following set of conditions was chosen to determine the reproducibility of the method, and also to serve as the basic condition for the rest of the work: 450 ppm $Cr_2O_7^{=}$, 1000 ppm $HC_2H_3O_2$, 200 cm^2 of steel surface, 35°C. Using these conditions, two separate runs gave the results plotted in Fig. 2. Although the two curves are not identical, they are nevertheless very similar, especially in the important values of initial slope and time at which the slope changes markedly. It is easily possible that difference in real steel surface area alone, e.g., due to type of finish, could cause this amount of variation (*ca.* 1

part in 100). Thus, it could be assumed that the runs were reproducible within experimental error.

Effect of decreasing dichromate concentration.—Runs were made using initial dichromate concentrations of 450, 400, 300, and 150 ppm. These results appear in Fig. 3, in which the loss of dichromate is plotted against time for each of the initial concentrations. Only one curve is drawn through points for the last two concentrations. Dichromate depletion was, in general, greater for lower initial dichromate concentration. The losses to the point of practical cessation of reaction were 14 per cent, 14 per cent, 30 per cent, and 67 per cent, respectively.

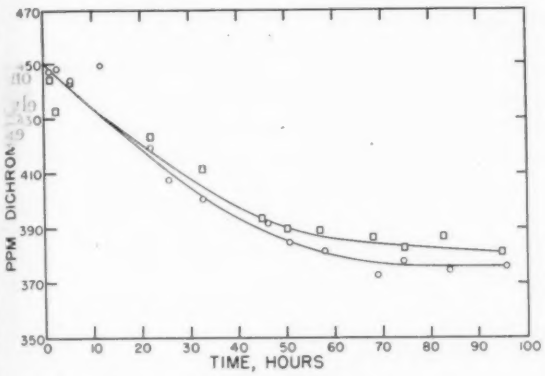

FIG. 2. Reproducibility of the method. □—run 1; ○—run 2. 1000 ppm acetic acid, 200 cm² steel area, 35°C.

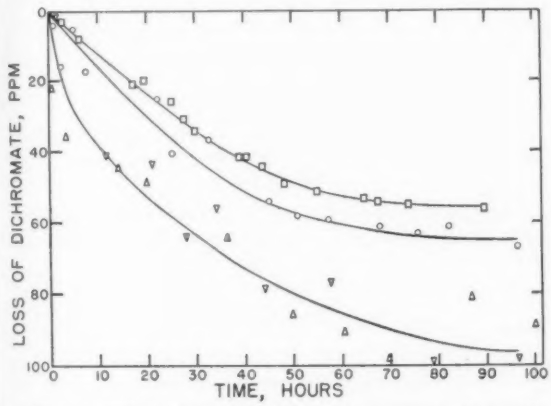

FIG. 3. Effect of initial dichromate concentration with 1000 ppm acetic acid, 200 cm² steel area, 35°C. ▽—150 ppm; △—300 ppm; □—400 ppm; ○—450 ppm.

Effect of increasing acetic acid concentration.—Runs were made using initial acetic acid concentrations of 1000, 2000, 4000, and 8000 ppm which gave pH values of 3.30, 3.19, 3.01, and 2.81, respectively. As expected, increasing acid concentrations accelerated the consumption of dichromate, except that the intermediate values of 2000 and 4000 ppm gave curves which did not deviate from each other by more than 7 or 8 ppm. The curves for 1000, 2000, and 8000 ppm are shown in Fig. 4. Leveling off of the effect of acid concentration at these two values, followed by sharp increase in consumption at 8000 ppm, is ascribed to an interaction of the ferric and acetate ions to form the ferric acetate complex. This complex was obviously present at the end of the reaction involving the 8000 ppm acid, as shown by the deep red color of the solution. The color was not visible at the other acid concentrations.

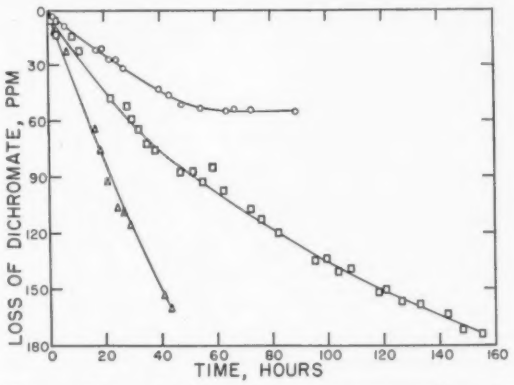

FIG. 4. Effect of initial acetic acid concentration with 400 ppm dichromate, 200 cm² steel area, 35°C. ○—1000 ppm; □—2000 ppm; △—8000 ppm.

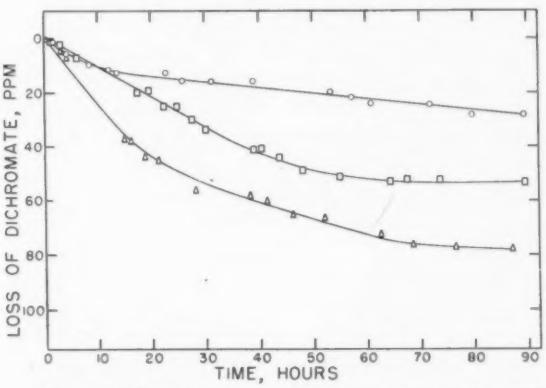

FIG. 5. Effect of steel area with 400 ppm dichromate, 1000 ppm acetic acid, 35°C. ○—100 cm²; □—200 cm²; △—400 cm².

Effect of varying the steel surface area.—Runs were made with steel surface areas of 100, 200, and 400 cm². As shown in Fig. 5, increasing the surface area increased the consumption of dichromate markedly, but the ratio of consumption values was closer to 1:3:4 than to the 1:2:4 value to be expected from a linear effect. As pointed out previously, the degree of finish on different coupons could cause the actual surface area of each coupon to vary considerably from run to run, so that this inexact relationship was not unexpected.

Effect of temperature.—The results of an experiment at 55°C are shown in Fig. 6, in which the dashed curve shows the equivalent run made at 35°C. There is a slight increase, about 25 per cent, in the initial rate of dichromate consumption, but the principal difference was in the failure of the curve to level off as it did at 35°C.

Effect of addition of oxygen.—Air was injected into the solution continuously during a run in which all other conditions were those mentioned previously as "basic conditions." The flow of air was maintained

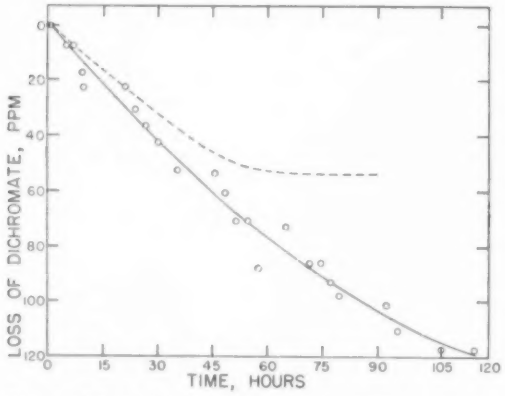

FIG. 6. Effect of temperature with 400 ppm dichromate 1000 ppm acetic acid, 200 cm² steel area. ----35°C; -○-55°C

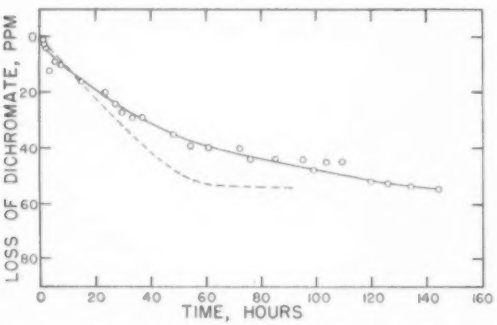

FIG. 7. Effect of the presence of NaCl with 400 ppm dichromate, 1000 ppm acetic acid, 200 cm² steel area, 35°C With 1000 ppm NaCl -○-, without NaCl ------.

at about 15 ml per minute. After 36 hours under these conditions there was no measurable change either in dichromate concentration or pH and the coupons, when removed, exhibited the same polished surface they possessed originally. At the end of experiments, in which air was excluded, the coupons were covered with a dark, reddish-black film, and exhibited some evidences of pitting, although attack was not severe in any case. Thus, the dichromate in conjunction with air, more specifically oxygen, served to inhibit the acid attack entirely. This mechanism was not investigated but the effect may be attributable to (*a*) still higher film pH (see below) than in the absence of oxygen, (*b*) oxide film repair, or (*c*) oxygen adsorption effects.

Effect of addition of NaCl.—Starting with the same basic set of conditions, the reaction solution was made up to 1000 ppm in NaCl also. According to Fig. 7 there was little effect from the presence of NaCl in this concentration except for a slight decrease in the rate of consumption of dichromate.

Effect of order of addition.—In this experiment a run was started with 4 steel coupons in a 1000 ppm acetic acid solution, but with no dichromate present. After 2 minutes, a solution containing both dichromate and acetic acid was added to the original solution, yielding a final solution containing 1000 ppm acetic acid and 450 ppm dichromate. This procedure prevented the dichromate ions from inhibiting the

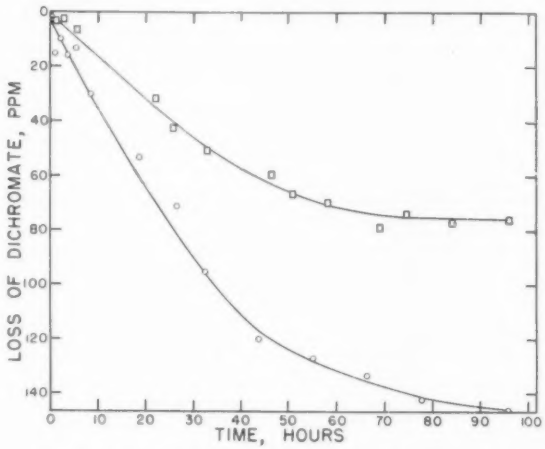

Fig. 8. Effect of delayed addition of dichromate solution with 400 ppm dichromate, 1000 ppm acetic acid, 200 cm² steel area, 35°C. □—simultaneous; ○—delayed.

surface before the acid attack could start. The results of this experiment are shown in Fig. 8, in which the top curve represents an experiment similar in all respects except for simultaneous addition of acid and dichromate. It is notable that the rate of dichromate consumption was about twice as great throughout for the delayed addition. Furthermore the loss of dichromate continued, although more slowly, in the latter stages of this run, whereas the slope became essentially zero for the experiments with simultaneous addition.

pH Changes.—An interesting effect was noted in that the pH of the solutions apparently increased discontinuously with time of reaction. This is shown in Fig. 9 for four of the experiments already discussed. The points on these curves are only half as large vertically as they should be, according to the precision of the pH measurements, in order to reduce

congestion. However, even with the points full scale the plateaus are evident. Close study of the dichromate reduction rate curves reveals that similar plateaus appear to exist. The data are not accurate enough to draw the curves in that manner, but the nature of these curves indicates a similar phenomenon might appear in the other rate curves.

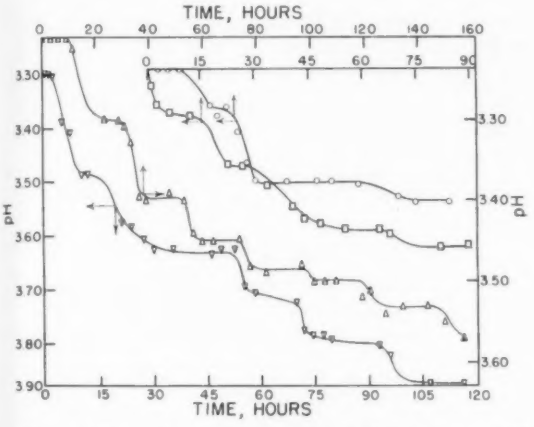

FIG. 9. Change in pH of reacting solution with time, 200 cm² steel area.

○—450 ppm dichromate; 1000 ppm acetic acid, 35°C
□—400 ppm dichromate; 1000 ppm acetic acid, 35°C
△—400 ppm dichromate; 2000 ppm acetic acid, 35°C
▽—400 ppm dichromate; 1000 ppm acetic acid, 55°C

DISCUSSION

One of the ways in which chromates retard corrosion is by the formation of films of mixed ferric and chromic hydroxides which act as a mechanical barrier between the metal and its environment. If the environment is acidic, such films should be sufficiently soluble so that their formation might be considered improbable. At pH 3.0 about 56 mg of ferric iron per liter must be present in order for ferric hydroxide to precipitate. In these experiments the steel coupons were the only source of iron-III ion, and in order to fulfill the concentration requirement indicated above, the attack on the metal would have had to be much more severe than it actually was. The solubility product of chromic hydroxide is slightly larger (10^{-33} vs. 10^{-36}) and a correspondingly larger amount of chromium-III ion could be tolerated in solution prior to precipitation.

The protection eventually achieved in all of the systems studied, and the small actual loss of iron, can be accounted for by postulating that the pH of the fluid adjacent to the steel surface was greater than that of the main bulk of the solution. Such a pH differential has been mentioned before (9) and can be readily explained by the chemistry of the system as described below.

Reaction between hydrogen ion and iron takes place first, thus

$$Fe\ (metal) + 2H^+ \rightarrow Fe^{++} + H_2\ (gas).$$

In the presence of dichromate in acid solution the iron-II ions are converted rapidly and quantitatively to iron-III ions,

$$6Fe^{++} + Cr_2O_7^{--} + 14H^+ \rightarrow 6Fe^{+++} + 2Cr^{+++} + 7H_2O.$$

Thus in the dissolution and oxidation of 6 atoms of iron to ferric ion the solution lost 26 hydrogen ions. There exists a layer of liquid next to the metal which is not in motion relative to the surface in spite of solution agitation, and it is this layer which furnishes the hydrogen ions for these reactions. The reactions take place much more rapidly than hydrogen ion can diffuse from the solution bulk and consequently the pH of the film adjacent to the metal surface rises. The acidity in this layer can decrease to the point at which both ferric ion and chromic ion precipitate onto the metal surface as hydroxides. Hydrogen ions may continue to diffuse into this region but it is now "buffered" by the presence of the insoluble hydroxide, which dissolves to some extent. Provided the solid film is reduced in thickness sufficiently, more iron can dissolve and the process repeats, but the hydroxide film grows slightly thicker with each cycle. Eventually a point is reached at which hydrogen ion is essentially unable to reach the steel surface and the reaction comes to a virtual standstill. It is likely that the first dichromate ions which actually reach the steel surface bring about a more fundamental change, e.g., passivation by virtue of electronic displacement, but the mechanism described here is suggested as a reasonable description of subsequent changes.

The best proof of the postulated mechanism would certainly be an actual measurement of the pH in the liquid film immediately adjacent to the steel. This was not feasible, but the results described here can be shown to support the postulate.

The steady decrease of dichromate concentration with time, down to virtually constant values, is indicative of the fact that the source of iron ions is eventually blocked off. This is substantiated by the consistent variation of dichromate consumption rate with varying initial concentration and the greater percentage loss at the lower concentrations. Since the rate of dichromate consumption was much faster when it was not added simultaneously with the acid solution (Fig. 8), it is probable that ferrous ions were not converted to ferric ions immediately after release from the steel (dichromate concentration at surface must build up by diffusion, also), but migrated outward into the body of the solution before reaction

took place. These ions then had no chance to precipitate onto the surface. Apparently, the region of reaction was eventually displaced toward the steel surface, but more chromate was reduced and a longer time was necessary before reaction ceased. The marked increase in reduction rate with the more acidic solutions (Fig. 4) may mean that the film pH was maintained more nearly equal to solution pH because of the increased diffusion rate of H^+. The reduction rate increase of only 25 per cent for a 20°C rise (Fig. 6) is also strong evidence for a diffusion controlled rate.

The stepwise changes in pH with time (Fig. 9) fit the proposed mechanism of alternate decrease in acidity with buffering by the solid hydroxide on the metal surface. As a matter of fact, if the curves in the other figures are drawn through each point, similar plateaus become apparent. Such periods, during which dichromate was presumably not being consumed, should correspond to the periods of constant pH. Unfortunately, this effect was not anticipated and there are not enough experimental points to state categorically that it is real.

The effect of steel surface area seems to be simply one of increasing the ferrous ion available for reducing the dichromate. Finally, NaCl had little effect on the reduction rate, probably because the acid solution supplies corroding agent at a rate in excess of that which controls the over-all reduction process. Hence the salt would have little effect except to cause the appearance of a few more ferrous ions.

Summary

1. Apparatus and method were described for determining the rate of reduction of dichromate ion in an air-free, acetic acid solution in which steel is corroding.

2. The effects of dichromate concentration, acid concentration, temperature, steel surface area, and order of addition of the chemicals, and presence of NaCl were studied.

3. It was shown that dichromate can be an effective corrosion inhibitor in these systems since the reduction rate eventually becomes negligible, indicating a cessation of $Fe \rightarrow Fe^{++}$ reaction.

4. A mechanism was presented based on high pH in the liquid film adjacent to the metal and control of the reaction rate by diffusion processes.

Any discussion of this paper will appear in a Discussion Section, to be published in the December 1951 issue of the Journal.

References

1. "Corrosion Handbook," H. H. Uhlig, Editor, p. 981, John Wiley & Sons, Inc., New York (1948).
2. R. B. Mears, *J. (and Trans.) Electrochem. Soc.*, **95**, 1 (1949).
3. T. P. Hoar and U. R. Evans, *J. Chem. Soc.*, **135**, 2476 (1932).
4. U. R. Evans, "Metallic Corrosion, Protection, and Passivity," 2nd Ed., pp. 26, 542, E. Arnold and Co., London (1946).
5. M. Darrin, *Ind. Eng. Chem. Anal. Ed.*, **13**, 755 (1941); *Ind. Eng. Chem.*, **37**, 741 (1945); *ibid.*, **38**, 368 (1946); Bulletins No. 33 and 34, Mutual Chemical Company of America, Baltimore, Md.; Paper presented at 31st Spring Meeting of the American Society of Refrigerating Engineers, Pittsburgh, Pa., June 5, 1944.
6. W. D. Yale, *Corrosion*, **2**, 85 (1946).
7. H. Schmidt, Ph.D. Dissertation, The University of Texas (1947).
8. L. Meites and T. Meites, *Anal. Chem.*, **20**, 984 (1948).
9. U. R. Evans, Foreword to paper by W. G. Palmer, *J. Iron Steel Inst.*, **1949**, 421.

Potential-pH Diagram of Lead and its Applications to the Study of Lead Corrosion and to the Lead Storage Battery[1]

PAUL DELAHAY

Louisiana State University, Baton Rouge, Louisiana

MARCEL POURBAIX

University of Brussels, Brussels, Belgium

AND

PIERRE VAN RYSSELBERGHE

University of Oregon, Eugene, Oregon

ABSTRACT

The reactions and equilibrium equations of the system lead-water are given in detail and are used in the construction of the potential-pH diagram of lead. Some important features of the diagram are discussed, in particular the solubilities of oxides and hydroxides and some of the important oxidation reduction reactions. A modified form of the potential-pH diagram of lead showing corrosion, passivity, and passivation domains is presented. The addition of passivation domains due to the presence of carbon dioxide and carbonates are determined. A modified potential-pH diagram taking into account the presence of sulfate in solution is also presented. Important features of the behavior of lead storage batteries are studied on the basis of this modified diagram.

The construction of potential-pH diagrams for the various elements has been previously discussed (1, 2, 3) and diagrams for iron, copper, chromium, and nitrogen have been presented. A particularly interesting and important case is that of lead which is discussed in the present paper. Applications of potential-pH diagrams in the study of the corrosion of lead and in the analysis of the behavior of lead storage batteries are also presented.

CONSTRUCTION OF THE POTENTIAL-pH DIAGRAM ITS USE IN THE INTERPRETATION OF ELECTROCHEMICAL PROPERTIES OF LEAD AND LEAD COMPOUNDS

THERMODYNAMIC FORMULAS

Since the theory of potential-pH diagram has been discussed elsewhere (1, 2, 3) we shall only present a short discussion of the thermodynamic formula applied in the construction of a potential-pH diagram.

The potential E corresponding to the equilibrium

$$x\ \mathrm{Ox} + mH^+ + ne^- = y\ \mathrm{Red} + z\ \mathrm{H_2O} \qquad \text{(I)}$$

is calculated by the following formula

$$E = \frac{x\Delta F^\circ_{\mathrm{Ox}} - y\Delta F^\circ_{\mathrm{Red}} - z\Delta F^\circ_{\mathrm{H_2O}}}{23{,}070n} - 0.0591\frac{m}{n}\,\mathrm{pH} + \frac{0.0591}{n}\log\frac{a^x_{\mathrm{Ox}}}{a^y_{\mathrm{Red}}} \qquad \text{(II)}$$

in which ΔF° are the standard free energies of formation of the reactants in calories and a the activities of the reactants. Formula II is valid for a temperature of 25°C.

The equilibrium constant K for the reaction

$$p\ A + m\ \mathrm{H^+} = q\ B + z\ \mathrm{H_2O} \qquad \text{(III)}$$

is calculated by the following formula

$$\log K \frac{p\Delta F^\circ_A - q\Delta F^\circ_B - z\Delta F^\circ_{\mathrm{H_2O}}}{2.3RT} \qquad \text{(IV)}$$

in which $2.3\ RT = 1363$ calories at 25°C. When A is a hydroxide and B the corresponding cation the activity of ion B is calculated by formula

$$\log a_B = \frac{1}{q}\frac{p\Delta F^\circ_A - q\Delta F^\circ_B - z\Delta F^\circ_{\mathrm{H_2O}}}{1363} - \frac{z}{p}\,\mathrm{pH} \qquad \text{(V)}$$

STANDARD FREE ENERGIES OF FORMATION

All standard free energies have been obtained from Latimer's book (4) except for the following cases.

The free energy of the PbO_3^{--} ion has been calculated on the basis of the value $E^\circ = 0.300$ volt given

[1] Manuscript received March 6, 1950. This paper prepared for delivery before the Buffalo Meeting, October 11 to 13, 1950.

by Glasstone (5) for the standard potential of the reaction

$PbO_3^{--} + 2H_2O + 2e^- = HPbO_2^- + 3OH^-$

which leads to −66,339 cal for this free energy of formation.

The free energies of PbO, Pb_3O_4, and PbO_2 have been recalculated from the data of Andrews and Brown (6) and of Spencer and Mote (7) by changing from −56,560 to −56,690 cal the free energy of water. The following values were used in our calculations: $\Delta F^\circ = -45{,}230$ cal for PbO, $\Delta F^\circ = -142{,}730$ cal for Pb_3O_4, and $\Delta F^\circ = -50{,}860$ cal for PbO_2.

The free energy −192,532 cal of $PbSO_4$ has been calculated on the basis of Latimer's value (4), −0.3563 volt for the standard potential of the reaction

$$PbSO_4 + 2e^- = Pb + SO_4^{--}$$

Equilibrium Equations

Equilibrium equations have been calculated by application of formulas I to V as follows

For Water

(*a*) $2H^+ + 2e^- = H_2$

$$E = -0.0591 \text{ pH} - 0.0295 \log P_{H_2}$$

(*b*) $O_2 + 4H^+ + 4e^- = 2H_2O$

$$E = 1.229 - 0.0591 \text{ pH} + 0.0148 \log P_{O_2}$$

For Lead and Its Compounds

A. Homogeneous Reactions

Without oxidation

(1) $HPbO_2^- + 3H^+ = Pb^{++} + 2H_2O$

$$\log \frac{a_{HPbO_2^-}}{a_{Pb^{++}}} = -28.17 + 3.00 \text{ pH}$$

(2) $PbO_3^{--} + 6H^+ = Pb^{+4} + 3H_2O$

$$\log \frac{a_{PbO_3^{--}}}{a_{Pb^{+4}}} = -23.13 + 6.00 \text{ pH}$$

With oxidation

(3) $Pb^{+4} + 2e^- = Pb^{++}$

$$E = 1.691 + 0.0295 \log \frac{a_{Pb^{4+}}}{a_{Pb^{++}}}$$

(4) $PbO_3^{--} + 6H^+ + 2e^- = Pb^{++} + 3H_2O$

$$E = 2.375 - 0.1773 \text{ pH} + 0.0295 \log \frac{a_{PbO_3^{--}}}{a_{Pb^{++}}}$$

(5) $PbO_3^{--} + 3H^+ + 2e^- = HPbO_2^- + H_2O$

$$E = 1.543 - 0.0886 \text{ pH} + 0.0295 \log \frac{a_{PbO_3^{--}}}{a_{HPbO_2^-}}$$

B. Heterogeneous Reactions Involving Two Solids

With oxidation

(6) $Pb(OH)_2 + 2H^+ + 2e^- = Pb + 2H_2O$

$$E = 0.242 - 0.0591 \text{ pH}$$

(7) $PbO_r + 2H^+ + 2e^- = Pb + 2H_2O$

$$E = 0.248 - 0.0591 \text{ pH}$$

(8) $Pb_3O_4 + 2H_2O + 2H^+ + 2e^- = 3Pb(OH)_2$

$$E = 1.101 - 0.0591 \text{ pH}$$

(9) $Pb_3O_4 + 2H^+ + 2e^- = 3PbO_r + H_2O$

$$E = 1.076 - 0.0591 \text{ pH}$$

(10) $PbO_2 + 2H^+ + 2e^- = Pb(OH)_2$

$$E = 1.113 - 0.0591 \text{ pH}$$

(11) $PbO_2 + 2H^+ + 2e^- = PbO_r + H_2O$

$$E = 1.107 - 0.0591 \text{ pH}$$

(12) $3PbO_2 + 4H^+ + 4e^- = Pb_3O_4 + 2H_2O$

$$E = 1.122 - 0.0591 \text{ pH}$$

C. Heterogeneous Reactions Involving One Solid

Without oxidation

(13) $Pb(OH)_2 + 2H^+ = Pb^{++} + 2H_2O$

$$\log a_{Pb^{++}} = 12.46 - 2.00 \text{ pH}$$

(14) $HPbO_2^- + H^+ = Pb(OH)_2$

$$\log a_{HPbO_2^-} = -15.68 + 1.00 \text{ pH}$$

(15) $PbO_r + 2H^+ = Pb + H_2O$

$$\log a_{Pb^{++}} = 12.67 - 2.00 \text{ pH}$$

(16) $HPbO_2^- + H^+ = PbO_r + H_2O$

$$\log a_{HPbO_2^-} = -15.49 + 1.00 \text{ pH}$$

(17) $PbO_2 + 4H^+ = Pb^{+4} + 2H_2O$

$$\log a_{Pb^{+4}} = -7.10 - 4.00 \text{ pH}$$

(18) $PbO_3^{--} + 2H^+ = PbO_2 + H_2O$

$$\log a_{PbO_3^{--}} = -30.24 + 2.00 \text{ pH}$$

With oxidation

(19) $Pb^{++} + 2e^- = Pb$

$$E = -0.126 + 0.0295 \log a_{Pb^{++}}$$

(20) $HPbO_2^- + 3H^+ + 2e^- = Pb + 2H_2O$

$$E = 0.706 - 0.0886 \text{ pH} + 0.0295 \log a_{HPbO_2^-}$$

(21) $PbO_3^{--} + 4H^+ + 2e^- = Pb(OH)_2 + H_2O$

$$E = 2.007 - 0.1182 \text{ pH} + 0.0295 \log a_{PbO_3^{--}}$$

(22) $PbO_3^{--} + 4H^+ + 2e^- = PbO_r + 2H_2O$

$$E = 2.001 - 0.1182 \text{ pH} + 0.0295 \log a_{PbO_3^{--}}$$

(23) $Pb_3O_4 + 8H^+ + 2e^- = 3Pb^{++} + 4H_2O$

$$E = 2.200 - 0.2364 \text{ pH} - 0.0886 \log a_{Pb^{++}}$$

(24) $Pb_3O_4 + 2H_2O + 2e^- = 3HPbO_2^- + H^+$

$$E = -0.297 + 0.0295 \text{ pH} - 0.0886 \log a_{HPbO_2^-}$$

(25) $3PbO_3^{--} + 10\,H^+ + 4e^- = Pb_3O_4 + 5H_2O$

$$E = 2.463 - 0.1477 \text{ pH} + 0.0443 \log a_{PbO_3^{--}}$$

(26) $PbO_2 + 4H^+ + 2e^- = Pb^{++} + 2H_2O$

$$E = 1.482 - 0.1182 \text{ pH} - 0.0295 \log a_{Pb^{++}}$$

(27) $PbO_2 + H^+ + 2e^- = HPbO_2^-$

$$E = 0.649 - 0.0295 \text{ pH} - 0.0295 \log a_{HPbO_2^-}$$

DESCRIPTION OF THE POTENTIAL-pH DIAGRAM OF LEAD

Fig. 1 has been established on the basis of formula (*a*) and (*b*), and (1) to (27) given above. It gives a fairly complete picture of the various thermodynamic equilibria of the system Pb–H_2O at 25°C. For the sake of simplicity the domain of stability of $Pb(OH)_2$, which is slightly larger than that of re

PbO has not been represented. The domain of Pb_2O_3 whose equilibrium properties are insufficiently known is not represented. When one ion is involved in a reaction, the equilibrium condition is represented for values of the activity of this ion equal to 1, 10^{-2}, 10^{-4}, and 10^{-6}. When two ions are involved in a reaction, the equilibrium condition is represented for a ratio of their activities equal to 1.

The domains of predominance of lead and its various derivatives, i.e., ions, oxides, and hydroxides, can be interpreted as follows. Line 19 for example represents the equilibrium between Pb^{++} ion and metallic lead. A point located below line 19 (−6) corresponds to a Pb^{++} activity smaller than 10^{-6} while a point located above 19 (0) corresponds to a Pb^{++} activity larger than 1. Therefore, the domain below line 19 (−6) essentially corresponds to the stability of metallic lead since the equilibrium activity of Pb^{++} ion is smaller than 10^{-6}. Similarly the domain above line 19 (0) corresponds to the stability of Pb^{++} ion.

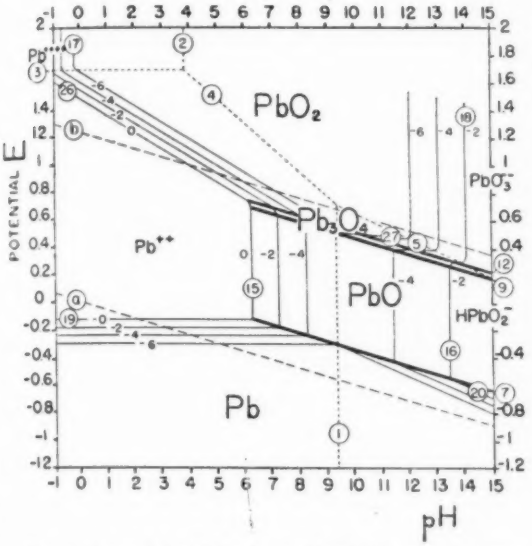

FIG. 1. Potential-pH diagram of lead. The area between lines *a* and *b* corresponds to thermodynamic stability of water. Thin lines represent equilibrium conditions between a solid phase and an ion at activities 1, 10^{-2}, 10^{-4}, 10^{-6}. Heavy lines represent equilibrium conditions between two solid phases. Dotted lines represent equilibrium conditions between two ions for a ratio of activities of these ions equal to unity. In this and subsequent figures circled figures and letters refer to the corresponding equations in the text.

The following domains of predominance are shown in Fig. 1.

Pb: below lines 19, 7, 20.

PbO (also approximately $Pb(OH)_2$): limited by lines 7, 9, 15.

PbO_2: limited by lines 12, 17, 18, 26, 27.

Pb_3O_4: limited by lines 9, 23, 24, 12.

Pb^{++}: limited by lines 3, 15, 19, 23, 26.

Pb^{+4}: limited by lines 3, 17.

$HPbO_2^-$: limited by lines 5, 16, 20, 24, 27.

PbO_3^{--}: limited by lines 5, 18.

Fig. 1 shows, among other things, that metallic lead, usually stable in presence of aqueous solutions free of oxidants, can be dissolved in oxidizing acid solutions with the resulting formation of divalent plumbous ions Pb^{++}. A very strong oxidizing action may transform these Pb^{++} ions directly into the brown tetravalent lead peroxide PbO_2 which is insoluble in neutral or moderately acid solutions, slightly soluble in strongly acid solutions with the resulting formation of plumbic ions Pb^{+4}, and very soluble in strongly alkaline solutions with the resulting formation of plumbate ions PbO_3^{--}.

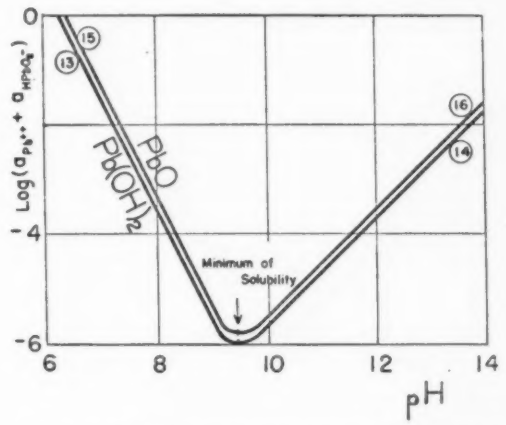

FIG. 2. Solubility of lead oxide and lead hydroxide as a function of pH.

Lead hydroxide $Pb(OH)_2$ and the oxide PbO exhibit a minimum of solubility at pH = 9.4 at which the concentration is $10^{-5.8}$ gram ion per liter or 0.33 mg of lead per liter in the case of red PbO, and $10^{-6.0}$ gram ion per liter or 0.21 mg of lead per liter in the case of $Pb(OH)_2$. This is shown in Fig. 2 which has been constructed by plotting the logarithm of the total lead activity ($a_{Pb^{++}} + a_{HPbO_2^-}$) against pH. Both PbO and $Pb(OH)_2$ dissolve in acid solutions with formation of Pb^{++} ion and in alkaline solutions with formation of biplumbite ion $HPbO_2^-$ and, to a lesser extent, plumbite PbO_2^{--}. The latter ion has not been represented on the diagram because of the lack of precise thermodynamic data.

The oxidation of PbO, of $Pb(OH)_2$, and of alkaline solutions of Pb^{++} can lead to Pb_3O_4, to PbO_2, and to solutions of tetravalent lead under the form of plumbate PbO_3^{--}. In very alkaline media Pb_2O_3 can also be formed. This oxide has not been represented on the diagram.

The dissolution of Pb_2O_3 in alkaline solutions according to the reaction

$$Pb_2O_3 + 3OH^- = HPbO_2^- + PbO_3^{--} + H_2O$$

which has been studied by Glasstone (4) leads to solutions containing equal amounts of the ions $HPbO_2^-$ and PbO_3^{--} whose equilibrium characteristics are represented by line 5. The oxide PbO_2 and plumbate solutions are stable in presence of alkaline solutions free of reducing agents because of the fact that, at pH values higher than 7, lines 26 and 27 are below line *b* which corresponds to the oxidation of water to oxygen. In presence of acid solutions PbO_2 is thermodynamically unstable under atmospheric pressure since, for such solutions, the 26 lines are under line *b*; PbO_2 then tends to reduce into plumbous ions Pb^{++}, water being decomposed with liberation of oxygen. The latter reaction, however, involves a large overvoltage and this circumstance favors the stability of plumbic salts.

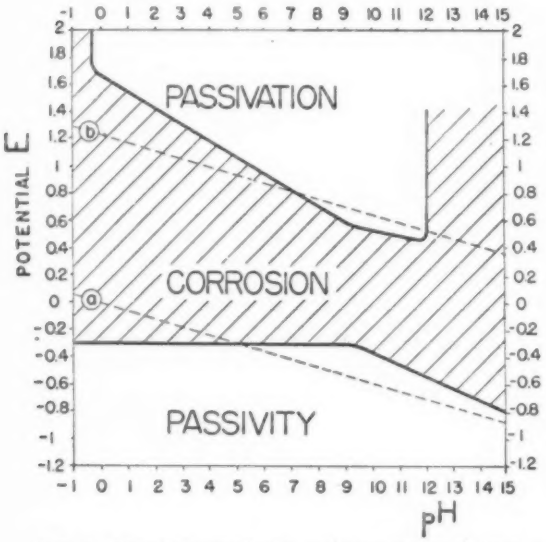

FIG. 3. Corrosion, passivity, and passivation of lead as deduced from Fig. 1.

Fig. 1 also shows that lead can generally be used as an electrolytic anode at pH values between 0 and 12, in which case it covers itself with PbO_2.

Metallic lead is thermodynamically stable in presence of neutral or alkaline solutions free of oxidants since, in such solutions, a portion of the domain of stability of lead is above line *a*. In acid solutions under atmospheric pressure lead generally tends to decompose water with evolution of hydrogen, in which case its potential exhibits a value between those of line *a* and those of the line of the 19 group which corresponds to the lead concentration of the solution. This decomposition of water by lead is, however, usually very slow on account of the high overvoltage of hydrogen on lead (8).

APPLICATION OF THE DIAGRAM TO THE STUDY OF THE CORROSION OF LEAD

In the present section of this paper, as well as in the next one, equilibrium diagrams are used in the study of phenomena which in practice may be subject to irreversible conditions. Nevertheless considerations based upon equilibrium theory are useful, indeed fundamental, since they give us the limits within which these corrosion phenomena can take place.

Corrosion of Lead in the Absence of Dissolved Carbon Dioxide

On Fig. 3 we have drawn the lines for which the total solubility of lead and its oxides under the form $Pb^{++} + HPbO_2^- + PbO_3^{--}$ has the value 10^{-6} gram atom of lead per liter (0.207 milligram Pb/liter). The lines are considered as separating the domain of corrosion from the domain of passivity which corresponds to the metallic lead area and from the domain of passivation corresponding to the lead dioxide area (See Fig. 1 and 2).

We use the terms passivity or passivation according to whether the protected surface is essentially metallic and cannot corrode or consists of a protective coating of oxide or other adherent compound. In the present case the distinction between passivity and passivation is a particularly clear one and there is no doubt that the use of both terms is advantageous.

This corrosion diagram of lead indicates that, in the absence of passivating substances (e.g., carbonates), any oxidizing action can cause the corrosion of lead except at the high potentials which correspond to the stability of lead dioxide PbO_2. As stated by Schikorr (9) lead oxide (PbO) is too soluble to give any protection to lead.

In the absence of complexing ions (e.g., tartrates) lead can be cathodically protected if its potential is lowered below about -0.3 volt in acid or neutral solutions or below -0.3 to -0.8 volt according to pH in alkaline solutions.

Corrosion of Lead in Presence of Carbonic Acid and Its Ions

In presence of aqueous solutions containing carbonates and bicarbonates lead may form lead carbonate $PbCO_3$ whose conditions of stability with respect to metallic lead, its oxides, and its ions are given by formulas (30) to (46) below. For the sake of simplicity conditions of stability of basic carbonates are not included.

Reactions and Equilibrium Conditions

A. Homogeneous Reactions without Oxidation

(28) $HCO_3^- + H^+ = H_2CO_3$

$$\log \frac{a_{HCO_3^-}}{a_{H_2CO_3}} = -6.37 + pH$$

(29) $CO_3^{--} + H^+ = HCO_3^-$

$$\log \frac{a_{CO_3^{--}}}{a_{HCO_3^-}} = -10.34 + pH$$

B. Heterogeneous Reactions Involving Two Solids and with Oxidation

(30) $PbCO_3 + H_2O = Pb(OH)_2 + CO_2(g)$

$$\log P_{CO_2} = -7.15$$

(31) $PbCO_3 = PbO + CO_2\ (g)$

$$\log P_{CO_2} = -7.36$$

(32) $PbCO_3 + 2H^+ + 2e^- = Pb + CO_2\ (g) + H_2O$

$$E = 0.031 - 0.0591\ pH - 0.0295 \log P_{CO_2}$$

(33) $PbCO_3 + 2H^+ + 2e^- = Pb + H_2CO_3$

$$E = 0.012 - 0.0591\ pH - 0.0295 \log a_{H_2CO_3}$$

(34) $PbCO_3 + H^+ + 2e^- = Pb + HCO_3^-$

$$E = -0.200 - 0.0295\ pH - 0.0295 \log a_{HCO_3^-}$$

(35) $PbCO_3 + 2e^- = Pb + CO_3^{--}$

$$E = -0.506 - 0.0295 \log a_{CO_3^{--}}$$

(36) $PbO_2 + CO_2\ (g) + 4H^+ + 2e^- = PbCO_3 + 2H_2O$

$$E = 1.324 - 0.0591\ pH + 0.0295 \log P_{CO_2}$$

(37) $PbO_2 + H_2CO_3 + 2H^+ + 2e^- = PbCO_3 + 2H_2O$

$$E = 1.367 - 0.0591\ pH + 0.0295 \log a_{H_2CO_3}$$

(38) $PbO_2 + HCO_3^- + 3H^+ + 2e^- = PbCO_3 + 2H_2O$

$$E = 1.555 - 0.0886\ pH + 0.0295 \log a_{HCO_3^-}$$

(39) $PbO_2 + CO_3^{--} + 4H^+ + 2e^- = PbCO_3 + 2H_2O$

$$E = 1.861 - 0.1182\ pH + 0.0295 \log a_{CO_3^{--}}$$

C. Heterogeneous Reactions Involving One Solid and without Oxidation

(40) $Pb^{++} + CO_2\ (g) + H_2O = PbCO_3 + 2H^+$

$$\log a_{Pb^{++}} = 5.31 - 2.00\ pH - \log P_{CO_2}$$

(41) $HPbO_2^- + CO_2\ (g) + H^+ = PbCO_3 + H_2O$

$$\log a_{HPbO_2^-} = -22.85 + pH - \log P_{CO_2}$$

(42) $Pb^{++} + H_2CO_3 = PbCO_3 + 2H^+$

$$\log a_{Pb^{++}} = 3.87 - 2.00\ pH - \log a_{H_2CO_3}$$

(43) $Pb^{++} + HCO_3^- = PbCO_3 + H^+$

$$\log a_{Pb^{++}} = -2.50 - pH - \log a_{HCO_3^-}$$

(44) $Pb^{++} + CO_3^{--} = PbCO_3$

$$\log a_{Pb^{++}} = -12.85 - \log a_{CO_3^{--}}$$

(45) $HPbO_2^- + HCO_3^- + 2H^+ = PbCO_3 + 2H_2O$

$$\log a_{HPbO_2^-} = -30.67 + 2.00\ pH - \log a_{HCO_3^-}$$

(46) $HPbO_2 + CO_3^{--} + 3H^+ = PbCO_3 + 2H_2O$

$$\log a_{HPbO_2^-} = -41.01 + 3.00\ pH - \log a_{CO_3^{--}}$$

Corrosion Diagram of Lead in Presence of Carbon Dioxide

The influence of pH on the solubility of lead carbonate is shown in Fig. 4 for activities or concentrations of total CO_2 (i.e., $H_2CO_3 + HCO_3^- + CO_3^{--}$) varying from 10^{-6} to 1 mole per liter, and in Fig. 5 for partial pressures of CO_2 varying from 10^{-6} to 1 atmosphere. The intersections of the horizontal line of ordinate 10^{-6} of Fig. 4 with the solubility curves of lead carbonate give the pH values corresponding to the boundaries between corrosion and its essential absence for various amounts of total CO_2. The additional domains of passivation resulting from the pres-

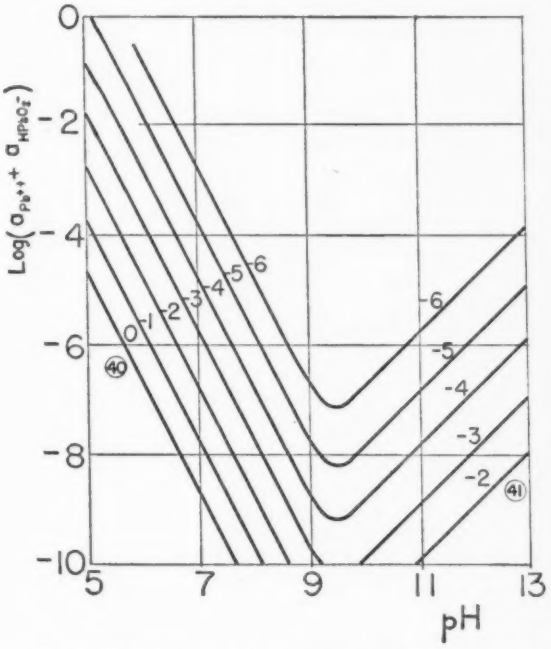

FIG. 4. Solubility of lead carbonate as a function of pH for a pressure of carbon dioxide varying from 1 to 10^{-6} atmosphere. The number indicated on each curve corresponds to the value of log P_{CO_2}.

ence of CO_2 are represented in Fig. 6 which is easily drawn on the basis of Fig. 1 and of the information obtained from Fig. 4. A similar diagram could be established from Fig. 1 and 5, the additional domains of passivation corresponding then to various pressures of CO_2.

The data shown in Fig. 6 indicate that minute traces of CO_2 in air suffice to cause the formation of lead carbonate in slightly alkaline solutions. This lead carbonate forms a protective layer on the metal which, in the absence of activating ions such as chloride, passivates the lead and protects it against corrosion.

It is well known (10) that, while distilled water

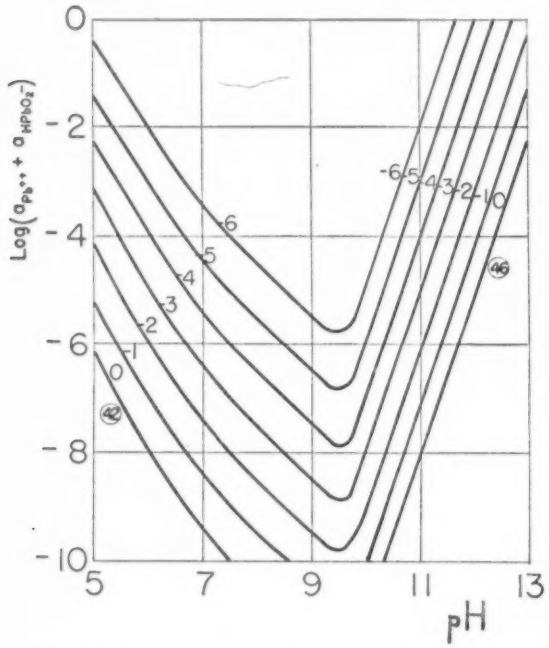

FIG. 5. Solubility of lead carbonate as a function of pH for a total activity $a_{H_2CO_3} + a_{HCO_3^-} + a_{CO_3^{--}}$ varying from 1 to 10^{-6}. The number indicated on each curve corresponds to the value of log $(a_{H_2CO_3} + a_{HCO_3^-} + a_{CO_3^{--}})$.

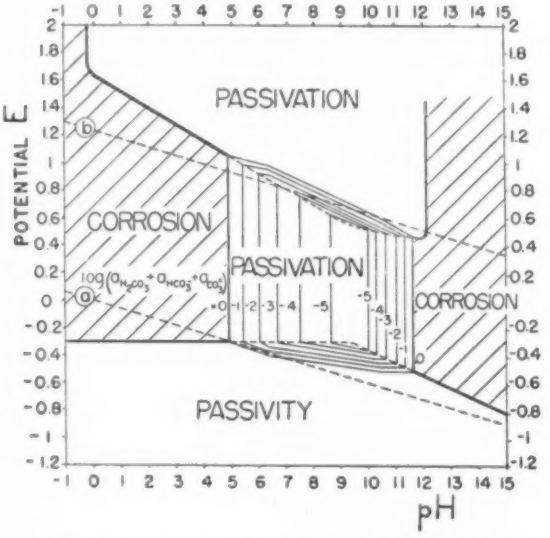

FIG. 6. Corrosion, passivity, and passivation of lead in presence of carbon dioxide, bicarbonate, and carbonate ions. Heavy lines correspond to log $(a_{H_2CO_3} + a_{HCO_3^-} + a_{CO_3^{--}}) = 0$. The passivation domain limited by thin lines corresponds to log $(a_{H_2CO_3} + a_{HCO_3^-} + a_{CO_3^{--}})$ equal to 0, −1, −2, −3, −4, and −5.

and rain water corrode lead, this metal is not corroded by waters containing bicarbonates but sufficiently free of aggressive CO_2. Fig. 6 gives a direct explanation of the fact that addition of CO_2 to rain water is not usually sufficient to render this water nonaggressive toward lead because the resulting pH is often too low (5.5 or less). On the contrary, good protection of lead can be accomplished if CO_2 is added to water at a pH close to 8 or 9, i.e., when CO_2 is added as bicarbonate.

Fig. 6 also shows that, on the basis of the views presented here, a certain passivating action could be expected to occur even at very low carbonate and bicarbonate contents of the water, e.g., 10^{-5} gram ion or 1 part per million of $CaCO_3$, at pH values of 9 to 10. At higher carbonate contents these pH limits are widened in both directions and chiefly toward neutrality.

Solutions having a pH of 7 are probably passivating when the amount of dissolved CO_2 is higher than $10^{-3.4}$ mole per liter, i.e., 40 parts per million of $CaCO_3$. The equilibrium pressure of CO_2 is then $10^{-2.7}$ atmosphere corresponding to 0.2 per cent of CO_2 in air. It is unlikely that carbonates could cause passivation of lead when the pH is higher than 12 because of the impossibility of obtaining sufficiently concentrated solutions.

APPLICATION OF THE DIAGRAM TO THE STUDY OF THE LEAD STORAGE BATTERY

When the sulfate ion is present additional equilibrium conditions have to be taken into account. These are equations (47) to (57) as follows.

A. Homogeneous Reaction without Oxidation

(47) $SO_4^{--} + H^+ = HSO_4^-$

$$\log \frac{a_{HSO_4^-}}{a_{SO_4^{--}}} = -1.92 + \text{pH}$$

B. Heterogeneous Reactions Involving Two Solids and with Oxidation

(48) $PbSO_4 + H^+ + 2e^- = Pb + HSO_4^-$

$$E = -0.300 - 0.0295\,\text{pH} - 0.0295 \log a_{HSO_4^-}$$

(49) $PbSO_4 + 2e^- = Pb + SO_4^{--}$

$$E = -0.356 - 0.0295 \log a_{SO_4^{--}}$$

(50) $Pb_3O_4 + 3SO_4^{--} + 8H^+ + 2e^- = 3PbSO_4 + 4H_2$

$$E = 2.912 - 0.2364\,\text{pH} + 0.0886 \log a_{SO_4^{--}}$$

(51) $PbO_2 + HSO_4^- + 3H^+ + 2e^- = PbSO_4 + 2H_2$

$$E = 1.655 - 0.0886\,\text{pH} + 0.0295 \log a_{HSO_4^-}$$

(52) $PbO_2 + SO_4^{--} + 4H^+ + 2e^- = PbSO_4 + 2H_2$

$$E = 1.712 - 0.1182\,\text{pH} + 0.0295 \log a_{SO_4^{--}}$$

C. Heterogeneous Reactions Involving One Solid

Without oxidation

(53) $Pb^{++} + HSO_4^- = PbSO_4 + H^+$

$$\log a_{Pb^{++}} = -5.87 - \text{pH} - \log a_{HSO_4^-}$$

(54) $Pb^{++} + SO_4^{--} = PbSO_4$

$$\log a_{Pb^{++}} = -7.79 - \log a_{SO_4^{--}}$$

(55) $HPbO_2^- + SO_4^{--} + 3H^+ = PbSO_4 + 2H_2O$

$$\log a_{HPbO_2^-} = -35.96 + 3pH - \log a_{SO_4^{--}}$$

With oxidation

(56) $Pb^{++} + HSO_4^- + 2e^- = PbSO_4 + H^+$

$$E = 1.865 + 0.0295\ pH + 0.0295 \log a_{Pb^{++}} \cdot a_{HSO_4^-}$$

(57) $PbO_3^{--} + SO_4^{--} + 6H^+ + 2e^- = PbSO_4 + 3H_2O$

$$E = 2.344 - 0.1773\ pH + 0.0295 \log a_{PbO_3^{--}} \cdot a_{SO_4^{--}}$$

Fig. 7 has been constructed on the basis of formulas (1) to (27) and (47) to (57). It gives a picture of the various thermodynamic equilibria of lead and its derivatives in presence of aqueous solutions containing a total sulfate activity $a_{HSO_4^-} + a_{SO_4^{--}}$ equal to 1 ion gram per liter. Comparing this figure with

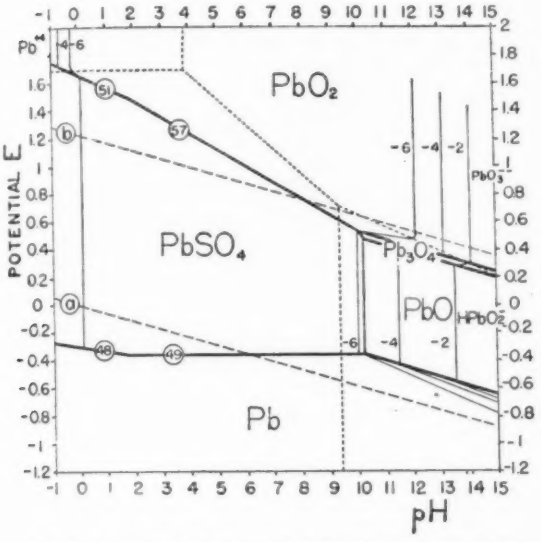

FIG. 7. Potentiai-pH diagram of lead in presence of sulfate ion. Same notations as Fig. 1. Note that line 52 is erroneously indicated as line 57.

Fig. 1, one observes that the presence of sulfate chiefly results in a considerable domain of stability of lead sulfate $PbSO_4$.

Fig. 7 shows that, in presence of solutions with a total sulfate activity of 1, Pb and $PbSO_4$ are in equilibrium for a potential which, at pH values between approximately 3 and 10, has a very definite value of −0.356 volt. In the whole portion of the domain of stability of $PbSO_4$ for which the lead and sulfate in solution exist essentially as Pb^{++} and SO_4^{--} ions, i.e., at pH values between 3 and 9, the stability of lead is constant and equal to $10^{-7.79}$ gram atom per liter (or 0.0033 milligram of Pb per liter). At pH values lower than 3 the solubility of lead sulfate increases on account of the formation of bisulfate ion HSO_4^-, reaction (48). At pH values higher than 9 the solubility of lead sulfate increases on account of the formation of biplumbite ion HPO_2^-. At pH = 9.4 the amounts of HPO_2^- and Pb^{++} are equal to each other and at pH = 10.0 the total amount of lead in solution is 10^{-6} gram atom per liter or 0.21 milligram per liter.

At pH = 10.2 $PbSO_4$ ceases to constitute the thermodynamically stable solid phase in presence of a molar activity of SO_4^{--} and it tends to transform itself into PbO or $Pb(OH)_2$ or into some basic salts which we have not included in our study.

The Pb-$PbSO_4$ electrode in solutions of total sulfate activity equal to 1, whose equilibrium characteristics are represented by lines 48–49, is thermodynamically stable in water under atmospheric pressure only for pH values between 6.0 and 10.2. At pH values lower than 6.0 this electrode tends to decompose water with evolution of hydrogen. However, this decomposition is very slow, and even negligible, on account of the high hydrogen overvoltage on lead [see, for instance, Creighton (8)].

At the high potentials corresponding to lines 51–52 the sulfate $PbSO_4$ is in equilibrium with PbO_2 in presence of 1 molar sulfate solutions. Along the portion of 52 between about pH = 3 and pH = 9 the amount of lead in solution is constant at the same small value (0.0033 milligram per liter) already men-

TABLE I. *Lead storage battery with 1 molar sulfate*

pH	Potentials volts		emf volts	Pb concentration mg/l	
	+ pole	− pole		+ pole	− pole
−1	1.74 ?	−0.27 ?	2.01 ?	165 ?	2.6 ?
0	1.65	−0.30	1.95	0.26	0.26
1	1.56	−0.33	1.89	0.026	0.026
2	1.47	−0.36	1.83	0.0065	0.0065
3	1.35	−0.36	1.71	0.0033	0.0033
4	1.24	−0.36	1.60	0.0033	0.0033
5	1.12	−0.36	1.48	0.0033	0.0033
6	1.00	−0.36	1.36	0.0033	0.0033
7	0.88	−0.36	1.24	0.0033	0.0033

TABLE II. *Lead storage batteries with various concentrations of sulfuric acid*

H_2SO_4 concentration moles/l	pH	Potentials volts		emf volts		Pb concentration mg/l	
		+ pole	− pole	calc.	expt.	+ pole	− pole
0.1	1.03	1.535	−0.301	1.84	—	0.2	0.2
0.5	0.48	1.603	−0.305	1.91	—	0.2	0.2
1	0.20	1.656	−0.309	1.96	1.919	0.2	0.2
2	−0.06	1.669	−0.307	1.98	1.971	0.2	0.2
3	−0.30	1.696	−0.305	2.00	2.014	0.5	0.2
4	−0.46	1.714	−0.304	2.02	2.053	1.3	0.2
5	−0.60	1.728	−0.303	2.03	2.090	4.3	0.2
6	−0.74	1.743	−0.301	2.04	2.123	14.0	0.3

tioned above in connection with the Pb-$PbSO_4$ electrode. At pH values lower than 3 the amount of lead in solution increases on account of the transformation of sulfate into bisulfate ions. This results in an increase of Pb^{++} ion concentration to 10^{-6} gram ion per liter or 0.21 milligram per liter at pH 0.1 and, at still lower pH values, plumbic ions Pb^{+4} are formed. At pH values higher than 9 the amount of lead in solution increases on account of the formation of biplumbite ions $HPbO_2^-$.

The PbO_2-$PbSO_4$ electrode in 1 molar sulfate solutions, whose equilibrium characteristics are represented by lines 51–52, is thermodynamically stable in presence of water under atmospheric pressure only for pH values between about 7.9 and 10.0. At pH values below 7.9 this electrode tends to decompose water with evolution of oxygen, but it is most likely that this decomposition is very slow.

Lead Storage Battery

Fig. 7, as well as similar diagrams which could be drawn for other sulfate concentrations, is useful in the study of the behavior of the lead storage battery since the equilibrium characteristics of the two electrodes of the battery are represented by lines 48–49 (Pb-$PbSO_4$ electrode, negative pole) and by lines 51–52 (PbO_2-$PbSO_4$ electrode, positive pole). Both electrodes are dipping in solutions saturated with $PbSO_4$.

The amount of dissolved lead, which is extremely low at pH values higher than 3 ($10^{-7.79}$ gram ion per liter or 0.0033 milligram per liter) increases as the pH diminishes ($10^{-6.0}$ gram ion per liter or 0.21 milligram per liter at pH = 0.1).

With the more acid solutions, which are used in practice in storage batteries, the solubility at the positive pole is greater than that at the negative pole on account of the dissolution of PbO_2 into plumbic ions Pb^{+4} which are not present in any appreciable amounts in less acid solutions.

The electromotive force of the storage battery, which is equal to the difference between the potentials of the two electrodes, is measured by the vertical distance separating the lines 48–49 from the lines 51–52. Table I gives, at different pH values, the potentials of the two electrodes, the electromotive force and the lead concentrations around the two electrodes in solutions of molarity 1 in $HSO_4^- + SO_4^{--}$. Differences between concentrations and activities are neglected and the concentrations of lead are approximate, particularly at pH = −1. Table I shows that storage batteries should be used with as high a acidity as possible.

Table II gives the characteristics of batteries functioning at various concentrations of sulfuric acid calculated from formulas 48 and 51.[2] In addition to the calculated electromotive forces we give the experimental values of Harned and Hamer (11) as quoted by Latimer (4). Their approximate character is sufficient for these calculations which neglect the differences between concentrations and activities. The Table shows that the calculated electromotive forces agree rather well with the experimental values. One also notices that an increase of acidity above 2 molar causes a rapid increase of the amount of dissolved lead around the positive pole on account of the dissolution of PbO_2 as Pb^{+4} ions.

Acknowledgments

The preparation of the present paper was started during the simultaneous presence of the three authors at the University of Oregon during the spring of 1949. Thanks are due to the Office of Naval Research and to the Belgian American Educational Foundation.

Any discussion of this paper will appear in a Discussion Section, to be published in the December 1951 issue of the Journal.

References

1. M. Pourbaix, "Thermodynamique des Solutions Aqueuses Diluées—Représentation Graphique du Rôle du pH et du Potentiel," Meinema, Delft (1945). Also Beranger, Paris (1948). An English translation by J. N. Agar has been published by Arnold, London (1949).
2. M. Pourbaix, *Corrosion*, **5**, 121 (1949).
3. P. Delahay, M. Pourbaix, and P. Van Rysselberghe, *J. Chem. Education* **27**, 683 (1950).
4. W. M. Latimer, "The Oxidation State of the Elements and their Potentials in Aqueous Solutions," Prentice-Hall, New York (1938).
5. S. Glasstone, *J. Phys. Chem.*, **121**, 1456 (1922).
6. L. V. Andrews and D. J. Brown, *J. Am. Chem. Soc.*, **56**, 388 (1934).
7. H. M. Spencer and H. Mote, *J. Am. Chem. Soc.*, **54**, 4618 (1932).
8. H. J. Creighton, "Principles and Applications of Electrochemistry," 4th ed., Vol. **1**, p. 249, John Wiley & Sons, Inc., New York (1943).
9. G. Schikorr, *Korrosion u. Metallschutz*, **16**, 181 (1940).
10. U. R. Evans, "Metallic Corrosion, Passivity and Protection," 2nd ed., pp. 394–398, Arnold, London (1946).
11. H. S. Harned and W. J. Hamer, *J. Am. Chem. Soc.*, **57**, 33 (1935).

[2] pH values measured by R. D. Williams.

Potential-pH Diagram of Silver

Construction of the Diagram—Its Applications to the Study of the Properties of the Metal, its Compounds, and its Corrosion[1]

PAUL DELAHAY

Louisiana State University, Baton Rouge, Louisiana

MARCEL POURBAIX

University of Brussels, Brussels, Belgium

AND

PIERRE VAN RYSSELBERGHE

University of Oregon, Eugene, Oregon

ABSTRACT

On the basis of methods and conventions previously described (1) and using the available thermodynamic and electrochemical data, the potential-pH diagram of silver has been constructed. A derived diagram showing domains of corrosion, passivity, and passivation is also presented.

REACTIONS AND EQUILIBRIUM CONDITIONS

The free energy values used in the present paper are those given by Latimer (2) except in the following two cases:

1. For the ion AgO^+ the $E°$ value estimated by Latimer (2) for the reaction

$$AgO^+ + 2H^+ + e^- = Ag^{++} + H_2O$$

is 2.1 volts. The corresponding $\Delta F°$ of AgO^+ is 54,907 calories (calculated with more figures than are significant for convenience in the construction of the diagram, observation of intersection requirements of certain lines, etc.).

2. For the oxide Ag_2O_3 the $E°$ given by Latimer (3) on the basis of the work of Luther and Pokorny (4) for the reaction

$$Ag_2O_3 + H_2O + 2e^- = 2AgO + 2OH^-$$

is 0.74 volt. The corresponding $\Delta F°$ of Ag_2O_3 is 20,864 calories. The same remark as that made for AgO^+ applies here. Both $\Delta F°$ values are uncertain.

We have the following reactions and equilibrium conditions:

FOR WATER

(a) $2H^+ + 2e^- = H_2$

$$E = -0.0591 \text{ pH} - 0.0295 \log P_{H_2}$$

(b) $O_2 + 4H^+ + 4e^- = 2H_2O$

$$E = 1.229 - 0.0591 \text{ pH} + 0.0148 \log P_{O_2}$$

FOR SILVER

A. Homogeneous Reactions with Oxidation

(1) $Ag^{++} + e^- = Ag^+$

$$E = 1.939 + 0.0591 \log \frac{a_{Ag^{++}}}{a_{Ag^+}}$$

(2) $AgO^+ + 2H^+ + 2e^- = Ag^+ + H_2O$

$$E = 2.019 - 0.0591\ p\text{H} + 0.0295 \log \frac{a_{AgO^+}}{a_{Ag^+}}$$

(3) $AgO^+ + 2H^+ + e^- = Ag^{++} + H_2O$

$$E = 2.100 - 0.1182 \text{ pH} + 0.0591 \log \frac{a_{AgO^+}}{a_{Ag^{++}}}$$

B. Heterogeneous Reactions Involving Two Solids with Oxidation

(4) $Ag_2O + 2H^+ + 2e^- = 2Ag + H_2O$

$$E = 1.173 - 0.0591 \text{ pH}$$

(5) $2AgO + 2H^+ + 2e^- = Ag_2O + H_2O$

$$E = 1.398 - 0.0591 \text{ pH}$$

(6) $Ag_2O_3 + 2H^+ + 2e^- = 2AgO + H_2O$

$$E = 1.568 - 0.0591 \text{ pH}$$

C. Heterogeneous Reactions Involving One Solid without oxidation

(7) $Ag_2O + 2H^+ = 2Ag^+ + H_2O$

$$\log a_{Ag^+} = 6.32 - \text{pH}$$

(8) $2AgO + 4H^+ = 2Ag^{++} + 2H_2O$

$$\log a_{Ag^{++}} = -2.83 - 2 \text{ pH}$$

(9) $Ag_2O_3 + 2H^+ = 2AgO^+ + H_2O$

$$\log a_{AgO^+} = -11.82 - \text{pH}$$

[1] Manuscript received April 13, 1950. This paper prepared for delivery before the Buffalo Meeting, October 11 to 13, 1950.

With oxidation

(10) $Ag^+ + e^- = Ag$

$E = 0.800 + 0.0591 \log a_{Ag^+}$

(11) $Ag^{++} + 2e^- = Ag$

$E = 1.369 + 0.0295 \log a_{Ag^{++}}$

(12) $2AgO + 4H^+ + 2e^- = 2Ag^+ + 2H_2O$

$E = 1.771 - 0.1182\ pH - 0.0591 \log a_{Ag^+}$

(13) $2AgO^+ + 2e^- = 2AgO$

$E = 2.267 + 0.0591 \log a_{AgO^+}$

(14) $Ag_2O_3 + 6H^+ + 4e^- = 2Ag^+ + 3H_2O$

$E = 1.670 - 0.0887\ pH - 0.0295 \log a_{Ag^+}$

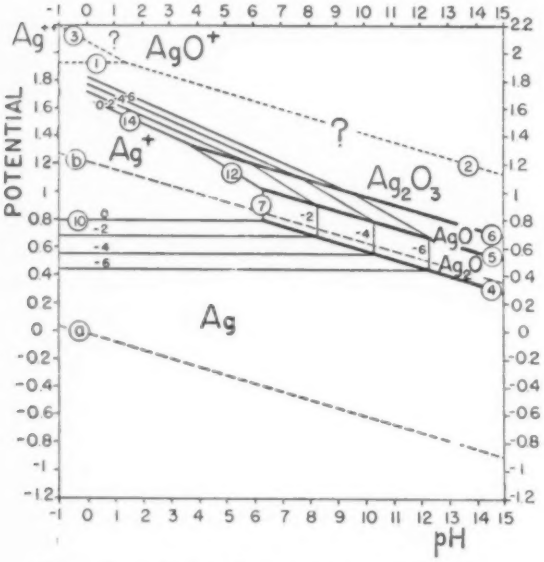

FIG. 1. Potential-pH diagram of silver at 25° C. The area between lines *a* and *b* corresponds to thermodynamic stability of water. Thin lines represent equilibrium conditions between a solid phase and an ion at activities 1, 10^{-2}, 10^{-4}, 10^{-6}. Heavy lines represent equilibrium conditions between two solid phases. Dotted lines represent equilibrium conditions between two ions for a ratio of activities of these ions equal to unity. Circled figures and letters refer to the corresponding equations in the text.

(15) $Ag_2O_3 + 6H^+ + 2e^- = 2Ag^{++} + 3H_2O$

$E = 1.401 - 0.1773\ pH - 0.0591 \log a_{Ag^{++}}$

Description of the Potential-pH Diagram

Fig. 1 has been established on the basis of equilibrium conditions (1) to (15) and represents the circumstances of thermodynamic equilibrium of the system Ag–H_2O at 25°C. The information given in this diagram concerning the oxide of trivalent silver, Ag_2O_3, and the ions Ag^{++} and AgO^+, should be regarded as provisional.

Metallic silver, generally stable in presence of aqueous solutions deprived of complexing substances, such as cyanides, ammonia, sulfite, and thiosulfate ions, can be dissolved by acid oxidizing solutions with the resulting formation of colorless univalent silver ions Ag^+.

In neutral or moderately acid solutions strong oxidants, as ozone and persulfates, oxidize solutions of silver ion Ag^+ with the resulting formation of black peroxides AgO and Ag_2O_3 which are unstable in presence of water and decompose it with evolution of oxygen. The corresponding ions Ag^{++} and AgO^+ probably do not exist in solution at any pH according to equations (8) and (9), although complexes of the Ag^{++} ion have been reported in nitric acid solutions (5–9). These solutions, whose potential is close to 1.9 volts, are strong oxidants. As has been shown by Noyes and his collaborators, they oxidize H_2O_2 to O_2, Mn^{++} to MnO_4^-, Ce^{3+} to Ce^{4+}, VO^{++} to VO_2^+, IO_3^- to IO_4^-, NH_4^+ to N_2 and nitrogen oxides (5–9).

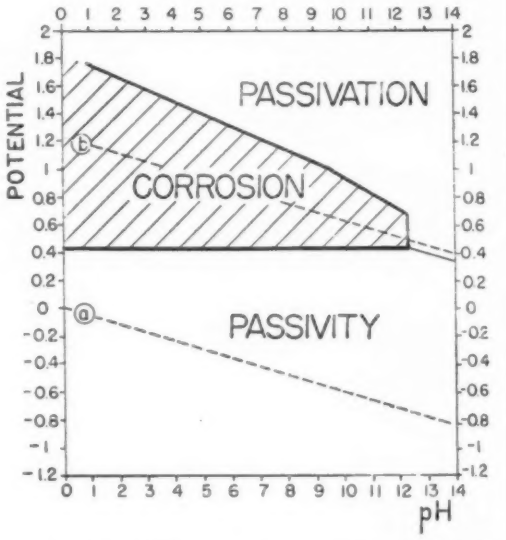

FIG. 2. Conditions of corrosion, passivity, and passivation of silver as determined from the potential-pH diagram.

In presence of definitely alkaline solutions, metallic silver is entirely stable. With an oxidant present, it then covers itself with a protective coating of brown Ag_2O.

The anodic polarization of silver in presence of a solution of sodium hydroxide leads first, as has been shown by Hickling and Taylor (10) on the basis of an oscillographic method, to the formation of a protective film of Ag_2O. This film seems to appear at potentials practically equal to those given by line 4 corresponding to the equilibrium Ag/Ag_2O.

At potentials higher than those given by lines 3 and 6 (for instance 0.88 volt at a pH around 13.8) the Ag_2O film covers itself with an unstable peroxide possibly Ag_2O_3, which decomposes with formation of AgO. During this decomposition the potential decreases and stabilizes itself in the neighborhood

line 5. The anode is then apparently covered with a mixture of Ag_2O and AgO and evolution of oxygen occurs at its surface. In less alkaline solutions, of pH less than 9, anodic passivation of silver is imperfect and the metal dissolves (10).

Electrolysis of solutions of silver ion Ag^+ under sufficiently low current density with a silver anode leads to anodic dissolution of silver as Ag^+ ion exclusively and to a quantitative cathodic deposition of the metal without any risk of secondary reactions. These conditions are those encountered in the perfect behavior of silver coulometers. Copper coulometers, as is well known, do not fulfill these conditions.

Electrolysis of solutions of silver ion Ag^+ under high current density, with a sufficiently high anodic potential, may lead to a deposition of black peroxides AgO and Ag_2O_3 on the anode. These peroxides are unstable in presence of water and decompose it with evolution of oxygen when the electrolysis current is interrupted.

Application of the Potential-pH Diagram to the Study of the Corrosion of Silver

Fig. 2 has been deduced from Fig. 1 on the basis of conventions previously presented (1). In particular it has been assumed that an ionic concentration of 10^{-6} gram-ion per liter represents the boundary between corrosion and its absence. It should also be recalled that the term passivity applies to the resistance to corrosion exhibited by uncoated metallic surfaces while the term passivation applies to the resistance to corrosion provided by coatings of insoluble oxides or other compounds.

Fig. 2 shows that, in the absence of complexing substances (cyanide, ammonia, sulfite, thiosulfate, etc.), no corrosion of silver could possibly occur in sufficiently alkaline solutions. Sufficiently strong oxidants can corrode silver in neutral or acid solution. By comparing the positions of lines *b* and 10 one sees that, on the basis of thermodynamic predictions, metallic silver should reduce oxygen with formation of Ag^+ ions. This reaction does not occur to any detectable extent because, as has been shown by one of us (11), the reduction of O_2 on a silver electrode involves a high overvoltage.

Acknowledgments

The preparation of the present paper, as well as that of several others concerning potential-pH diagrams, was started during the simultaneous presence of the three authors at the University of Oregon during the spring of 1949. Thanks are due to the Belgian American Educational Foundation and to the Office of Naval Research.

Any discussion of this paper will appear in a Discussion Section, to be published in the December 1951 issue of the Journal.

References

1. P. Delahay, M. Pourbaix, P. Van Rysselberghe, *J. Electrochem. Soc.*, **98**, 57 (1951).
2. W. M. Latimer, "The Oxidation States of the Elements and Their Potentials in Aqueous Solutions," p. 181, Prentice-Hall, New York (1938).
3. *Ibid.*, p. 182.
4. R. Luther and F. Pokorny, *Z. anorg. Chem.*, **57**, 291 (1908).
5. A. A. Noyes, J. L. Hoard, and K. S. Pitzer, *J. Am. Chem. Soc.*, **57**, 1221 (1935).
6. A. A. Noyes, K. S. Pitzer, and C. L. Dunn, *J. Am. Chem. Soc.*, **57**, 1229 (1935).
7. A. A. Noyes and A. Kossiakoff, *J. Am. Chem. Soc.*, **57**, 1238 (1935).
8. A. A. Noyes, C. D. Coryell, F. Stitt, and A. Kossiakoff, *J. Am. Chem. Soc.*, **59**, 1316 (1937).
9. A. A. Noyes, D. De Vault, C. D. Coryell, and T. J. Deahl, *J. Am. Chem. Soc.*, **59**, 1326 (1937).
10. A. Hickling and D. Taylor, *Faraday Soc. Disc.*, **1**, 277 (1947).
11. P. Delahay, *J. Electrochem. Soc.*, **97**, 198, 205 (1950).

Electronic Instrumentation for Overvoltage Measurements[1]

DIMITRIOS STAICOPOULOS, ERNEST YEAGER, AND FRANK HOVORKA

Department of Chemistry, Western Reserve University, Cleveland, Ohio

ABSTRACT

Electronic instrumentation has been developed for the measurement of overvoltage by the commutator or indirect method. With this apparatus current may be interrupted for periods ranging in length from 5 microseconds through one-half the repetition rate for repetition rates from 20 sec^{-1} through 3000 sec^{-1}. Potential measurements may be made at any time while current is either off or on during periods as short as 5 microseconds. Typical accuracy of the potential measurements is $\pm$ 5 mv for measurement periods of 5 microseconds duration at a repetition rate of 1000 sec^{-1}. The potential measurements involve the use of a gated-bridge null detector in conjunction with an ordinary potentiometer.

INTRODUCTION

Two methods are available for overvoltage measurements (1): the direct method and the indirect or commutator method. With the direct method, the potential of the polarized electrode is measured against a reference electrode while current is flowing. To minimize any ohmic voltage drop in the measured potential, the tip (Luggin capillary) of the solution bridge connecting the compartment of the polarized electrode to that of the reference electrode is pressed against the surface of the polarized electrode. With the commutator method, measurements are made while the current is interrupted for a short period and a Luggin capillary is not necessary.

In the past some controversy has existed concerning the reliability of the commutator method because of the difficulty in extrapolating the measured values back to the instant when the current is interrupted. In 1937, Hickling (2) constructed an electronic commutator with which measurements can be made with a precision of 10 mv at the end of interruption periods with a lower limit of 50 microseconds. Because of the rapid decay of hydrogen overvoltage on many metals during the first few microseconds, the extrapolation from 50 microseconds to zero time is difficult, particularly in view of a precision of 10 mv for each measurement. Results (3) obtained with this equipment, however, have been found to be in general agreement (20-30 mv) with the measurements of Bockris (4) who used the direct method. Since the errors associated with the two methods are expected to act in opposite directions, this has served to establish confidence in both methods.

[1] Manuscript received August 14, 1950. This paper prepared for delivery before the Cleveland Meeting, April 19 to 22, 1950. The work reported herein has been partially supported by the Office of Naval Research under Contract No. N7 onr 47002, Project No. NR 051 162.

DESIGN AND CONSTRUCTION

In designing equipment for the measurement of overvoltage by the commutator method, the authors have attempted to incorporate the following features:

1. An interruption period of variable length with a lower limit of 5 microseconds and an upper limit of the order of 1000 microseconds or one-half the repetition period (depending on which is smaller).
2. A variable repetition or recursion rate with a lower limit of 20 sec^{-1} and an upper limit of 3000 sec^{-1}.
3. Polarizing currents variable from 10^{-6} through 10^{-1} amp.
4. Provisions for measuring potentials during periods as short as 5 microseconds at any known time after the interruption or initiation of the polarizing current.
5. An accuracy for the potential measurements of 5 mv for measurement periods as short as 5 microseconds.

In terms of these provisions it is possible to establish quantitatively the decay and build-up curves for overvoltage. The present unit can be used to measure cathodic and anodic polarization.

Fig. 1 shows a block diagram which indicates the functions of the various components of the apparatus. The output from a multivibrator (shown in detail in Fig. 2) is differentiated and the resulting positive pulses deleted by means of a diode, while the remaining negative pulses are subsequently amplified (A). In turn, these pulses trigger a univibrator or one-shot multivibrator (U_1) which produces rectangular pulses of controllable duration. After adequate amplification, the rectangular pulses are used to activate the current interruptor (I). The latter (Fig. 3) consists of a duo-triode, type 6N7 (V_7) with the two sections connected in parallel. Higher polarizing currents may be obtained by the introduction of one or more duo-triodes (6N7) in parallel with

V_7) in Fig. 3. The electrolytic cell to be polarized is placed in series with these triodes. The bias of the tubes is such that the triodes normally conduct and the current may be abruptly reduced to zero when negative pulses are introduced in the grid circuit. The magnitude of the polarizing current is controlled by adjusting the filament current, and hence, the filament temperature of the duo-triodes.

The same pulses which trigger the univibrator (U_1) also trigger a similar unit (U_2) which serves effectively as a pulse delay stage. The rectangular pulses from this univibrator (U_2) are differentiated and the leading negative edges are deleted with a diode while the trailing positive pulses are used to trigger a third univibrator (U_3). When the rectangular pulses produced by univibrator (U_2) are lengthened, the leading edge of each pulse remains fixed with respect to the trigger pulse while the trailing edge lags farther behind. Hence, a variable delay time is involved in the triggering of univibrator (U_3) relative to the triggering of univibrator (U_1). The delay time is essentially equal to the pulse duration obtained with univibrator (U_2). Univibrator (U_3) then produces rectangular pulses of variable duration which after amplification are used to control the on-off action of the gated-bridge null detector.

The null detector effectively serves as a galvanometer in the potential measurements and is used in conjunction with a Leeds & Northrup student-type potentiometer (P in Fig. 3). The duo-triode 6N7 (V_3 in Fig. 3) with the two triodes in parallel is normally conducting and biases the high-mu triodes 6SF5 (V_1 and V_2 in Fig. 3) in the arms of the bridge well beyond cutoff. With the introduction of a negative pulse on the grids of the duo-triode (V_3), this tube is cut off sharply and the bias on tubes (V_1) and (V_2) drops to a value at which the tubes conduct. If there is any potential difference between the grids of the tubes (V_1) and (V_2) when the tubes are conducting, an unbalanced condition results in the bridge and is registered as a sound in the earphones. The triodes (V_1) and (V_2) are carefully matched for linear performance over the range of grid potentials from -2.5 to 0 volts[2]. A biasing cell (B.C. in Fig. 3) has also been incorporated in the grid circuit to insure that the grid potential is in the linear range during the overvoltage measurements. The grid circuits of both triodes, as well as the potentiometer, have been shielded in order to prevent stray pickup, particularly 60 cycle. Due to the grid-to-plate capacity of the duo-triode (V_7) and the grid-to-cathode capacity of the duo-triode (V_3), the two negative pulses applied at (A) and (B) appear differentiated at the plates of (V_7) and at the cathode of the duo-triode (V_3), respectively, owing to the relatively low resistance of the electrolytic cell and the low cathode resistance (R_1) of (V_3) in Fig. 3. The resulting negative and positive "spikes" at the beginning and the

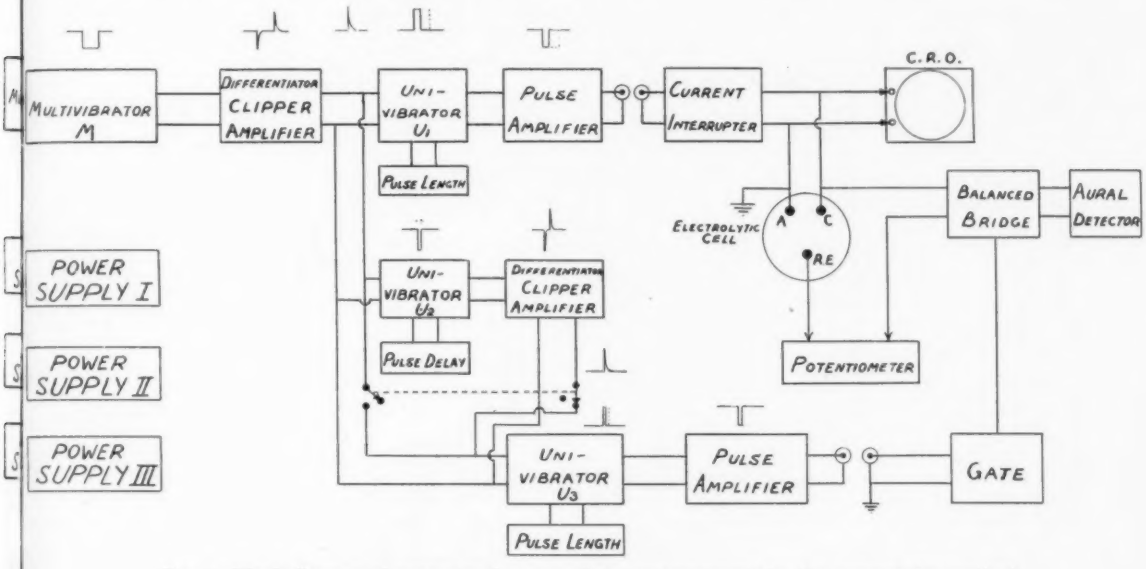

FIG. 1. Block diagram of apparatus for overvoltage measurements by the commutator method

[2] At the present time a modification of this circuit is being used which involves the introduction of a second potentiometer in place of the bias cell. By using this potentiometer in conjunction with a gated-bridge detector, it is possible to adjust the potential of the grids of each triode (V_1) and (V_2) always to the same potential with respect to ground; thus, the matching of the tube characteristics over a wide range of grid potentials is no longer a necessity.

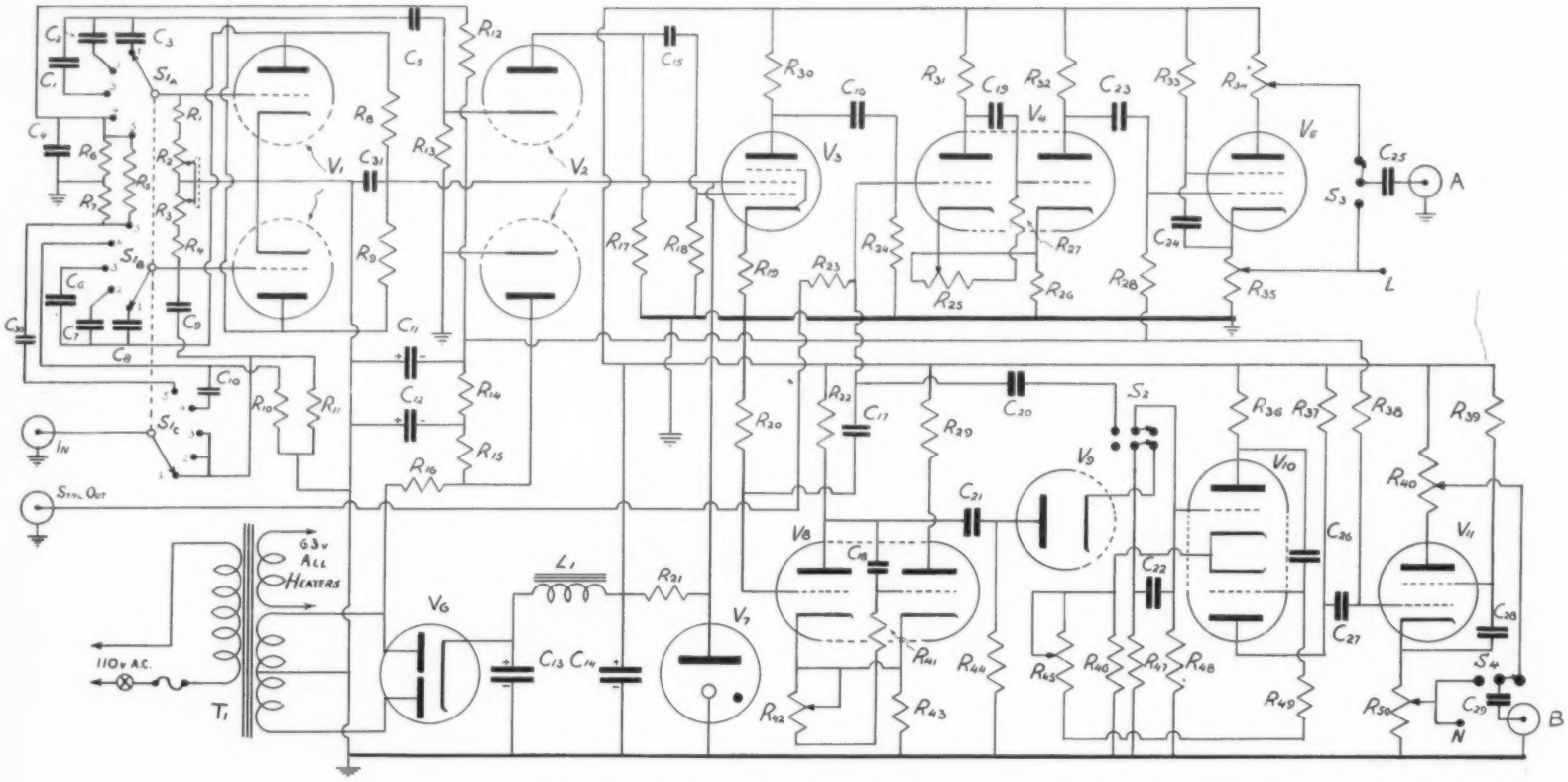

FIG. 2. Circuit diagram of rectangular pulse generator

R_1, R_4, R_{29}, R_{32}, R_{37}	15,000 ohms	R_{27}, R_{41}	250 ohms	C_{13}, C_{14}	20 microfarads (450 volts)
R_2, R_3	250,000 ohms (dual potentiometer)	R_{28}, R_{38}, R_{42}	500,000 ohms	C_{15}, C_{16}	0.00027 microfarads
R_5, R_{12}	100,000 ohms	R_{30}	4,700 ohms	C_{17}, C_{18}, C_{19}, C_{26}	0.001 microfarads
R_6, R_7, R_{10}, R_{14}, R_{15}, R_{45}	50,000 ohms	R_{34}, R_{35}, R_{40}, R_{50}	500 ohms	C_{20}	0.00018 microfarads
R_8, R_{11}	20,000 ohms	R_{49}	200 ohms	C_{21}	0.00007 microfarads
R_9	12,000 ohms	C_1, C_6	0.0005 microfarads	L_1	10 henrys (75 ma)
R_{13}, R_{19}	510 ohms	C_2, C_7	0.003 microfarads		
R_{16}, R_{22}, R_{31}, R_{36}	30,000 ohms	C_3, C_8, C_{22}, C_{23}, C_{27}	0.005 microfarads	V_1, V_4, V_8, V_{10}	6J6
R_{17}, R_{33}, R_{39}, R_{44}, R_{47}	10,000 ohms	C_4, C_{24}, C_{25}, C_{28}, C_{29}	0.1 microfarads	V_2, V_9	6AL5
R_{18}	220,000 ohms	C_5	0.00005 microfarads	V_3	6AG5
R_{20}, R_{23}, R_{24}, R_{48}	51,000 ohms	C_9	0.0002 microfarads	V_5, V_{11}	6AQ5
R_{21}	4,000 ohms	C_{10}, C_{30}	0.0001 microfarads	V_6	6X4
R_{25}	200,000 ohms	C_{11}	10 microfarads (450 volts)	V_7	OA2
R_{26}, R_{43}, R_{46}	1,500 ohms	C_{12}	30 microfarads (150 volts)		

end of … overvolt… at "zero… the con… at the … (Fig. 2) … (V_3) (F… cancella… The ad…

R_1
R_2, R_3,
R_3, R_4,
R_7
R_9
R_{10}
R_{11}
C_1, C_2,

assure… will … ground… plate … a regu… a-c so… drift …

Th… urem…

PULSE INPUT B

PULSE INPUT A

0-5…

end of each pulse influence the measurements of overvoltage, particularly at low current densities and at "zero" time. With the superposition, however, of the concurrent positive pulses which are obtained at the points (L) and (N) of the pulse generator (Fig. 2), on the plates of (V_7) and the cathode of (V_3) (Fig. 3), respectively, nearly complete mutual cancellation of the resulting "spikes" is accomplished. The addition of the diode (V_8), as shown in Fig. 3, assures that the potential at the cathode of (V_3) will never become less negative with respect to ground than a certain predetermined value. The plate voltage for the bridge circuit is obtained from a regulated power supply. Although an unregulated a-c source is used for the filaments, no appreciable drift of the balance has been observed.

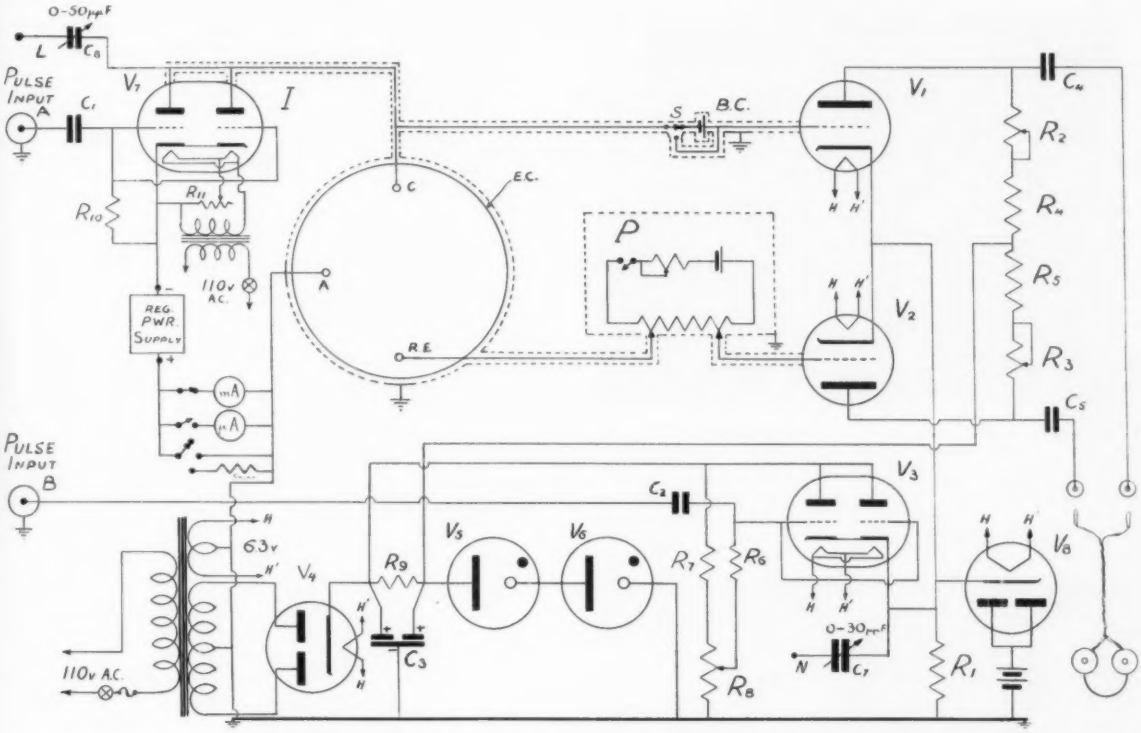

FIG. 3. Circuit diagram of current interruptor and gated-bridge null detector

R_1	500 ohms	C_2 (dual)	20–20 microfarads (450 volts)	V_1, V_2	6SF5
R_2, R_5, R_8	50,000 ohms			V_3, V_7	6N7
R_3, R_4, R_6	100,000 ohms	C_7	0.000030 microfarad variable condenser	V_5, V_6	VR 150
R_7	200,000 ohms			V_4	6X5
R_9	1,500 ohms			V_8	6AL5
R_{10}	1 megohm				
R_{11}	20 ohms	C_8	0.000050 microfarad variable condenser		
C_1, C_2, C_4, C_5	0.1 microfarads				

PERFORMANCE

Three preliminary steps are involved in the measurement of overvoltage with this unit. First, the potentiometer is balanced against a standard cell with an ordinary galvanometer. Following this, the grids of the tubes (V_1) and (V_2) are adjusted to the same potential with respect to ground and the gated-bridge null detector is balanced by means of the plate resistances in the other arms of the bridge (Fig. 3). The overvoltage is measured by connecting the polarized electrode and the reference electrode to the null detector and the potentiometer as shown in Fig. 3. The time-average value for the polarizing current is measured with an ammeter (Fig. 3), while the instantaneous value is determined with the gated-bridge null detector by measuring the potential difference across a resistance which is placed in series with the cell.

In Fig. 4 and 5 are oscillograms obtained with the electronic commutator at a repetition rate of 1200 sec^{-1} and an interruption period of 300 microseconds. Trace (A) in Fig. 4 represents the polarizing current with an average value of 30 ma. The narrow pulses,

superimposed on the trace, are the rectangular pulses which are used to activate the gated-bridge null detector and are approximately 5 microseconds wide and 250 microseconds delayed with respect to the interruption of the polarizing current. Trace (B) in Fig. 4 was obtained by connecting the cathode-ray oscillograph between a bright-platinum cathode and an anode. Anodic variations in terms of oxygen overvoltage have been rendered essentially negligible by

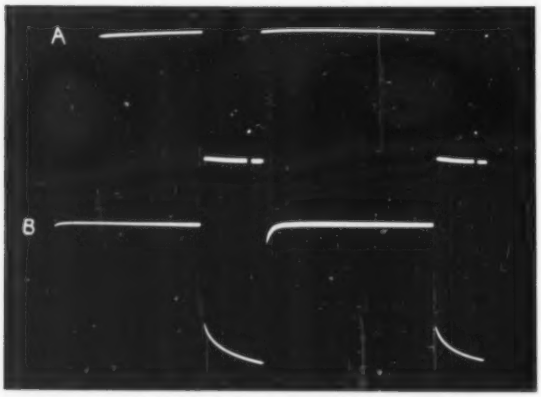

FIG. 4. Oscillograms of the polarizing current (A) and the build-up and decay curves of hydrogen overvoltage on a bright platinum cathode (B). Polarizing current, 30 ma; repetition rate, 1200 sec^{-1}; "Current-off" period, 300 microseconds.

conditions between two ions for a ratio of activities of these ions equal to unity. Circled figures and letters refer to the corresponding equations in the text.

(15) $Ag_2O_3 + 6H^+ + 2e^- = 2Ag^{++} + 3H_2O$
$E = 1.401 - 0.1773\ pH - 0.0591 \log a_{Ag^{++}}$

DESCRIPTION OF THE POTENTIAL-pH DIAGRAM

Fig. 1 has been established on the basis of equilibrium conditions (1) to (15) and represents the circumstances of thermodynamic equilibrium of the system Ag–H_2O at 25°C. The information given in this diagram concerning the oxide of trivalent silver, Ag_2O_3, and the ions Ag^{++} and AgO^+, should be regarded as provisional.

Metallic silver, generally stable in presence of aqueous solutions deprived of complexing substances, such as cyanides, ammonia, sulfite, and thiosulfate ions, can be dissolved by acid oxidizing solutions

interruption of the current. The polarization as shown by trace (B) in Fig. 4 attains a constant value during the period when current is flowing. Trace (B) in Fig. 5, however, indicates that at lower current densities a longer "on" period and a shorter interruption period are required for the polarization to reach a constant value. This can be accomplished with the present apparatus by lowering the frequency of the multivibrator (M in Fig. 1) or reducing the width of the pulses from the univibrator (U_2), or both.

In Fig. 6 typical values for the hydrogen overvoltage on smooth platinum at various times following the interruption of the polarizing current have been superimposed on the trace obtained with a DuMont cathode-ray oscillograph (model 304 TH)

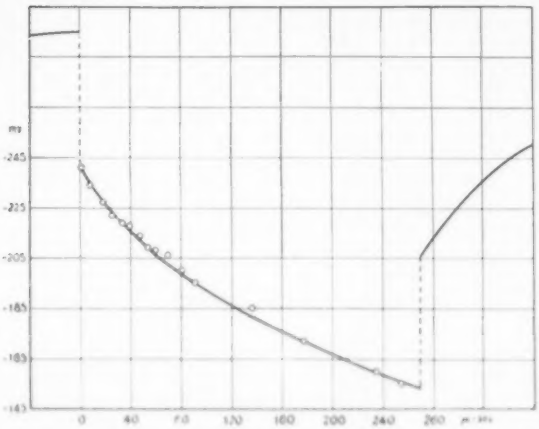

FIG. 6. Decay of hydrogen overvoltage on bright platinum. Prepolarization, 2 hr; current density, 8 ma/cm^2; solution, 0.1*N* HCl. Trace from cathode-ray oscillograph compared with values obtained by the gated detector in conjunction with the potentiometer.

tion of silver as determined from the pote... pH ... dant

In presence of definitely alkaline solutions, metalli... silver is entirely stable. With an oxidant present, i... then covers itself with a protective coating of brown... Ag_2O.

The anodic polarization of silver in presence of a... solution of sodium hydroxide leads first, as has been shown by Hickling and Taylor (10) on the basis of an... oscillographic method, to the formation of a protective film of Ag_2O. This film seems to appear at potentials practically equal to those given by line 4 corresponding to the equilibrium Ag/Ag_2O.

At potentials higher than those given by lines ... and 6 (for instance 0.88 volt at a pH around 13.8) the Ag_2O film covers itself with an unstable peroxide, possibly Ag_2O_3, which decomposes with formation of AgO. During this decomposition the potential decreases and stabilizes itself in the neighborhood ...

developed as part of a research program involving the application of ultrasonics to electrochemistry. The commutator method is particularly suited to the study of the rate of decay of overvoltage in the presence of ultrasonic radiations because small symmetrical electrodes (e.g., short, thin wires) with unobstructed surfaces may be used. The measurement of hydrogen overvoltage both with and without ultrasonics is in progress with this apparatus at the present time and results will be reported in the near future.

Summary

An electronic commutator has been constructed with the following features:

1. Variable current interruption periods with a lower limit of 5 microseconds and an upper limit of 1000 microseconds or one-half the repetition period, whichever is smaller.

2. A variable repetition rate of 20 sec^{-1} through 3000 sec^{-1}.

3. Polarizing currents continuously variable from 10^{-6} through 10^{-1} amp.

4. Provisions for measuring rapidly varying potentials during periods as short as 5 microseconds at any known time after the interruption or the initiation of the polarizing current, thus permitting a quantitative study of the decay as well as the build-up of cathodic or anodic polarization.

5. An accuracy for the potential measurements within ± 5 mv.

Any discussion of this paper will appear in a Discussion Section, to be published in the December 1951 issue of the Journal.

References

1. J. O'M. Bockris, *Chem. Revs.*, **3,** 525 (1948).
2. A. Hickling, *Trans. Faraday Soc.*, **33,** 1540 (1937).
3. A. Hickling and F. W. Salt, *Trans. Faraday Soc.*, **36,** 1226 (1940).
4. J. O'M. Bockris, *Trans. Faraday Soc.*, **43,** 417 (1947).

ions can corrode silver in neutral or acid solution.

11. P. Delahay, *J. Electrochem. Soc.*, **97,** 198, 205 (1950).

Electronic Instrumentation for Overvoltage Measurements[1]

DIMITRIOS STAICOPOULOS, ERNEST YEAGER, AND FRANK HOVORKA

Department of Chemistry, Western Reserve University, Cleveland, Ohio

ABSTRACT

Electronic instrumentation has been developed for the measurement of overvoltage by the commutator or indirect method. With this apparatus current may be interrupted for periods ranging in length from 5 microseconds through one-half the repetition rate for repetition rates from 20 sec^{-1} through 3000 sec^{-1}. Potential measurements may be made at any time while current is either off or on during periods as short as 5 microseconds. Typical accuracy of the potential measurements is $\pm$ 5 mv for measurement periods of 5 microseconds duration at a repetition rate of 1000 sec^{-1}. The potential measurements involve the use of a gated-bridge null detector in conjunction with an ordinary potentiometer.

INTRODUCTION

Two methods are available for overvoltage measurements (1): the direct method and the indirect or commutator method. With the direct method, the potential of the polarized electrode is measured against a reference electrode while current is flowing. To minimize any ohmic voltage drop in the measured potential, the tip (Luggin capillary) of the solution bridge connecting the compartment of the polarized electrode to that of the reference electrode is pressed against the surface of the polarized electrode. With the commutator method, measurements are made while the current is interrupted for a short period and a Luggin capillary is not necessary.

In the past some controversy has existed concerning the reliability of the commutator method because of the difficulty in extrapolating the measured values back to the instant when the current is interrupted. In 1937, Hickling (2) constructed an electronic commutator with which measurements can be made with a precision of 10 mv at the end of interruption periods with a lower limit of 50 microseconds. Because of the rapid decay of hydrogen overvoltage on many metals during the first few microseconds, the extrapolation from 50 microseconds to zero time is difficult, particularly in view of a precision of 10 mv for each measurement. Results (3) obtained with this equipment, however, have been found to be in general agreement (20-30 mv) with the measurements of Bockris (4) who used the direct method. Since the errors associated with the two methods are expected to act in opposite directions, this has served to establish confidence in both methods.

[1] Manuscript received August 14, 1950. This paper prepared for delivery before the Cleveland Meeting, April 19 to 22, 1950. The work reported herein has been partially supported by the Office of Naval Research under Contract No. N7 onr 47002, Project No. NR 051 162.

DESIGN AND CONSTRUCTION

In designing equipment for the measurement of overvoltage by the commutator method, the authors have attempted to incorporate the following features:

1. An interruption period of variable length with a lower limit of 5 microseconds and an upper limit of the order of 1000 microseconds or one-half the repetition period (depending on which is smaller).
2. A variable repetition or recursion rate with a lower limit of 20 sec^{-1} and an upper limit of 3000 sec^{-1}.
3. Polarizing currents variable from 10^{-6} through 10^{-1} amp.
4. Provisions for measuring potentials during periods as short as 5 microseconds at any known time after the interruption or initiation of the polarizing current.
5. An accuracy for the potential measurements of 5 mv for measurement periods as short as 5 microseconds.

In terms of these provisions it is possible to establish quantitatively the decay and build-up curves for overvoltage. The present unit can be used to measure cathodic and anodic polarization.

Fig. 1 shows a block diagram which indicates the functions of the various components of the apparatus. The output from a multivibrator (shown in detail in Fig. 2) is differentiated and the resulting positive pulses deleted by means of a diode, while the remaining negative pulses are subsequently amplified (A). In turn, these pulses trigger a univibrator or one-shot multivibrator (U_1) which produces rectangular pulses of controllable duration. After adequate amplification, the rectangular pulses are used to activate the current interruptor (I). The latter (Fig. 3) consists of a duo-triode, type 6N7 (V_7) with the two sections connected in parallel. Higher polarizing currents may be obtained by the introduction of one or more duo-triodes (6N7) in parallel with

(V_7) in Fig. 3. The electrolytic cell to be polarized is placed in series with these triodes. The bias of the tubes is such that the triodes normally conduct and the current may be abruptly reduced to zero when negative pulses are introduced in the grid circuit. The magnitude of the polarizing current is controlled by adjusting the filament current, and hence, the filament temperature of the duo-triodes.

The same pulses which trigger the univibrator (U_1) also trigger a similar unit (U_2) which serves effectively as a pulse delay stage. The rectangular pulses from this univibrator (U_2) are differentiated and the leading negative edges are deleted with a diode while the trailing positive pulses are used to trigger a third univibrator (U_3). When the rectangular pulses produced by univibrator (U_2) are lengthened, the leading edge of each pulse remains fixed with respect to the trigger pulse while the trailing edge lags farther behind. Hence, a variable delay time is involved in the triggering of univibrator (U_3) relative to the triggering of univibrator (U_1). The delay time is essentially equal to the pulse duration obtained with univibrator (U_2). Univibrator (U_3) then produces rectangular pulses of variable duration which after amplification are used to control the on-off action of the gated-bridge null detector.

The null detector effectively serves as a galvanometer in the potential measurements and is used in conjunction with a Leeds & Northrup student-type potentiometer (P in Fig. 3). The duo-triode 6N7 (V_3 in Fig. 3) with the two triodes in parallel is normally conducting and biases the high-mu triodes 6SF5 (V_1 and V_2 in Fig. 3) in the arms of the bridge well beyond cutoff. With the introduction of a negative pulse on the grids of the duo-triode (V_3), this tube is cut off sharply and the bias on tubes (V_1) and (V_2) drops to a value at which the tubes conduct. If there is any potential difference between the grids of the tubes (V_1) and (V_2) when the tubes are conducting, an unbalanced condition results in the bridge and is registered as a sound in the earphones. The triodes (V_1) and (V_2) are carefully matched for linear performance over the range of grid potentials from -2.5 to 0 volts[2]. A biasing cell (B.C. in Fig. 3) has also been incorporated in the grid circuit to insure that the grid potential is in the linear range during the overvoltage measurements. The grid circuits of both triodes, as well as the potentiometer, have been shielded in order to prevent stray pickup, particularly 60 cycle. Due to the grid-to-plate capacity of the duo-triode (V_7) and the grid-to-cathode capacity of the duo-triode (V_3), the two negative pulses applied at (A) and (B) appear differentiated at the plates of (V_7) and at the cathode of the duo-triode (V_3), respectively, owing to the relatively low resistance of the electrolytic cell and the low cathode resistance (R_1) of (V_3) in Fig. 3. The resulting negative and positive "spikes" at the beginning and the

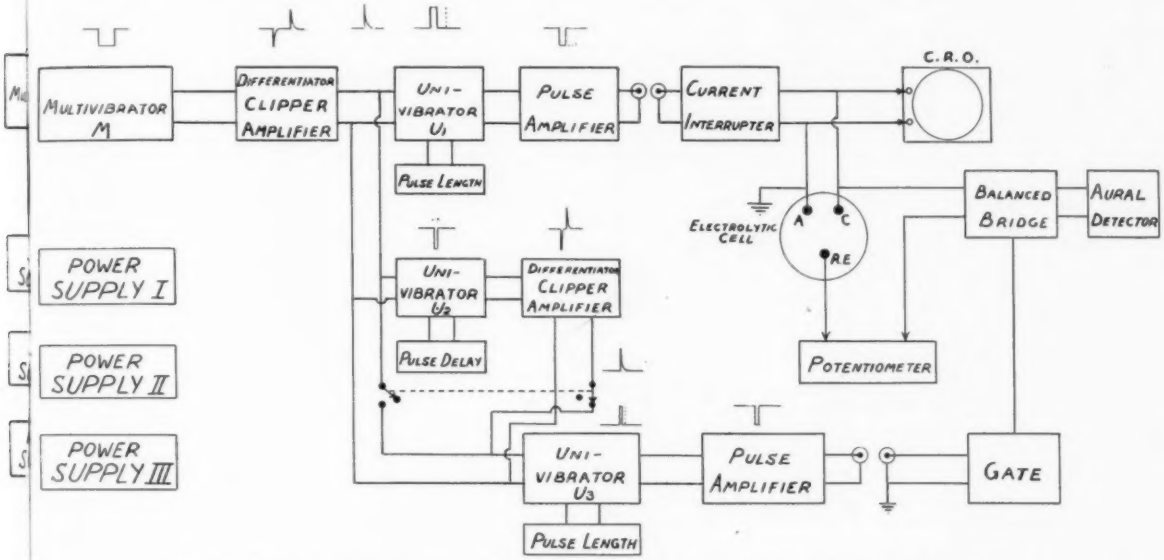

FIG. 1. Block diagram of apparatus for overvoltage measurements by the commutator method

[2] At the present time a modification of this circuit is being used which involves the introduction of a second potentiometer in place of the bias cell. By using this potentiometer in conjunction with a gated-bridge detector, it is possible to adjust the potential of the grids of each triode (V_1) and (V_2) always to the same potential with respect to ground; thus, the matching of the tube characteristics over a wide range of grid potentials is no longer a necessity.

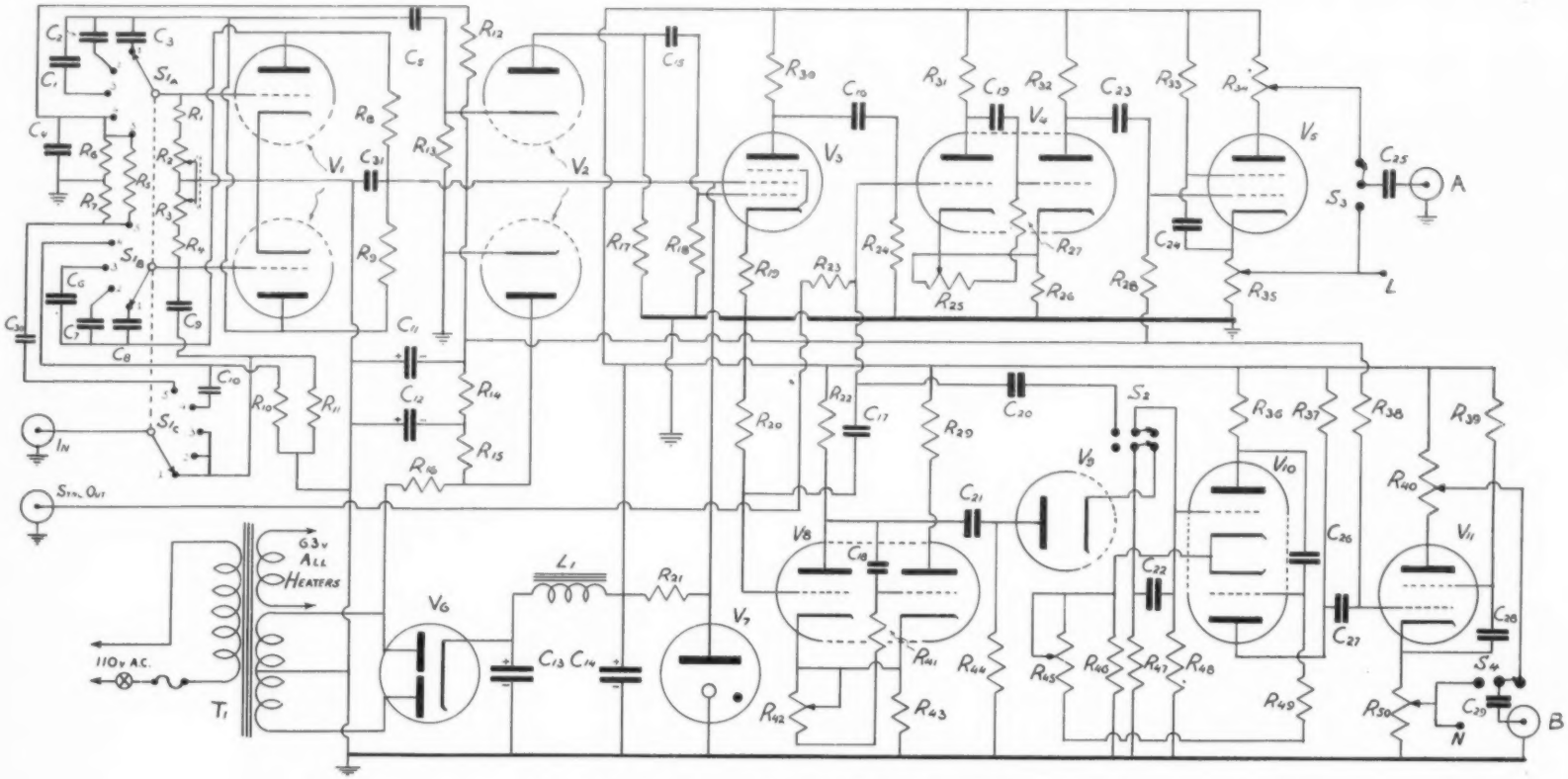

FIG. 2. Circuit diagram of rectangular pulse generator

R_1, R_4, R_{29}, R_{32}, R_{37}	15,000 ohms	R_{27}, R_{41}	250 ohms	C_{13}, C_{14}	20 microfarads (450 volts)
R_2, R_3	250,000 ohms (dual potentiometer)	R_{28}, R_{38}, R_{42}	500,000 ohms	C_{15}, C_{16}	0.00027 microfarads
		R_{30}	4,700 ohms	C_{17}, C_{18}, C_{19}, C_{26}	0.001 microfarads
R_5, R_{12}	100,000 ohms	R_{34}, R_{35}, R_{40}, R_{50}	500 ohms	C_{20}	0.00018 microfarads
R_6, R_7, R_{10}, R_{14}, R_{15}, R_{45}	50,000 ohms	R_{49}	200 ohms	C_{21}	0.00007 microfarads
R_8, R_{11}	20,000 ohms				
R_9	12,000 ohms	C_1, C_6	0.0005 microfarads	L_1	10 henrys (75 ma)
R_{13}, R_{19}	510 ohms	C_2, C_7	0.003 microfarads		
R_{16}, R_{22}, R_{31}, R_{36}	30,000 ohms	C_3, C_8, C_{22}, C_{23}, C_{27}	0.005 microfarads	V_1, V_4, V_8, V_{10}	6J6
R_{17}, R_{33}, R_{39}, R_{44}, R_{47}	10,000 ohms	C_4, C_{24}, C_{25}, C_{28}, C_{29}	0.1 microfarads	V_2, V_9	6AL5
R_{18}	220,000 ohms	C_5	0.00005 microfarads	V_3	6AG5
R_{20}, R_{23}, R_{24}, R_{48}	51,000 ohms	C_9	0.0002 microfarads	V_5, V_{11}	6AQ5
R_{21}	4,000 ohms	C_{10}, C_{20}	0.0001 microfarads	V_6	6X4
R_{25}	200,000 ohms	C_{11}	10 microfarads (450 volts)	V_7	OA2
R_{26}, R_{43}, R_{46}	1,500 ohms	C_{12}	microfarads (150 volts)		

end of
overvo
at "zer
the co
at the
(Fig. 2
(V_3) (
cancell
The ac

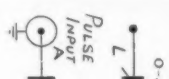

R_1
R_2, R_3
R_5, R_{12}
R_7
R_9
R_{10}
R_{11}
C_1, C_2

assur
will
groun
plate
a reg
a-c s
drift

The
urem

end of each pulse influence the measurements of overvoltage, particularly at low current densities and at "zero" time. With the superposition, however, of the concurrent positive pulses which are obtained at the points (L) and (N) of the pulse generator (Fig. 2), on the plates of (V_7) and the cathode of (V_3) (Fig. 3), respectively, nearly complete mutual cancellation of the resulting "spikes" is accomplished. The addition of the diode (V_8), as shown in Fig. 3, assures that the potential at the cathode of (V_3) will never become less negative with respect to ground than a certain predetermined value. The plate voltage for the bridge circuit is obtained from a regulated power supply. Although an unregulated a-c source is used for the filaments, no appreciable drift of the balance has been observed.

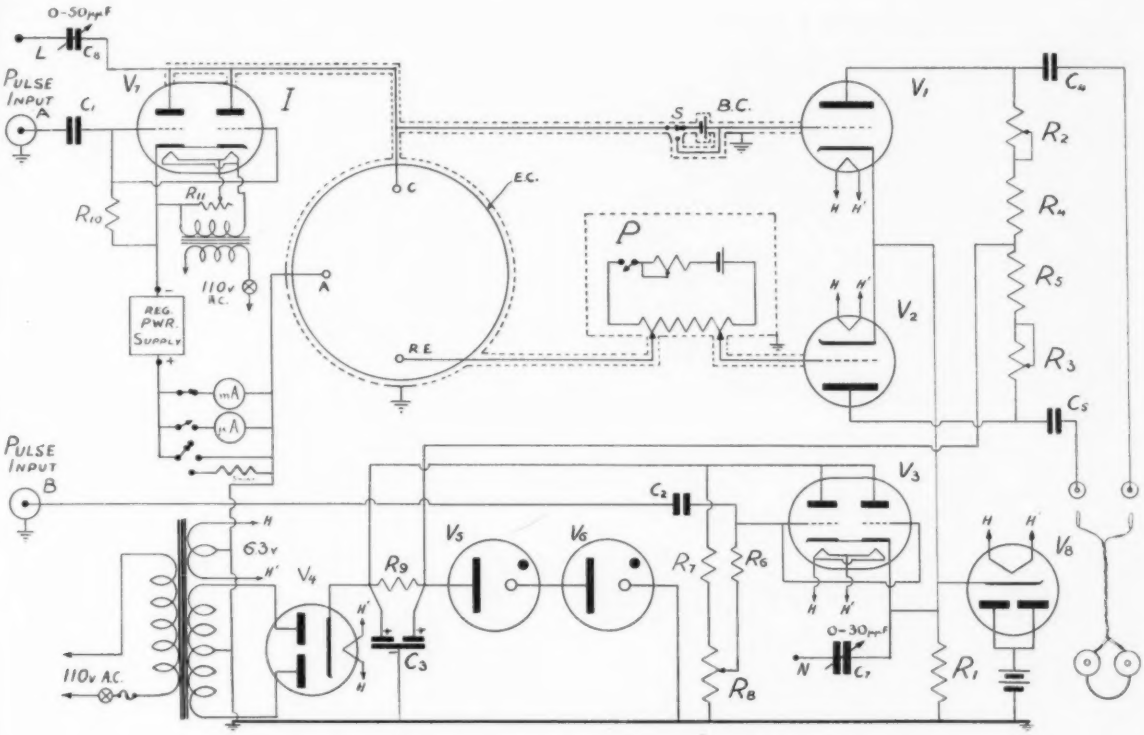

FIG. 3. Circuit diagram of current interruptor and gated-bridge null detector

R_1	500 ohms	C_3 (dual)	20–20 microfarads (450 volts)	V_1, V_2	6SF5
R_2, R_5, R_3	50,000 ohms			V_3, V_7	6N7
R_3, R_4, R_6	100,000 ohms	C_7	0.000030 microfarad variable condenser	V_5, V_6	VR 150
R_7	200,000 ohms			V_4	6X5
R_9	1,500 ohms			V_8	6AL5
R_{10}	1 megohm				
R_{11}	20 ohms	C_8	0.000050 microfarad variable condenser		
C_1, C_2, C_4, C_5	0.1 microfarads				

PERFORMANCE

Three preliminary steps are involved in the measurement of overvoltage with this unit. First, the potentiometer is balanced against a standard cell with an ordinary galvanometer. Following this, the grids of the tubes (V_1) and (V_2) are adjusted to the same potential with respect to ground and the gated-bridge null detector is balanced by means of the plate resistances in the other arms of the bridge (Fig. 3). The overvoltage is measured by connecting the polarized electrode and the reference electrode to the null detector and the potentiometer as shown in Fig. 3. The time-average value for the polarizing current is measured with an ammeter (Fig. 3), while the instantaneous value is determined with the gated-bridge null detector by measuring the potential difference across a resistance which is placed in series with the cell.

In Fig. 4 and 5 are oscillograms obtained with the electronic commutator at a repetition rate of 1200 sec^{-1} and an interruption period of 300 microseconds. Trace (A) in Fig. 4 represents the polarizing current with an average value of 30 ma. The narrow pulses,

superimposed on the trace, are the rectangular pulses which are used to activate the gated-bridge null detector and are approximately 5 microseconds wide and 250 microseconds delayed with respect to the interruption of the polarizing current. Trace (B) in Fig. 4 was obtained by connecting the cathode-ray oscillograph between a bright-platinum cathode and an anode. Anodic variations in terms of oxygen overvoltage have been rendered essentially negligible by

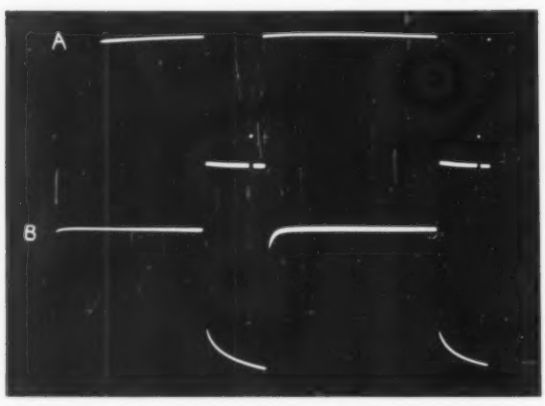

FIG. 4. Oscillograms of the polarizing current (A) and the build-up and decay curves of hydrogen overvoltage on a bright platinum cathode (B). Polarizing current, 30 ma; repetition rate, 1200 sec^{-1}. "Current-off" period, 300 microseconds.

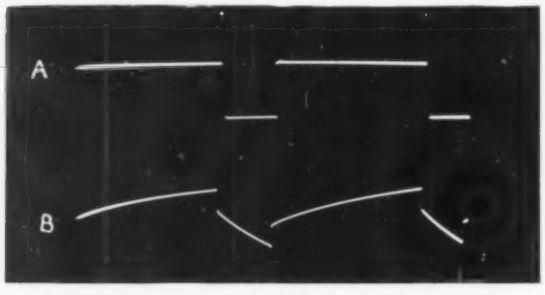

FIG. 5. Oscillograms of the polarizing current (A) and the build-up and decay curves of hydrogen overvoltage on a bright platinum cathode (B). Polarizing current, 0.7 ma; repetition rate, 1200 sec^{-1}. "Current-off" period, 300 microseconds.

the use of a large platinized-platinum anode (approximately 100 times the apparent area of the cathode) with hydrogen gas bubbling through the anode compartment. For the current trace (A) as well as the rectangular pulses used to activate the detector, the rise time is a fraction of a microsecond. The traces in Fig. 5 are analogous to those of Fig. 4 except that the average value for the polarizing current is 700 microamp and the gated-bridge null detector is activated within a fraction of a microsecond after the interruption of the current. The polarization as shown by trace (B) in Fig. 4 attains a constant value during the period when current is flowing. Trace (B) in Fig. 5, however, indicates that at lower current densities a longer "on" period and a shorter interruption period are required for the polarization to reach a constant value. This can be accomplished with the present apparatus by lowering the frequency of the multivibrator (M in Fig. 1) or reducing the width of the pulses from the univibrator (U_2), or both.

In Fig. 6 typical values for the hydrogen overvoltage on smooth platinum at various times following the interruption of the polarizing current have been superimposed on the trace obtained with a DuMont cathode-ray oscillograph (model 304 TH)

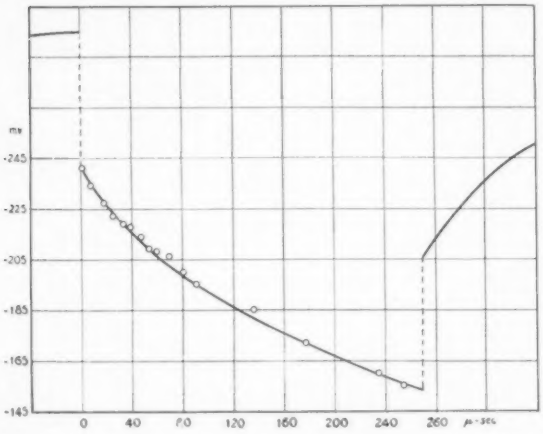

FIG. 6. Decay of hydrogen overvoltage on bright platinum. Prepolarization, 2 hr; current density, 8 ma/cm^2; solution, 0.1*N* HCl. Trace from cathode-ray oscillograph compared with values obtained by the gated detector in conjunction with the potentiometer.

during the same period. The agreement between the circled points representing the measured potentials and the continuous curve representing the oscillogram is generally indicative of an accuracy of the order of 5 mv or less.

In using the electronic commutator for the measurement of overvoltage, it is important that the internal resistance between the polarized hydrogen electrode and the anode, which is grounded, be low compared to the impedance of the measuring circuit. The latter is almost entirely capacitive and includes the capacity of the grid circuit to ground as a result of the shielding. In the present unit the input capacity is approximately 100 micro-microfarads. For an internal resistance of less than 500 ohms, no appreciable distortion of the decay or build-up curves for the polarization should result.

The apparatus described in this paper has been

developed as part of a research program involving the application of ultrasonics to electrochemistry. The commutator method is particularly suited to the study of the rate of decay of overvoltage in the presence of ultrasonic radiations because small symmetrical electrodes (e.g., short, thin wires) with unobstructed surfaces may be used. The measurement of hydrogen overvoltage both with and without ultrasonics is in progress with this apparatus at the present time and results will be reported in the near future.

Summary

An electronic commutator has been constructed with the following features:

1. Variable current interruption periods with a lower limit of 5 microseconds and an upper limit of 1000 microseconds or one-half the repetition period, whichever is smaller.

2. A variable repetition rate of 20 sec^{-1} through 3000 sec^{-1}.

3. Polarizing currents continuously variable from 10^{-6} through 10^{-1} amp.

4. Provisions for measuring rapidly varying potentials during periods as short as 5 microseconds at any known time after the interruption or the initiation of the polarizing current, thus permitting a quantitative study of the decay as well as the build-up of cathodic or anodic polarization.

5. An accuracy for the potential measurements within ± 5 mv.

Any discussion of this paper will appear in a Discussion Section, to be published in the December 1951 issue of the Journal.

References

1. J. O'M. Bockris, *Chem. Revs.*, **3,** 525 (1948).
2. A. Hickling, *Trans. Faraday Soc.*, **33,** 1540 (1937).
3. A. Hickling and F. W. Salt, *Trans. Faraday Soc.*, **36,** 1226 (1940).
4. J. O'M. Bockris, *Trans. Faraday Soc.*, **43,** 417 (1947).

Luminescence of K_4MnCl_6 and KCl (Pb + Mn)[1]

ROBERT J. GINTHER

Crystal Branch, Metallurgy Division, Naval Research Laboratory, Washington, D. C.

ABSTRACT

Excitation and emission spectra of K_4MnCl_6 and KCl (Pb + Mn) are reported. A method for the preparation of K_4MnCl_6 from solution at room temperature is described. Lead and thallium are shown to produce sensitized luminescence in this phosphor.

INTRODUCTION

In the course of an investigation of the sensitized luminescence of the alkali halide phosphors, it was found that no manganese-activated luminescent potassium chloride phase could be prepared by the method used by Schulman, *et al.*, (1) for sodium chloride. This method employed precipitation from a mixed solution of potassium, lead, and manganous chloride with concentrated hydrochloric acid. The only visibly luminescent phase obtained from the above solution proved to be K_4MnCl_6.

Preparation of this compound from solution at elevated temperatures (2) and by solid phase reaction (3) has been reported, and it is found in nature as the mineral chloromanganokalite. Its structure has been determined by Bellanca (4). However, neither its luminescent properties nor a method for its preparation from solution at room temperature have been described.

PROCEDURE AND RESULTS

Preparation

To prepare the phosphor from solution, 250 ml of concentrated hydrochloric acid were added to 100 ml of a solution of potassium and manganous chlorides. Lead or thallium was introduced into the phosphor by adding $PbCl_2$ or TlCl to the salt solution before precipitation. The optimum potassium and manganese concentrations in solution were found to be dependent upon the lead concentration. The optimum manganese content of a solution of 0.117 g KCl per ml and up to 0.030 g $PbCl_2$ per ml was found to be 0.350 g $MnCl_2 \cdot 4H_2O$ per ml. For solutions of the same KCl concentration, but containing from 0.075 to 0.225 g $PbCl_2$ per ml, the optimum $MnCl_2 \cdot 4H_2O$ concentration was 0.250 g per ml. The effect of either raising the potassium or lowering the manganese concentration from the optimum is to contaminate the product with KCl. Increasing the manganese concentration causes the precipitate to be diluted with a nonluminescent manganese-bearing phase, while decreasing the KCl concentration seriously reduces the yield.

To prepare K_4MnCl_6 by solid phase reaction, stoichiometric quantities of KCl and $MnCl_2$, with or without lead or thallium, were melted together in either an HCl atmosphere or in vacuo and then annealed below 430°C.

KCl(Pb + Mn) phosphor has been prepared previously by melt techniques (5, 6), but no detailed information as to its luminescent properties is available. In order to compare its properties with those of K_4MnCl_6 a series of compositions were prepared by melting together the component halides in HCl atmosphere or in vacuo.

A luminescent combination of KCl, $MnCl_2 \cdot 4H_2O$, and $PbCl_2$ can be prepared by simply grinding these materials together in a mortar. The concentrations of the components are not at all critical, but for rapid reaction large quantities of lead should be used. Thallium cannot be substituted for lead in this process.

Identification and Analysis

Phase identification was based upon microscopic and x-ray examination. Lead, thallium, and manganese were determined polarographically.

The most efficient and homogeneous phosphors were those prepared by precipitation. Even the most uniform samples contained traces of free KCl and of an unidentified manganese-containing phase. However, all of the precipitated samples selected for optical testing were essentially K_4MnCl_6, and their compositions ranged only from 3.9–4.2 moles of KCl per mole of $MnCl_2$. The lead contents were found to be low: about one hundredth of the lead content of KCl precipitated from solution of the same lead concentration but of a manganese concentration which permitted the precipitation of only KCl. This is shown in Table I where the lead and manganese contents of a series of precipitates are tabulated. Table II gives the lead contents of several preparations all of which were essentially K_4MnCl_6.

It is seen that the lead content of the precipitate

[1] Manuscript received July 31, 1950. This paper prepared for delivery before the Washington Meeting, April 8 to 12, 1951.

does not vary continuously with the lead content of the solution. This is not believed to be significant for two reasons: (*a*) the height of the lead excitation band was found to be dependent upon the lead concentration of the solution not upon the lead concentration in the precipitate; (*b*) all samples contain small amounts of KCl as a separate phase. It was shown in Table I that the Pb/K ratio can be expected to be nearly seventy times greater in the KCl phase than in the K_4MnCl_6 composition produced from solutions of the same lead concentration. The lead content of the K_4MnCl_6 precipitate will, therefore, be greatly influenced by the amount of free KCl present along with it. For instance, according to the data of Table I the Pb/K ratio of KCl precipitated from a solution of 0.001 g $PbCl_2$ per ml is about 8.0×10^{-3} while the Pb/K ratio of K_4MnCl_6 produced from a solution of the same lead concentration is only 1.1×10^{-4}. If the K_4MnCl_6 contained one per cent of free KCl of Pb/K ratio of 8.0×10^{-3} this free KCl would provide over seventy per cent of the lead found in the sample. For these reasons it is believed that the lead analysis, although precise, gives only a value which the real lead content of the luminescent phase does not exceed.

The precipitated phosphors containing thallium were less uniform and efficient than the lead-bearing precipitates. From solutions of from 3.0×10^{-5} to 2.25×10^{-3} g Tl per ml phosphors were precipitated which contained from 2.0×10^{-5} to 4.1×10^{-3} mole thallium per mole of potassium. The interpretation of the thallium analyses is subject to the same restriction mentioned for the lead analyses.

Dry reaction produced inefficient phosphors. K_4MnCl_6 could always be identified as a major component in samples prepared from KCl and $MnCl_2$ in the 4-1 ratio, but a large excess of KCl and another manganese-bearing phase were always present. KCl (Pb + Mn) and KCl (Tl + Mn) phosphors consisted of a single phase, but were very inefficient. Lead and thallium both volatilize at the melting point of KCl, so that the lead or thallium concentration of phosphors prepared by this technique will be lower than the concentration added to the melt. The samples prepared by dry reaction were not of sufficient interest to warrant their analysis because of the poor efficiency of the KCl phosphor and the lack of homogeneity of the K_4MnCl_6 composition.

The identity of the phosphor prepared by grinding together KCl, $MnCl_2 \cdot 4H_2O$, and $PbCl_2$ remains obscure. It could not be identified microscopically or by x-ray methods because of the large excess of the reactants. Its luminescence properties resemble those of KCl (Pb + Mn) rather than those of K_4MnCl_6.

Luminescence Emission

The emission spectra were determined with an automatic recording spectroradiometer. Three different sources of excitation were used. A "Mineralite" lamp with Corning #9863 filter was used as a source of 2537 Å while a CH-4 type mercury lamp with Corning #5860 filter provided 3650 Å radiation. To obtain a strong source of radiation between these wavelengths, the quartz burner was removed from a CH-4 lamp and sealed into a fused silica envelope with one third of an atmosphere of argon. This lamp, when used with a Corning #9863 filter, is an excellent source of excitation in the region 2700–3000 A. It made possible the measurement of the spectral distribution of emission of the KCl (Pb + Mn) phosphors which could not be determined with either 2537Å or 3650 A radiation. It also provided a source for the excitation of K_4MnCl_6(Pb) in the lead excitation band at 2900 Å.

TABLE I. *KCl concentration 0.117 g/ml; $PbCl_2$ concentration 0.001 g/ml*

Conc. $MnCl_2 \cdot 4H_2O$ (g/ml)	Conc. Pb in precipitate (mole %)	Mole ratio Pb/K in precipitate	Conc. Mn in precipitate (mole %)	Phase produced
0.000	0.74	7.4×10^{-3}	<0.01	KCl
0.005	0.74	7.4×10^{-3}	<0.01	KCl
0.035	0.80	8.0×10^{-3}	<0.01	KCl
0.250	0.045	1.1×10^{-4}	19.1	K_4MnCl and KCl

TABLE II. *KCl concentration 0.117 g/ml*

Conc. $MnCl_2 \cdot 4H_2O$ (g/ml)	Conc. $PbCl_2$ (g/ml)	Conc. Pb in precipitate (mole %)	Mole ratio Pb/K in precipitate
0.350	0.00000	<0.003	
0.350	0.00003	0.02	5×10^{-5}
0.350	0.00015	0.06	1.5×10^{-4}
0.350	0.00030	0.01	2.5×10^{-5}
0.250	0.00075	0.12	3×10^{-4}
0.250	0.00150	0.079	2×10^{-4}
0.250	0.00225	0.094	2.4×10^{-4}

The emission spectra are shown in Fig. 1. All the precipitated samples gave the same emission in the wavelength range 5000–7000 Å. Using all three types of excitation, the same 6000 Å–6100 Å peaked band was obtained. In addition, ultraviolet emission from both the lead- and thallium-bearing phosphors was observed under the shorter wavelength excitation sources, but not under 3650 Å. Since at least some part of this ultraviolet emission is certainly from the lead or thallium-activated KCl phase present, there seems to be no justification for attributing any ultraviolet emission to the K_4MnCl_6 phase without further evidence. This phase of the investigation

was not of sufficient interest to warrant further study.

Of the KCl (Pb + Mn) phosphors, only those of about 0.01 mole per cent Pb and 0.20 mole per cent Mn were bright enough to permit the determination of their emission spectra. The peak for this phosphor was found to be at 6300 Å. Lower manganese concentrations gave very dim phosphors, while the excitation data indicated the presence of K_4MnCl_6 in preparations in which the manganese concentration was increased to only 2.0 mole per cent.

Beckman quartz monochromator. A Corning #2424 filter was used between the sample and phototube to separate the orange-red manganese emission from any ultraviolet emission or reflected light from the sample. Correction to equal energy of excitation was not made, but adequate precautions were taken to assure that all the observed peaks were real.

The excitation spectrum of the precipitated sample containing neither lead nor thallium is shown in Fig. 2. It consists of nine distinct peaks between 2200 Å and 5600 Å. Since the spectrum of the hydrogen

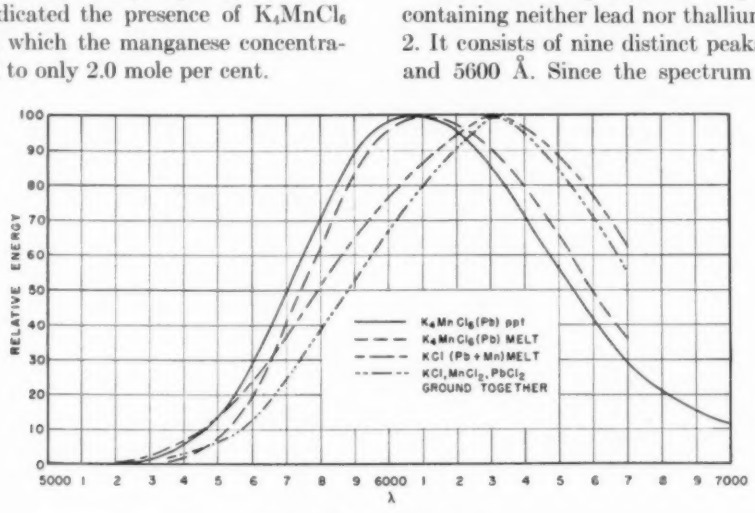

FIG. 1. Emission spectra

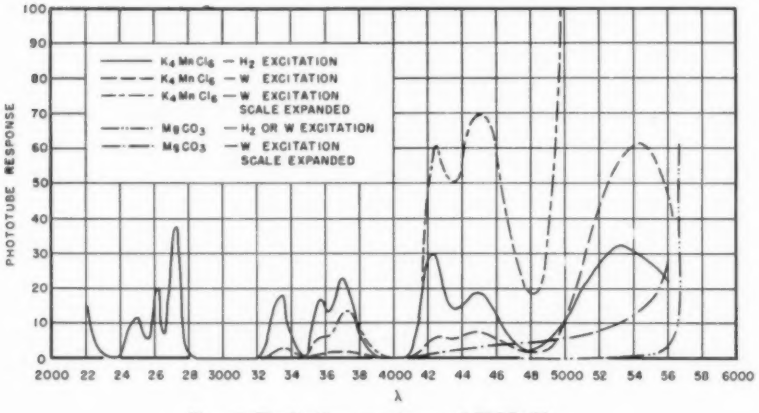
PHOTOTUBE RESPONSE
λ
K_4MnCl_6 — H_2 EXCITATION
K_4MnCl_6 — W EXCITATION
K_4MnCl_6 — W EXCITATION SCALE EXPANDED
$MgCO_3$ — H_2 OR W EXCITATION
$MgCO_3$ — W EXCITATION SCALE EXPANDED

FIG. 2. Excitation spectrum of K_4MnCl_6

The K_4MnCl_6 composition prepared from the melt has essentially the same emission spectrum as that of the precipitated phosphor. A minor shift to longer wavelengths is evident, as might be expected from the Pb + Mn activation of the relatively large amount of free KCl known to be associated with it.

The emission of the phosphor prepared by grinding together KCl, $MnCl_2 \cdot 4H_2O$, and $PbCl_2$ resembles that of KCl (Pb + Mn).

Excitation Spectra

The excitation spectra were measured in the usual manner, using a Beckman hydrogen lamp, and a discharge lamp was known to contain lines at wavelengths longer than about 3500 Å, it remained to prove that none of the observed peaks were due to structure in the hydrogen discharge. The results obtained by replacing the hydrogen lamp with a tungsten lamp are reproduced in the same figure. Two curves are shown. One, using the same amplifier sensitivity used with the hydrogen lamp, clearly resolves the visible bands. The second curve, for which a tenfold greater amplifier sensitivity was used, reproduces the peaks in the blue and near ultraviolet. Blank runs at both sensitivities in which the sample was replaced by a plaque of $MgCO_3$ smoked with

MgO proved that neither transmission nor fluorescence of the filter was introducing any spurious results.

The excitation spectra of some precipitates containing lead are shown in Fig. 3. As little as 3×10^{-5} g $PbCl_2$ per ml, in the solution from which the phosphor was precipitated, produces a new excitation peak at about 2900 Å. The height of this peak rises continuously with increasing lead concentration of solution. The curves in this figure are plotted out to only 4000 Å, but all the precipitated samples had all

The possiblity that the 2730 Å peak might be due to lead impurity (which seems to be present in all available KCl), and that the peak position is concentration dependent, or that any of the short wave peaks are due to impurities, was quickly disproved. A sample was prepared from specially purified materials[2] without addition of lead. Its excitation spectrum contained the same nine peaks with the same relative heights as found previously.

Fig. 4 gives the excitation spectra of the precipitated K_4MnCl_6 containing thallium. Two new peaks

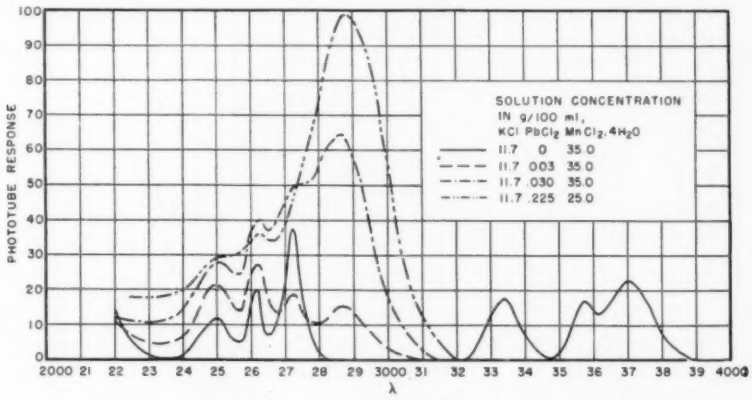

FIG. 3. Excitation spectra of precipitated K_4MnCl_6(Pb)

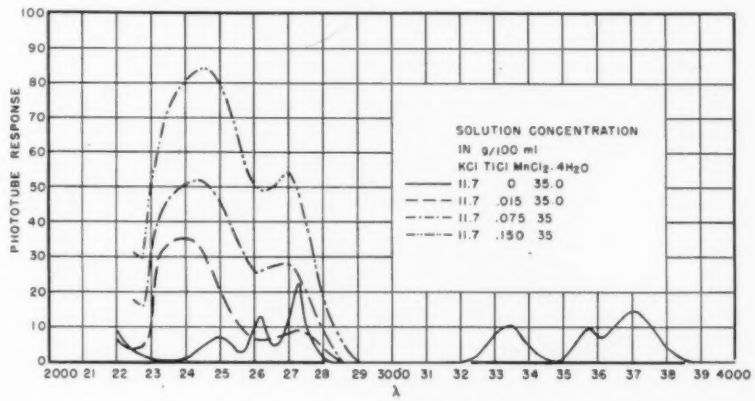

FIG. 4. Excitation spectra of precipitated K_4MnCl_6(Tl)

six peaks at wavelengths longer than 3200 Å, and the relative heights of these six peaks were the same in all samples. The curves were plotted by setting the peak height at 3340 Å equal in all samples whereupon the heights of all the peaks at longer wavelengths coincided. There is a real change in the relative heights of the three short wavelength peaks upon the addition of lead. The increased height of the 2500 Å and 2630 Å peaks could be attributed to their superposition upon the tail of the lead peak, but superposition could not be made to account for the reduction in the 2730 Å peak which was coincident with the first appearance of the 2900 Å peak.

one at about 2450 Å and one at 2700 Å, are found. Again the spectra are shown only out to 4000 Å, but the excitation spectra of all the precipitated samples were identical both as to position and relative height of peak at wavelengths greater than 3200 Å.

[2] $MnCl_2$ was purified by partial precipitation of the carbonate. Impurities were extracted from KCl with dithizone. The efficacy of the latter procedure in removing lead is best indicated by the absence of any ultraviolet luminescence in the purified KCl under 2730 Å excitation. This test is sensitive to much less lead than can be detected spectrographically in our laboratory. Our lower limit for spectrographic detection of lead in KCl is about half a part per million.

To determine whether the position of the lead excitation peak is in any way concentration dependent, a series of samples of K_4MnCl_6 composition with increasing lead concentration was prepared by solid phase reaction. The excitation spectra of these phosphors are shown in Fig. 5. It is seen that the lead peak remained at about 2900 Å for the range of lead additions from 5×10^{-4} to 0.5 mole per cent. Most of the phosphors of this series were too inefficient to permit the use of the 0.5-mm slit width needed to clearly resolve all the peaks. However, per cent causes only the growth of this same band. It seems logical to conclude, therefore, that the 2750 band in the sample to which no lead was added is due to lead impurity in the KCl. This is in accord with the observations made upon the ultraviolet luminescence of the KCl raw material as described previously. New excitation peaks appear with lead additions of 0.05 mole per cent and higher, but little attention was paid to these samples except to ob serve that their excitation spectra resembled that o the phosphor prepared by grinding together KC

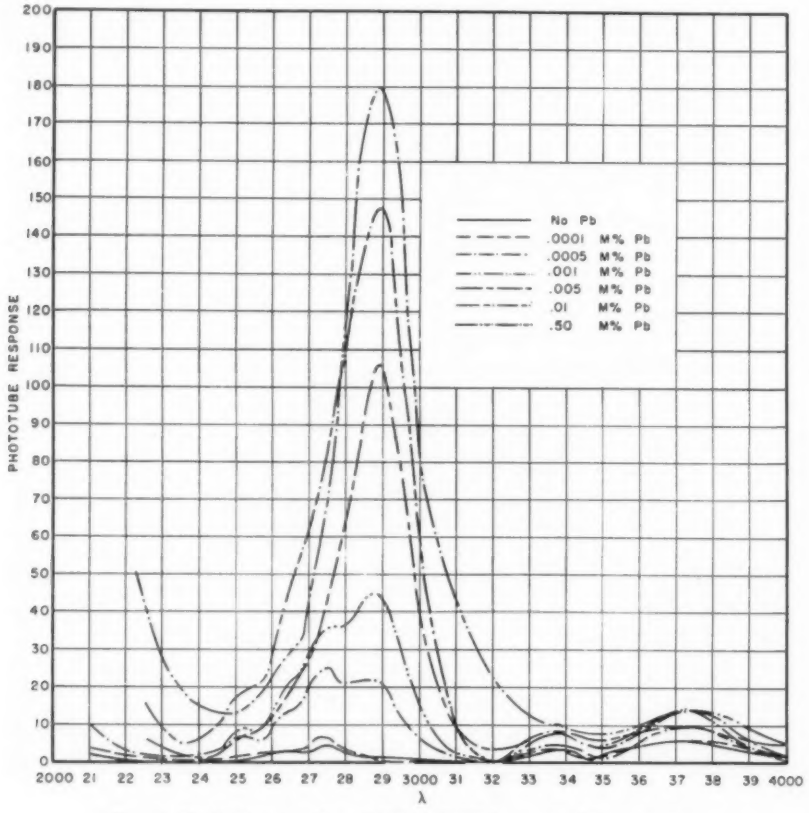

FIG. 5. Excitation spectra of K_4MnCl_6(Pb) prepared from melts

evidence that the long wave ultraviolet peaks are present is unmistakable. The samples were not uniform and were difficult to reproduce from the viewpoint of emission efficiency. Hence it is apparent that any lead analysis or attempt to determine the true solubility of lead by x-ray diffraction methods would be impractical.

The KCl(Pb + Mn) phosphors were very inefficient, but their excitation spectra provide some interesting data. Fig. 6 represents the excitation spectra of a series of KCl (0.20 mole % Mn) phosphors with increasing additions of lead. The sample to which no lead was added has a very weak excitation peaked at 2750 Å. Addition of lead up to 0.01 mole $MnCl_2 \cdot 4H_2O$, and $PbCl_2$. Neither the latter material nor any of the melts of low manganese content had any of the characteristic excitation peaks of K_4MnCl_6 in the long wave ultraviolet or visible region.

The excitation spectra of a series of KCl (0.01 mole per cent Pb) phosphors with increasing manganese concentration are shown in Fig. 7. Again the 0.5-mm slit width could not be used, but in some of the samples the characteristic peaks of K_4MnCl_6 are easily distinguishable although unresolved. The long wavelength peaks are apparent in the record of the sample containing only 10.0 mole per cent Mn and to a less extent in that of the 5.0 mole per cent sample. The 2900 Å peak is evident as a broadening

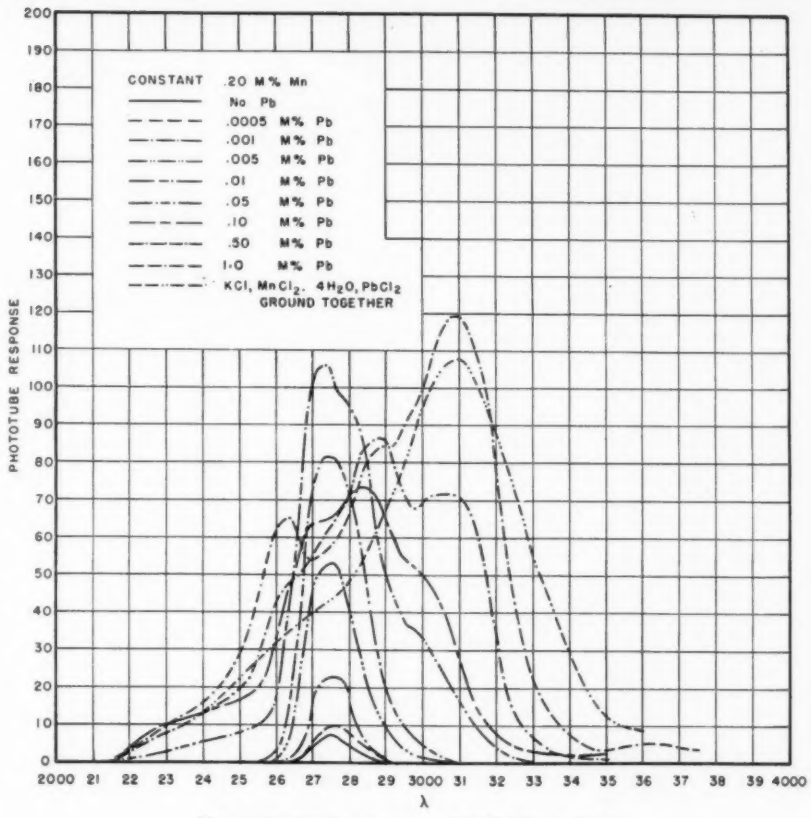

FIG. 6. Excitation spectra of KCl (Pb + Mn)

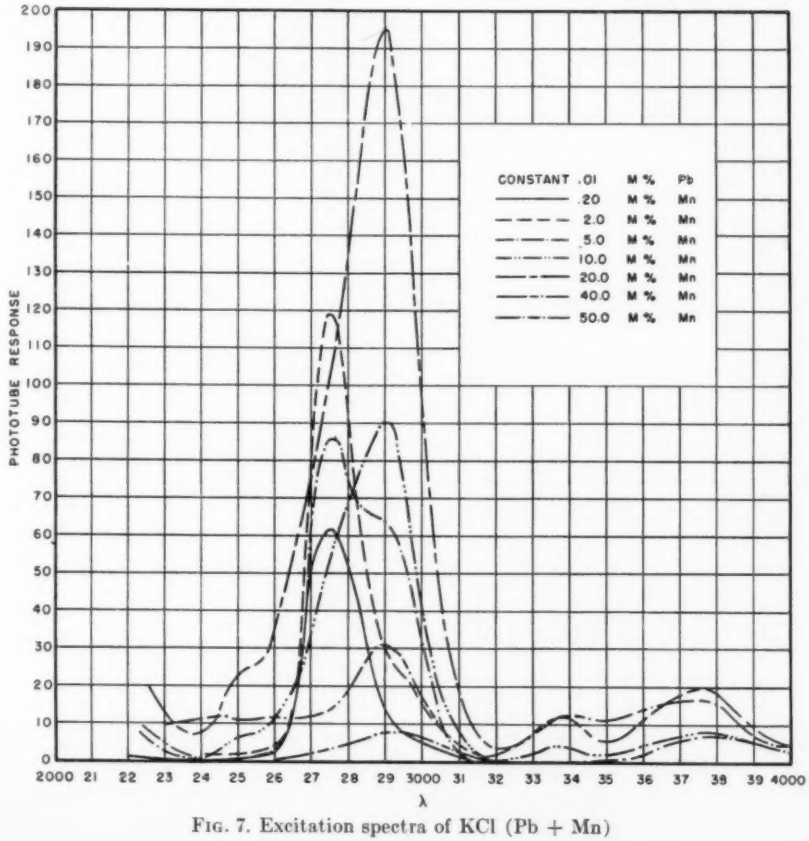

FIG. 7. Excitation spectra of KCl (Pb + Mn)

of the excitation curve of the 2.0 mole per cent sample. It is clearly resolved in the 5.0 mole per cent sample. The fact that this peak is due to K_4MnCl_6 is readily seen by its progressive increase in height to a maximum upon increasing the manganese concentration to 20.0 mole per cent. Further increase in manganese reduces the efficiency of the phosphor without introducing any new excitation peaks. At 50 mole per cent manganese, the composition of the compound $KMnCl_3$, only a very weak excitation at 2900 Å is observed. This small peak is very likely due to the presence of a small amount of K_4MnCl_6 and it may be concluded that $KMnCl_3$ is not excited in the wavelength range 2200–5600 Å at room temperature.

The excitation spectrum of the phosphor prepared by grinding together KCl, $MnCl_2 \cdot 4H_2O$, and $PbCl_2$ is also shown in Fig. 6. Its excitation spectrum resembles that of the high lead-containing samples of KCl (0.20 mole % Mn).

TABLE III

Sample	Excitation wavelength	Relative emission intensity
$(Zn, Be)_2SiO_4$ (Mn)	2500	100
K_4MnCl_6 (Pb) ppt.	2900	60.7
K_4MnCl_6 (Tl) ppt.	2450	56.9
K_4MnCl_6 ppt.	2720	17.5
K_4MnCl_6 (Pb) melt	2900	12.2
KCl (Pb + Mn)	2730	5.8

The relative efficiencies of several preparations under equal energy of excitation at the optimum excitation wavelength for each phosphor are shown in Table III.

Discussion

It is obvious that the luminescence emission of K_4MnCl_6 is similar to that of many manganese-activated compounds. The familiar 6000 Å–6100 Å peak is typical of this class of phosphors. The emission of KCl(Pb + Mn) is similar, but the displacement of the peak renders the two phosphors easily distinguishable by their emission spectra. The luminescence emission of manganese-activated alkali halides has not been discussed in terms of the coordination hypothesis as proposed for oxygen-bearing systems by Linwood and Weyl (7) and by Schulman (8). However, it has been observed that in alkali chlorides the six- (1) or eightfold (9) coordinated manganese emits an orange to red band. Without consideration of the question of whether coordination with chlorine should be analogous to coordination with oxygen, one might expect from the hypothesis that the coordination of manganese in K_4MnCl_6 should be similar to its coordination in the alkali chlorides. The work of Bellanca reveals that such is the case. Manganese is sixfold coordinated with chlorine as shown in the schematic representation of the structure in Fig. 8. The structure is very nearly cubic with three equal axes at an angle of 89° 32′ from each other. Manganese lies at the centers of alternate cubes whose eight corners are potassium ions. Chloride ions are at the faces of the cubes. The structure provides very nearly the same environment for all of the ions as might be found upon the orderly replacement of one third of the potassium ions in a potassium chloride crystal by an equivalent number of manganous ions and positive ion vacancies, if it were possible to retain the potassium chloride structure under such conditions. The coordination of both potassium and manganese with chlorine is sixfold in both structures. Chloride ions in K_4MnCl_6 are surrounded by four potassium ions and one manganous ion. The same chloride environment would be expected in the conjectured potassium chloride structure.

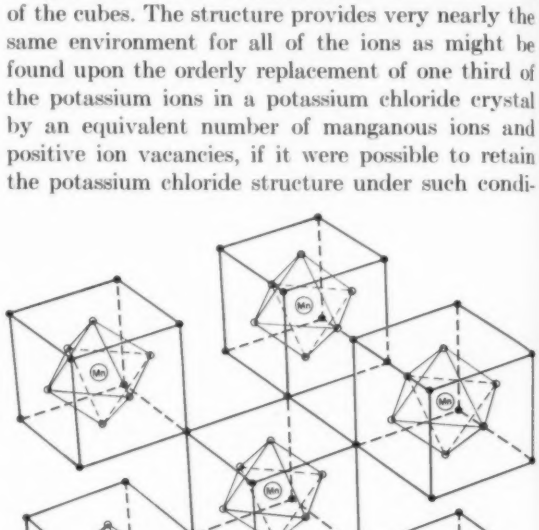

Fig. 8. Structure of K_4MnCl_6

From the excitation curves it may be seen that K_4MnCl_6 is not excited in the wavelength range 2800–3200 Å in the absence of lead or thallium. Lead introduces a strong excitation peak in this region. Since the same emission spectrum is obtained upon excitation in the lead band as is produced by excitation in the K_4MnCl_6 bands, the system must be one of sensitized luminescence when excitation occurs in the band introduced by lead. Excitation of lead-bearing preparations between 2200–2800 Å is seen to occur in a superposition of the characteristic K_4MnCl_6 bands upon the broad lead band. Lumi-

nescence excited in this region is, therefore, only partially due to a sensitized process since absorption occurs in both the sensitizer and the manganese ion. Excitation at wavelengths longer than 3200 Å results from absorption in the manganese ion and no sensitized process is involved.

Thallium does not introduce an excitation peak in a region where excitation of K_4MnCl_6 does not occur in its absence. However, it is seen that thallium provides two excitation peaks which greatly increase the excitation in the region 2200–2900 Å. Excitation in this range is, therefore, partially due to sensitization.

Manganese-activated potassium chloride phosphors were not studied very extensively in this investigation, but enough information was obtained to ascertain that the presence of a sensitizer is necessary to produce luminescence under ultraviolet excitation in the wavelength range 2200–4000 Å. The excitation curves of Fig. 6 show only a weak excitation of KCl(Mn) in this range. The excitation peak position is identical with the one produced by the introduction of lead and is increased by increasing lead concentration. The 2750 Å peak found in the absence of lead additions can be correlated with lead impurity in the KCl. The photoluminescence observed in this phosphor can, therefore, be entirely attributed to a sensitized process.

Neither of the two systems studied seems to be well adapted to providing fundamental information concerning the process of sensitized luminescence. The KCl-type phosphors are too inefficient to permit either the accurate optical measurements needed for such a study, or any justifiable conclusions from such measurements. The K_4MnCl_6 is complex and difficult to obtain as a completely homogeneous material. The presence of lead or thallium in the free KCl which accompanies this phosphor is a serious complication. Moreover, whether lead and thallium substitute for potassium or for manganese in K_4MnCl_6 seems to be an open question. One might expect that thallium, resembling potassium more than manganese in both ion size and valence, would substitute for an alkali ion. Lead, however, although very similar to potassium in ionic radius, is divalent. The author is inclined to believe that both thallium and lead substitute for potassium but no proof can be offered. However, the excitation spectrum of the K_4MnCl_6 phosphor contains a number of quite distinct peaks which may offer a clue to the nature of the electronic levels of the manganese taking part in the luminescence process. It is likely that further investigation of this compound would most profitably be made along these lines.

Acknowledgments

The author wishes to express his indebtedness to Dr. J. H. Schulman for many suggestions and discussions, to Mrs. E. W. Claffy and Mr. F. Von Batchelder for the x-ray diffraction data and polarographic analyses, to Drs. O. F. Tuttle and S. Zerfoss for the microscopic identification of phases, and to Dr. L. S. Birks for the interpretation of the data of Bellanca.

Any discussion of this paper will appear in a Discussion Section, to be published in the December 1951 issue of the Journal.

References

1. J. H. Schulman, E. Burstein, R. J. Ginther, M. White, and L. W. Evans, *Bull. Am. Phys. Soc.*, **24,** 25 (1949).
2. J. Süss, *Z. Krist. Mineral.*, **51,** 248 (1912).
3. C. Sandonnini and G. Scarpa, *Atti accad. naz. Lincei*, **22,** II, 163 (1913).
4. A. Bellanca, *Ricerca sci. e ricostruz.*, **16,** 1109 (1946); *Periodico mineral. (Rome)*, **16,** 73 (1947).
5. German Pat. 709,330, Aug. 1941.
6. M. Kato, *Sci. Papers Inst. Phys. Chem. Research Tokyo*, **41,** 113 (1943).
7. S. H. Linwood and W. A. Weyl, *J. Optical Soc. Am.*, **32,** 443 (1942).
8. J. H. Schulman, *J. Applied Phys.*, **17,** 902 (1946).
9. J. H. Schulman, Unpublished Data on Caesium Chloride.

THE ELECTROCHEMICAL SOCIETY, INC.

The Electrochemical Society is an international organization of individuals and companies concerned with or interested in Electrochemistry and allied subjects.

The Society is dedicated to the advancement of the theory and practice of Electrochemistry and related subjects, as shown in the following divisions:

Battery	Electro-Organic
Corrosion	Electrothermic
Electric Insulation	Industrial Electrolytic
Electrodeposition	Theoretical Electrochemistry
Electronics	

Among the means to this end are the holding of meetings for the reading and discussion of professional and scientific papers on these subjects, the publication of such papers, discussions, and communications as may seem appropriate, and cooperation with chemical, electrical, and other scientific and technical societies.

It is an incorporated society without capital stock. The affairs of the Society are managed by a Board of Directors under a Constitution and By-Laws. Officers are nominated by a nominating committee appointed by the Board of Directors and elected by the members.

Direct all general correspondence and inquiries regarding membership to Society headquarters at 235 West 102nd Street, New York 25, N. Y., c/o Mr. W. J. Holian, Assistant Secretary.

Officers of the Society

President ..... Charles L. Faust
Past President ..... Alfred L. Ferguson
Vice-President ..... Ralph M. Hunter
Vice-President ..... J. C. Warner
Vice-President ..... Robert J. McKay
Treasurer ..... E. Gideon Widell
Secretary ..... Henry B. Linford